MACCS VERIFICATION REPORT

Prepared for

U.S. Nuclear Regulatory Commission
Contract 31310018D0002
Task Order No. 31310020F0081

Prepared by

Osvaldo Pensado

Center for Nuclear Waste Regulatory Analyses
San Antonio, Texas

October 2021

ABSTRACT

This report documents systematic testing of the MELCOR Accident Consequence Code System (MACCS) functions by a third party (the Center for Nuclear Waste Regulatory Analyses at the Southwest Research Institute®) not involved in MACCS software development. Testing focused on verifying equations and algorithms of the MACCS code, as described in the MACCS Theory Manual. It is not practical to generate independent benchmarks that reproduce details of the MACCS code, given that MACCS has been developed over decades. Instead, simplified systems were examined that allowed for direct comparison to closed-form equations. Other tests were designed by predicting non-trivial trends and relationships of different outputs of the MACCS code. It was verified that MACCS outputs satisfied those predicted relationships.

The project began with testing MACCS Version 4.0. A small number of issues were identified through that testing, which were addressed in MACCS Version 4.1. Examples include expanding the domain of the independent variables (related to the effective plume size and receptor distance) in the lookup table used to compute the cloudshine factor, and imposing constraints on the extent of the lateral spread of simulated plumes. This report documents only tests applied to MACCS Version 4.1. The MACCS 4.1 code successfully satisfied the designed benchmarks and tests.

This report is structured in a modular manner, with tests of specific features documented in independent and stand-alone sections, thus allowing further documentation of additional tests later, if desired. Testing covered a broad range of features and functions of the MACCS code. Results are organized according to the three basic modules of the MACCS code: ATMOS, EARLY, and CHRONC. Only a small number of MACCS features were tested and documented in this report; complementary tests are expected in the future.

This report supplements information provided in the MACCS Theory Manual. The user is referred to the MACCS Theory Manual for a detailed discussion of models and solution algorithms; however, key equations of the MACCS Theory Manual are replicated in this report, with minor modifications for the sake of clarity, to serve as a stand-alone document. The graphic display of results and the designed benchmarks provide insights into models, equations, algorithms, and methods of the MACCS code as described in the Theory Manual.

CONTENTS

LIST OF FIGURES

LIST OF TABLES

Page

ACKNOWLEDGMENTS

This report was prepared to document work performed by the Center for Nuclear Waste Regulatory Analyses (CNWRA®) for the U.S. Nuclear Regulatory Commission (NRC) under Contract No. 31310018D0002, for Task Order No. 31310020F0081. The activities reported here were performed on behalf of the NRC Office of Nuclear Regulatory Research, Division of Systems Analysis. The author benefited from multiple discussions on MACCS algorithms with A.J. Nosek, K. Compton, and S. Haq of NRC, and with D. Clayton and J. Leute, MACCS software developers affiliated with the Sandia National Laboratories. The author recognizes the technical review by G. Adams and the editorial and programmatic review by W. Patrick. Appreciation is extended to L. Neill and A. Ramos for assistance in preparation of the report.

QUALITY OF DATA, ANALYSES, AND CODE DEVELOPMENT

DATA: All CNWRA-generated original data contained in this report meet the quality assurance (QA) requirements described in the CNWRA QA Manual.

ANALYSES AND CODES: The Windows version of the MACCS code (SNL, 2021), WinMACCS Version 4.1, was used to compute consequences of postulated accidents. Consequence outputs and input values were extracted from WinMACCS output files. Python 3 was used to translate MACCS outputs to Excel® files. Mathematica® 12 (Wolfram Research, 2021) was used to import values from WinMACCS output files, to plot results, and to compute expected results. Mathematica 12, Python 3, and Excel are general use software classified as "exempt from control" by TOP–018. Relevant electronic files and scripts were archived in the CNWRA QA records system.

References

SNL. "MELCOR Accident Consequence Code System (MACCS)." Albuquerque, New Mexico: Sandia National Laboratories. 2021. <https://maccs.sandia.gov/maccs.aspx>

Wolfram Research. "Wolfram Mathematica 12." Champaign, Illinois: Wolfram Research. 2021. <https://www.wolfram.com/mathematica/?source=nav> (Accessed date 21 September 2021).

1 INTRODUCTION

MACCS is a short name for MELCOR Accident Consequence Code System (SNL, 2021). The MACCS code is aimed at modeling the impact of severe accidents at nuclear power plants on the surrounding environment. Impacts are quantified as radiological doses and health effects (e.g., the number of people with immediate injury due to exposure to a cloud of radiation, or affected by cancer developed after a long-term), as well as measured in economic terms from loss of productivity and compromised land. The consequence analysis is a tool to inform adequate levels protection to the public, emergency planning, and gain insights on hazards posed by nuclear installations including nuclear power plants. Consequence analyses have been used, for example, in environmental assessments, regulatory cost-benefit analyses, and the State-of-the-Art Reactor Consequence Analyses (SOARCA) project (SNL, 2017a; SNL, 2019; Chang, et al., 2012).

MACCS has been developed by Sandia National Laboratories (SNL) for the U.S. Nuclear Regulatory Commission (NRC), over a span of more than two decades. Version 1.12 of MACCS was released in 1997 (Bixler, et al., 2017; SNL, 2015a), and the Windows-interface version of MACCS (WinMACCS) was released in 2008 (SNL, 2015b). MACCS has been produced under a software quality assurance program (SNL, 2017b), which calls for verification testing of its functions. However, there are only limited benchmark studies on MACCS functions by independent parties (Thoman, et al., 2009; Molenkamp, et al., 2004). This report documents systematic testing of MACCS functions implemented by a third party, Center for Nuclear Waste Regulatory Analyses, not involved in MACCS software development. This project initiated with testing MACCS Version 4.0, released on June 5, 2020. A small number of issues were identified as part of that initial testing and communicated to the SNL software developer. Those issues were addressed in the latest version of the MACCS code, Version 4.1, released on July 30, 2021 (SNL, 2021). The initial set of tests were repeated with the MACCS Version 4.1 to verify those issues were addressed, as documented in this report.

The MACCS is organized into three basic modules: ATMOS, EARLY, and CHRONC. The ATMOS module includes a model for the release of radionuclides from a source, a model for propagation of the plume (or finite plume segments) based on steady-state Gaussian dispersion plume functions or the HYSPLIT model, and a description of dynamic weather patterns (e.g., windspeed and direction, atmospheric stability index, rain rate). The EARLY module simulates the early phase of the accident with a duration of up to 40 days. During this time, people could be exposed to radionuclides in the plume cloud and to ground contamination. Several protective actions in the early phase are accounted for in the EARLY module, including sheltering, evacuation, dose-dependent early relocation, and ingestion of potassium iodide pills to mitigate effects of inhalation of radio-iodine. The CHRONC module models consequences in the intermediate and long-term phase. The intermediate phase is modeled as an optional phase (i.e., it can be bypassed or disabled) and it can last up to one year after the end of the EARLY phase; the exposure pathways are associated with ground contamination, and the only protective action is relocation. CHRONC also simulates the long-term phase, including exposure pathways arising from ground contamination (which could contaminate farm food products and water, which then become indirect exposure pathways). The long-term phase accounts for protective actions such as habitation and farming restrictions (including interdiction and condemnation of property), and land decontamination. Those protective actions constrain radiological doses but at an economic cost, also quantified by the CHRONC module. The duration of the long-term phase is limited to 50 years. Tests in this report were aimed at checking features and functions of the ATMOS, EARLY, and CHROC modules, and the testing

is organized into three main sections separately addressing these three modules (ATMOS tests are included in Section 2, EARLY tests in Section 3, and CHRONC tests in Section 4).

The MACCS software quality assurance plan (SNL, 2017b) defines *validation testing* as the process to ensure that the algorithms and models used in the program correctly describe the physical events that are being modeled. On the other hand, *verification testing* is defined as the process to ensure that the program/code correctly solves equations as intended. In this report, the focus is on verification testing; however, by examining assumptions and technical bases of those assumptions model confidence is gained, which relates to validation testing. This is a reason why this report is titled MACCS *Verification* Report, although it indirectly covered a level of model validation testing by the examination of the underlying models including discussion of those models with peers and technical counterparts at the NRC.

Given the more than two decades of development of the MACCS code, it is impractical to reproduce the functionality and complexity of the MACCS code by independent means. Instead, the main verification strategy adopted in this project was to examine very simple systems (e.g., constant wind speed and direction, one plume segment, one cohort, one single long-lived radionuclide, no mitigation actions, no evacuation, no relocation) where analytical equations can be used to compute radionuclide concentrations in air and on the ground, as well as dose consequences and health effects. Only a sample of the MACCS functions were tested but covering a broad range of features of the ATMOS, EARLY, and CHRONC modules. The emphasis of the testing was on radionuclide concentrations, dose computations, and health effects. MACCS functions to model protective actions and socioeconomic impacts and costs were not included in tests in this report. Complexities of the MACCS model such as plumes specified in multiple discrete segments, weather patterns, multiple cohorts, evacuation paths, and sampling of input parameters from distribution functions were also not included in tests in this report.

The MACCS Theory Manual (Nosek, et al., 2021) was the document consulted to guide the development of tests. Equations of the MACCS Theory Manual used in the tests are reproduced in this report to add specificity on the MACCS functions tested and numerical approaches adopted. A table in Section 5 compares the table of contents of the MACCS Theory Manual to tests documented in this report. This report covered a broad range of features of the MACCS code but keeping in mind that the systems modeled in the MACCS runs represented simple systems.

The tests in this report refer to multiple outputs of the MACCS code, such as Type A, Type C, Type 1, etcetera. Effort is made in the test documentation to add a description to the output such as Type A maximum dose, Type C sector average dose, Type 6 centerline dose. Those outputs are printed in blocks in three MACCS output files, Model1.out, Summary.txt, and tbl_outStat.txt. Scripts were prepared to extract information from those blocks of text into multi-worksheet Excel files or CSV files that are much easier to read and query. Those Excel® and CSV files were archived with the quality assurance records of this report, as well as the original MACCS output files. The reader is referred to the MACCS Theory Manual (Nosek, et al., 2021), Sections 2.9, 3.5, and 6.3 for a detailed description of the MACCS model outputs.

The food chain model of the CHRONC module was not tested. However, the reader is referred to another independent report (Pensado, et al., 2020), which includes a sensitivity analysis of input parameters of the MACCS food chain model named COMIDA, and a description of each of those input parameters. The COMIDA sensitivity analysis revealed aspects of model implementation, addressing aspects of model validity and verification testing.

2 ATMOS MODULE

2.1 Test 2.1: Air Concentrations

The objective of the test was to verify the use of Gaussian plume equations for the computation of concentrations in air, centerline (z=h) and ground level (z=0). The Gaussian plume equations are defined in Section 2.5.1 of the MACCS Theory Manual (Nosek, et al., 2021)

$$\chi(x,y,z) = \frac{Q}{u}\frac{1}{\sqrt{2\,\pi}\,\sigma_y(x)}\exp\left(-\frac{1}{2}\frac{y^2}{\sigma_y(x)^2}\right)\psi(x,z) \tag{2-1}$$

with

$$\psi(x,z) = \frac{1}{\sqrt{2\,\pi}\,\sigma_z(x)}\sum_{n=-N}^{N}\left\{\exp\left[-\frac{1}{2}\frac{(z-h+2\,n\,H)^2}{\sigma_z(x)^2}\right]+\exp\left[-\frac{1}{2}\frac{(z+h+2\,n\,H)^2}{\sigma_z(x)^2}\right]\right\} \tag{2-2}$$

χ	—	time-integrated concentration (Bq-s/m^3)
Q	—	total activity in the plume segment (Bq)
u	—	windspeed (m/s)
h	—	centerline height (=plume release height in case of no plume rise) (m)
H	—	plume ceiling, maximum plume height (m)
n	—	integer
N	—	series limit
x	—	longitudinal distance (m)
y	—	lateral, across wind, distance (m)
z	—	vertical distance from the ground (m)
$\sigma_y(x)$	—	lateral Gaussian dispersion coefficient (m)
$\sigma_z(x)$	—	vertical Gaussian dispersion coefficient (m)

Equation (2-2) accounts for mirror boundary at z = 0 and z = H (particles reaching the ground and the plume ceiling are assumed to bounce back and remain in the region 0 ≤ z ≤ H). The accurate solution is an infinite series (N=∞); however, in practice the series converges after a few terms. In the tests, it was in general sufficient to consider N = 5 in the computation of $\psi(z)$, but more terms in the series were required when the Gaussian vertical dispersion coefficient, $\sigma_z(x)$, was large.

A second objective of the test was verifying the computation of a cloudshine dose for a simple case (one radionuclide, one organ). This test complements tests in Section 3 aimed at verifying computations by the EARLY module. From Section 3.3.1 of the MACCS Theory Manual, for organ k the cloudshine centerline dose is computed as

$$DC_k = \left[\sum_i DRCC_{\infty ik}\,\chi(x, y=0, z=h)\right] C\;F\;SFC \tag{2-3}$$

DC_k	—	cloudshine centerline dose to organ k (Sv)
$DRCC_{\infty ik}$	—	semi-infinite cloudshine dose coefficient to organ k by radionuclide i (Sv-m^3/Bq-s)
C	—	cloudshine factor, function of the plume height, h, and the dispersion coefficients σ_y and σ_z

F — fraction of the exposure time (=1, for non-evacuating and non-relocating individuals)

SFC — cloudshine protection factor specified by CSFACT in WinMACCS (CSFACT = 1 in the problem examined)

For the simple case of one radionuclide, non-evacuating and non-relocating individuals, and SFC=CSFACT=1, Eq. (2-3) becomes

$$DC_k = DRCC_{\infty ik}\ \chi(x, y = 0, z = h)\ C \tag{2-4}$$

Equation (2-4) was used to examine the computation of the cloudshine factor C.

2.1.1 Test input

Default inputs from the LNT sample input file distributed with the MACCS code were selected, with modifications to simulate a simple case with the following features:

- One radionuclide, Cs-137
- One long-lasting plume segment, without plume rise
- Simple weather pattern: constant windspeed (10 m/s) blowing north
- One cohort, non-evacuating and non-relocating
- Cloudshine dose pathway only

The following were the explicit changes implemented to the MACCS inputs through the WinMACCS interface:

General Properties

- SCOPE
  - Atmospheric Transport and Dispersion: Gaussian
  - Early Consequences (no Late Consequences)
- TRANSPORT
  - Power Law Functions (NUM_DIST=0)
  - Plume Meander: None (MNDMOD=OFF)
- WEATHER
  - METCOD=4: constant weather
- PLUME
  - Plume Source: Area Source
  - Plume Rise: Power Model (plume rise controlled by power law and heat output, PLHEAT)
  - Plume Trapping/Downwash: Briggs (buoyancy flux)
- SITE DATA
  - Uniform: uniform population density
- DOSE
  - Linear No Threshold
  - Activate KI Model: FALSE (no KI ingestion model)
- EVAC/ROTATION
  - None (LASMOV=0): no evacuation
  - Wind Shift and Rotation: no wind shift with rotation (IPLUME = 1)
    - No wind shift: plume segments move with constant direction and speed
    - Rotation: means that wind direction is rotated according to user-defined

probabilities
    - Number of cohorts = 1
- WIND ROSE
    - User Supplied (OVRRID = True)
- ANIMATION/HEALTH EFFECTS
    - AniMACCS files disabled under IPLUME=1
    - Early Effects: Early Fatality Effects, Early Injury Effects, Latent Cancer Effects from Early Exposure

ATMOS

- Spatial Grid
    - NUMCOR=16: compass subdivisions
    - SPAEND (km) defines the radial grid. Adjacent radial segments must be greater or equal than 0.1 km. The grid was log-spaced, from 0.1 to 100 km
- Deposition
    - Dry/Wet Depos Flags
        - DRYDEP = FALSE for Cs and Ba: no dry deposition
        - WETDEP = FALSE for Cs and Ba: no wet deposition
- Dispersion
    - Dispersion Function
        - CYSIGA, CYSIGB, CZSIGA, CZSIGB according to Table 2-5 of the MACCS Theory Manual (Nosek, et al., 2021)
    - Scaling Factors
        - YSCALE =1, factor for σ_y
        - ZSCALE = 1.0, 0.1, 0.01, factor for σ_z
- Plume Specifications
    - Plume Rise Scale Factor
        - SCLCRW = 0.001
        - SCLADP = 0.01
        - SCLEFP = 0.01
        - The smallest factors were selected to avoid plume rise. These factors should not matter when PLHEAT=0
- Radionuclides
    - Radionuclides
        - NUMISO = 16
        - CORINV (Bq): inventory for all isotopes, all 0 except for Cs-137 = 10^{15} Bq
    - Pseudostable radionuclides
        - NUMSTB = 17
        - Added Ba-137m, so that it would not contribute to dose computations with Cs-137 inventories
        - Removed Ba-137m from NUCNAM
- Release Description
    - Plume Parameters
        - One plume segment: variables NUMREL, PDELAY, PLHITE, REFTIM, PLUDUR
        - PDELAY = 18,000 s
        - PLHITE (m) = 500 m: plume release height (mid distance to ceiling)
        - REFTIM = 0.5 (midpoint representative location of plume segment)
        - PLUDUR = 18000 s

    - Daughter Ingrowth Flag
        - APLFRC = PROGENY: initial release controlled by chemical group
    - Release fractions: RELFRC
        - RELFRC = 1 for Cs, Plume 1, 0 for everything else
    - Release Fraction Scale Factors
        - NUMISO = 16
        - IGROUP: parameter defining the chemical group. Isotopes are part of the same chemical group
        - Reduced the radionuclide set until a minimum set was achieved that could run, including Cs-137
    - Heat
        - PLHEAT = 0, disables plume rise, sensible heat using ambient temperature as reference
    - Building Height Data
        - BUILDH (m) = 40 m
    - Initial Area Source
        - SIGYINIT (m) = SIGZINIT (m) = 0.1 m: initial values of the Gaussian dispersion coefficients
- Weather
    - Constant or Boundary Conditions
        - BNDMXH (m) = 1000: plume ceiling
        - IBDSTB = 4: stability class
        - BNDRAN (mm/hr) = 0: rain rate
        - BNDWND (m/s) = 10: windspeed
    - Fixed Start Time Data
        - ISTRDY = 1: day of the year when weather sequence starts
        - ISTRHR = 1: starting time of the weather trial (first hour)

EARLY

- Wind Rose Probabilities
    - WINROS: Segment 1 (north) = 1, 0 for all other segments. The wind was assumed to blow north.
- Uniform Site Data
    - IBEGIN = 1
    - POPDEN (1/km^2) = 10 people/km^2, population density
    - FRACLD = 1.0 land fraction
- Normal Relocation
    - DOSNRM (Sv) = 10^{10} Sv, set to high threshold to avoid normal relocation
- Hot Spot Relocation
    - DOSHOT (Sv) = 10^{10} Sv, set to high threshold to avoid relocation
- Emergency Phase Resuspension
    - RESCON (1/m) = 0
    - RESHAF (s) = 10^{10} s: long half-life to avoid resuspension
    - Parameters selected to avoid resuspension
- Emergency Cohort One
    - Cohort Fraction
        - WTFRAC = 1.0 (weight fraction)
    - Shielding and Exposure
        - CSFACT = 1 (cloudshine), and 0 for all other shielding factors

Output Controls

- Type 0 (NUM0) ATMOS Outputs
  - INDREL = 1 (plume segment)
  - INRAD = 1, 2, 3, …, 26 (all radial segments)
  - NUCOUT = Cs-137: radionuclide output by NUM0
- Type 6 (NUM6) Centerline Dose
  - ORGNAM = L-ICRP60ED
  - PATHNM = CLD: cloudshine
  - I1DIS6=1, I2DIS6=26: all radial segments
- Type A (NUMA) Peak Dose in a Grid Ring
  - NAME = L-ICRP60ED
  - I1DISA=1, I2DISA=26: all radial ring segments
- Type C (NUMC) Average Sector Dose
  - ORGNAM = L-ICRP60ED
  - ELEVDOSE (Sv) = 0: outputs all grid elements with dose > 0 Sv
  - PRINT_FLAG_C = True: outputs information for all grid elements

2.1.2 Test procedure

Three different MACCS runs were executed with different values of ZSCALE (=0.01, 0.1, 1, 5, 10), to consider different cases of vertical plume spread, including very narrow plumes along the vertical direction. Results were extracted from MACCS output files Model1.out and tbl_outStat.txt. Python scripts were written to translate information in those files to Excel. Information in the Excel files were imported into Mathematica (Wolfram Reseach, 2021), to be queried, plotted, and compared to benchmark solutions.

Equations (2-1) and (2-2) were used to independently compute air concentrations along the centerline (y = 0, z=500 m) and along the ground (y = 0, z=0). The MACCS power law option was used to define the Gaussian dispersion coefficients, σ_y and σ_z as functions of the position x. The gaussian dispersion coefficients were computed using the coefficients for stability class D (class 4) of Table 2-5 of the MACCS Theory Manual, and the power law function (Eq. 2.21 of the MACCS Theory Manual) to compute $\sigma_y(x)$ and $\sigma_z(x)$. In addition, the virtual source position correction (Section 2.5.4 of the MACCS Theory Manual) was applied in the independent computations to match the assumed initial values of the dispersion coefficients at the source; i.e., $\sigma_y(x{=}0) = \text{SIGYINIT} = 0.1$ m, and $\sigma_z(x{=}0) = \text{SIGZINIT} = 0.1$ m.

Type 0 MACCS results (ATMOS module outputs) were compared to results directly computed based on Eqs. (2-1) and (2-2). Type 6 centerline doses and Type A peak doses were compared to Cs-137 cloudshine dose computed using Eq. (2-4).

Information output by the ATMOS module was also verified considering basic relationships, such as constant plume segment speed (= 10 m/s, controlled by the windspeed input) and decay rates of Cs-137.

2.1.3 Test results

Results of the air concentration tests are presented in Figure 2-1. The MACCS outputs were extracted from the file tbl_outStat.txt marked by the following labels

- Centerline Air Concentration (Bq-s/m3)
- Ground-Level Air Concentration (Bq-s/m3)

Excellent agreement was attained between the centerline and air concentrations computed with Eqs. (2-1) and (2-2) and the MACCS outputs, demonstrating that MACCS computes air concentrations using the Gaussian plume equations, with Gaussian dispersion coefficients that have variable values as function of the downwind distance x.

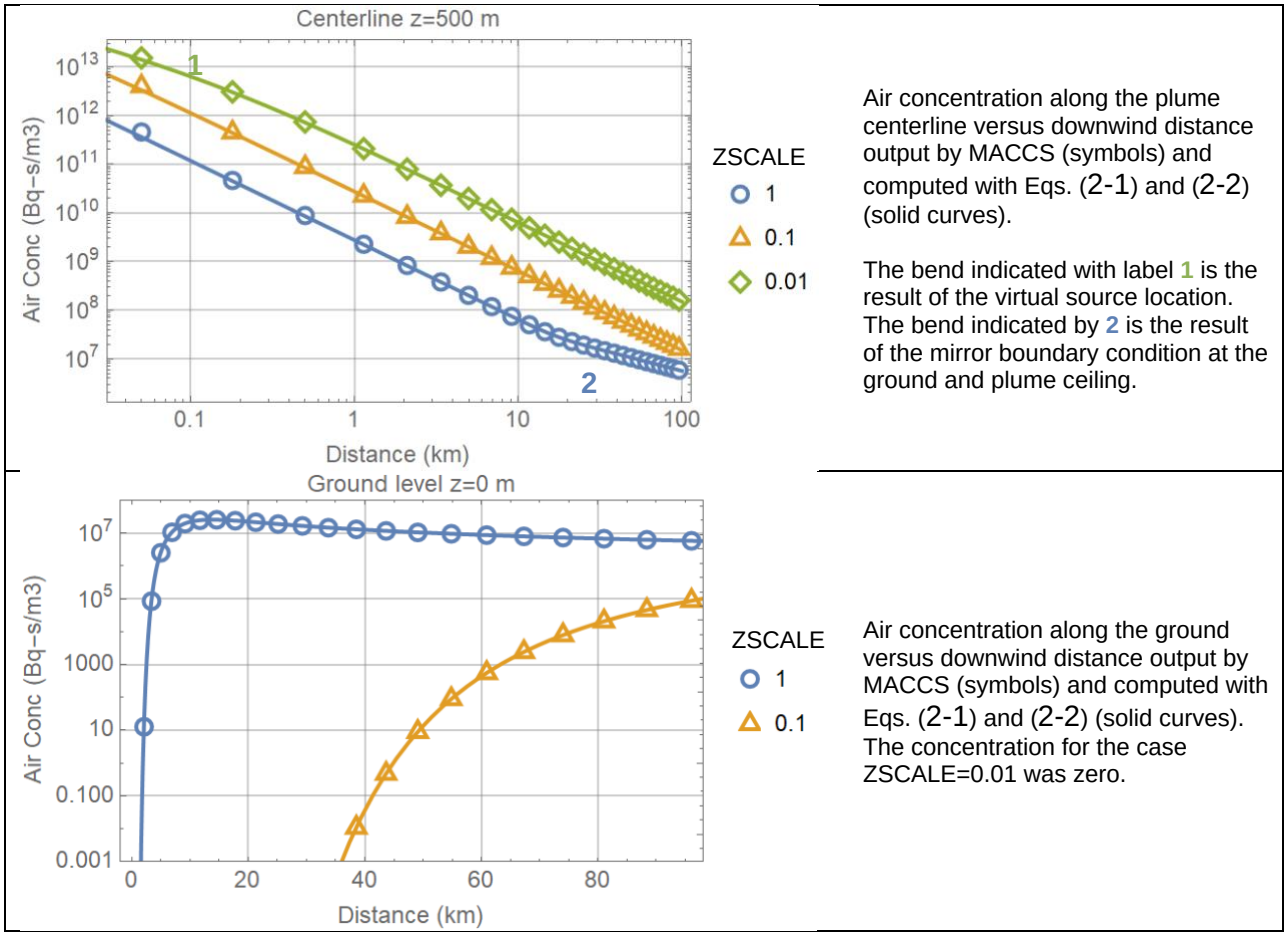

Figure 2-1. Air concentration along the centerline (y=500 m) and at the ground level (y=0 m) versus downwind distance. Symbols represent MACCS output; solid curves represent independent computations.

The file tbl_outStat.txt includes additional outputs that allow for straightforward verification with simple independent computations. For example, values for the Gaussian dispersion coefficients σ_y and σ_z are tracked in tbl_outStat.txt under

- Plume Crosswind Dispersion (m)
- Plume Vertical Dispersion (m)

were verified by direct comparison to dispersion coefficients independently computed using the power law function and the virtual source correction. Results of the verification are displayed in Figure 2-2. The independently computed dispersion coefficients match the MACCS outputs in tbl_outStat.txt.

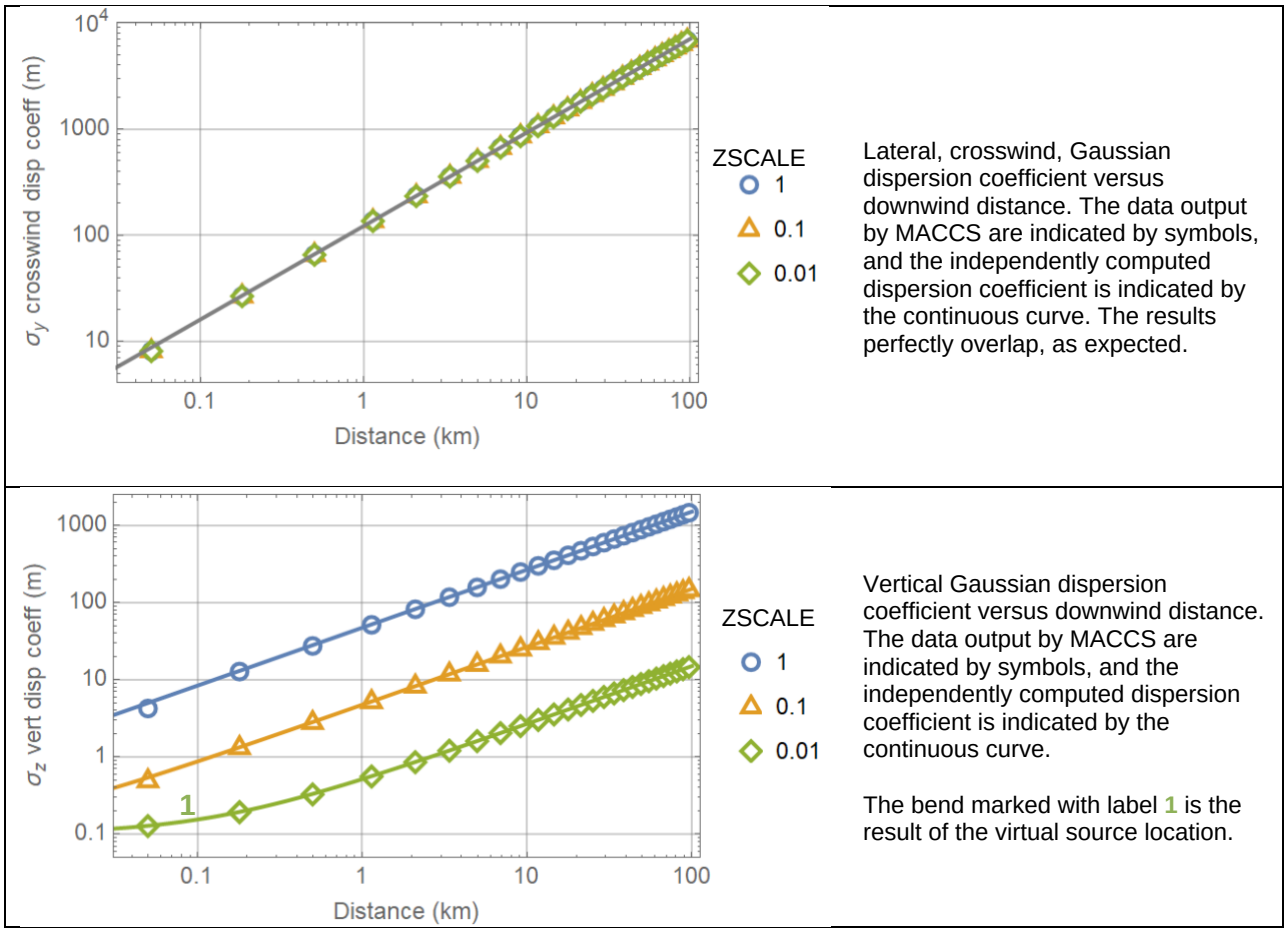

Figure 2-2. Lateral and vertical Gaussian dispersion coefficient versus downwind distance. Symbols represent MACCS output; solid curves represent independent computations.

The file tbl_outStat.txt includes information on the plume travel time and the adjusted source strength under

- Plume Arrival Time (s)
- Adjusted Source Strength (Bq)

The results can be directly verified based on the windspeed (BNDWND=10 m/s), the plume delay (PDELAY = 18,000 s), and the Cs-137 decay rate (half-life = 30.08 years). The verification

results are included in Figure 2-3. The results agree with expected results. A straight line fits the normalized source strength versus time, because the decay rate is small, and the exponential decay can be accurately approximated as a first order Taylor expansion.

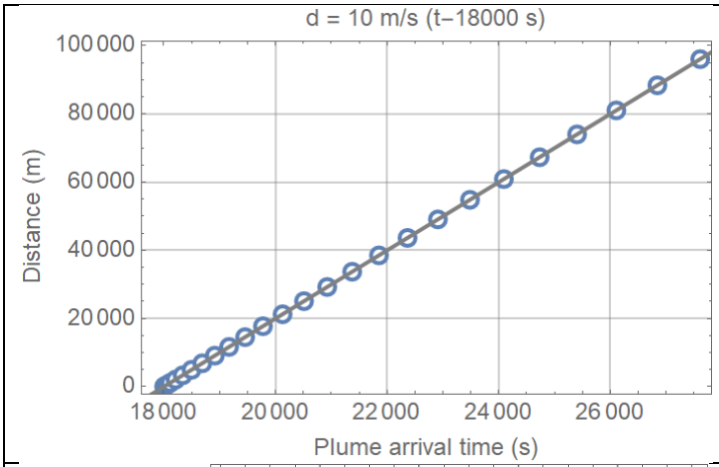

Plume distance versus time. MACCS output data are indicated by symbols, and the straight line was computed with the equations $d = 10\frac{m}{s}(t - 18000\ s)$, consistent with a windspeed BNDWND=10 m/s, and a delay PDELAY = 18,000 s provided as input.

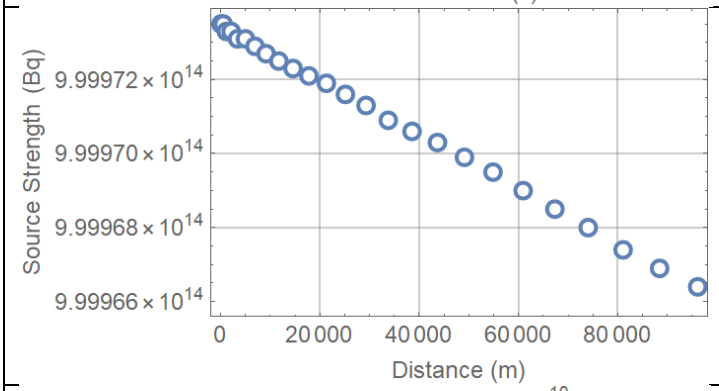

Source strength versus distance. The initial assumed inventory of Cs-137 was 10^{15} Bq (CORINV=10^{15} Bq).

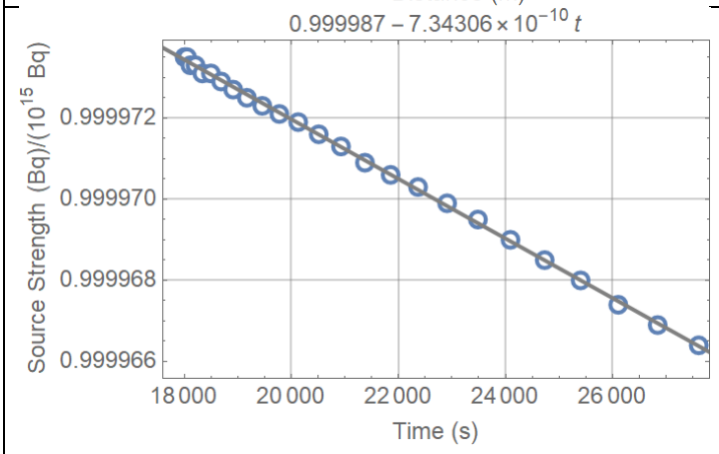

Normalized source strength versus time. The time was computed as a function of distance as

$$t = \frac{d}{10\ m/s} + 18000\ s$$

A straight line was fit, with a resulting slope of 7.34×10^{-10} 1/s. This slope corresponds to a half-life of 29.93 yr, which compares well to the Cs-137 half-life of 30.08 yr. A straight line fits the normalized source strength versus time because the decay rate is small, and a first order Taylor expansion is an accurate approximation:

$$\frac{Q}{Q_o} = e^{-\lambda t} \approx 1 - \lambda t$$

Q: source strength (Bq)
Q_o: initial source strength (CORINV=10^{15} Bq)

Figure 2-3. Plume travel time and source strength.

The following tests are focused on dose estimates associated with the cloudshine pathway. The dose computations are implemented by the EARLY module and corresponding tests are described in Section 3 of this report. However, a test of a cloudshine dose computation is included in the current Test 2.1 because it relates to air concentrations along the plume centerline, and data are readily available in the executed MACCS runs to complete a

supplemental test (cloudshine dose) to tests documented in Section 3.

Type 6 (centerline doses) and Type A (peak dose) are output in the file Model1.out. It was verified that Type 6 and Type A doses are practically identical; however, the comparison is not shown herein, for brevity. The value of the Cs-137 cloudshine dose coefficient factor was extracted from the MACCS input database (file named Fgr13dcf.inp), $DRCC_{\infty ik}$ = 9.28×10^{-17} Sv-m^3/Bq-s for the test. From Eq. (2-4), the cloudshine factor is computed from MACCS outputs as the ratio

$$C = \frac{DC_k}{DRCC_{\infty ik}\ \chi(x, y = 0, z = h)} \tag{2-5}$$

The numerator DC_k is the Type 6 centerline doe, the centerline concentration $\chi(x, y = 0, z = h = 500\ \mathrm{m})$ can be independently computed or extracted from the output Centerline Air Concentration (Bq-s/m^3) in the file tbl_outStat.txt.

The cloudshine factor C, computed from the MACCS outputs as described in Eq. (2-5), was compared to a cloudshine factor directly computed from a lookup table provided by the SNL software developers.[1] A plot of the cloudshine factor as a function of the effective plume size and the receptor distance from the centerline to the receptor location (located on the ground) is provided in Figure 2-4.

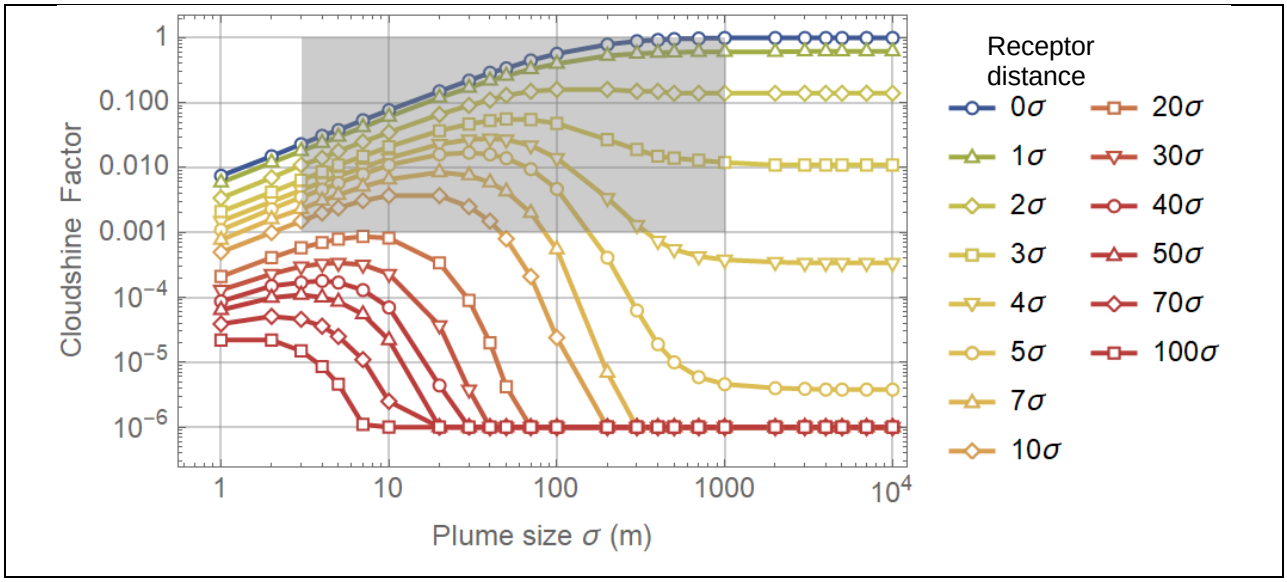

Figure 2-4. Cloudshine factor versus the effective plume size and the receptor distance to the plume centerline. This is lookup table data provided by MACCS software developers.[1] Markers represent points in the lookup table, which are joined by same-color lines to facilitate the visualization. The gray rectangle represents the domain considered in the prior MACCS Version 4.0.

[1]Data obtained through personal communication. Update data in Figure 2-4 are not included in the MACCS Theory Manual (Nosek, et al., 2021).

The effective plume size, σ, is defined as the geometric mean of the lateral Gaussian dispersion coefficient, σ_y, and the vertical Gaussian dispersion coefficient, σ_z:

$$\sigma(x) = \sqrt{\sigma_y(x)\,\sigma_z(x)} \tag{2-6}$$

The relative receptor distance, rrd, is defined as

$$rrd = \frac{receptor\ distance}{\sigma} = \frac{\sqrt{h^2 + y^2}}{\sigma} \tag{2-7}$$

where h is the plume centerline height (=500 m in the test problem), and the receptor is located at coordinates (x, y, z=0). The cloudshine factor lookup table updated for MACCS Version 4.1 defines the cloudshine factor as a function of σ ranging from 1 to 10,000, and rrd ranging from 0 to 100.

The gray box in Figure 2-4 represents the approximated domain of the lookup table of MACCS Version 4.0 (σ ranged from 3 to 1,000, and rrd from 0 to 5). Initial testing of MACCS Version 4.0 identified artefacts associated with effective plume sizes and relative receptor distances in the extrapolation domain of the cloudshine factor lookup table. Extending the (σ, rrd) domain of the cloudshine factor lookup table in MACCS Version 4.1 reduced the frequent need of extrapolation (implemented as edge interpolation in the MACCS algorithms) in the test problems in this report and associated artefacts.

Figure 2-5 displays the MACCS cloudshine factor. The symbols were computed based on Eq. (2-5) and MACCS outputs (centerline cloudshine dose and centerline concentration of Cs-137), and the continuous curves were computed from the lookup table (Figure 2-4), using a linear interpolation function available in Mathematica 12. The MACCS results are excellent in agreement with the independent computations.

Figure 2-6 displays the cloudshine factor versus the downwind distance for a wider range of ZSCALE factors (multiplicative factor to compute the vertical Gaussian dispersion coefficient σ_y), from 0.01 to 10. The independently computed cloudshine factor (solid curves) is in perfect agreement with the MACCS data for ZSCALE factors of 1 or less. The MACCS data exhibit a jump close to a value of 1 for the cases ZSCALE 5 and 10 possibly due to different and practical interpolation approaches to compute the cloudshine factor in the cases of broad plumes (large σ) and small relative receptor distance, rrd.

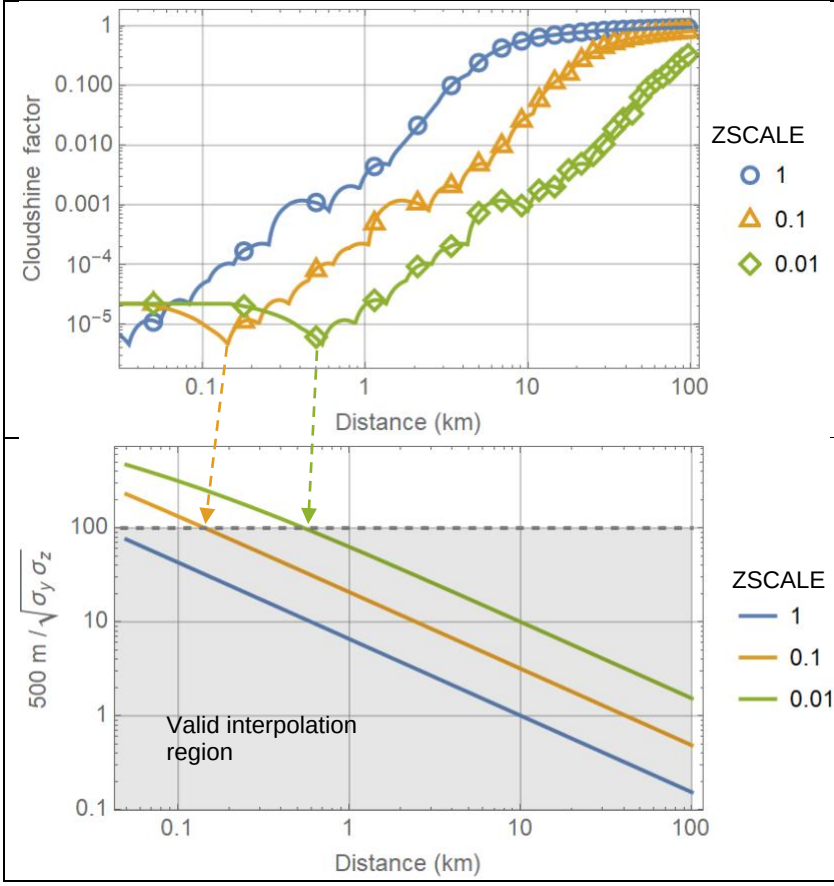

The symbols represent the MACCS cloudshine factor, computed as described in Eq. (2-5). The solid curves were independently computed using the lookup table provided by the software developers. There is complete agreement between the MACCS outputs and the independent computations.

The bumps arise from the use of linear interpolation to compute the cloudshine factor.

Relative receptor distance to the plume centerline versus downwind distance. Standard linear interpolation techniques to compute the cloudshine factor are used when the relative receptor distance is below the dashed line. The anomalous tails on the top plot, on the left of the downwind distance axis, result from using edge interpolation techniques for relative receptor distances above the dashed line.

Figure 2-5. Cloudshine factor versus downwind distance and relative receptor distance versus the downwind distance.

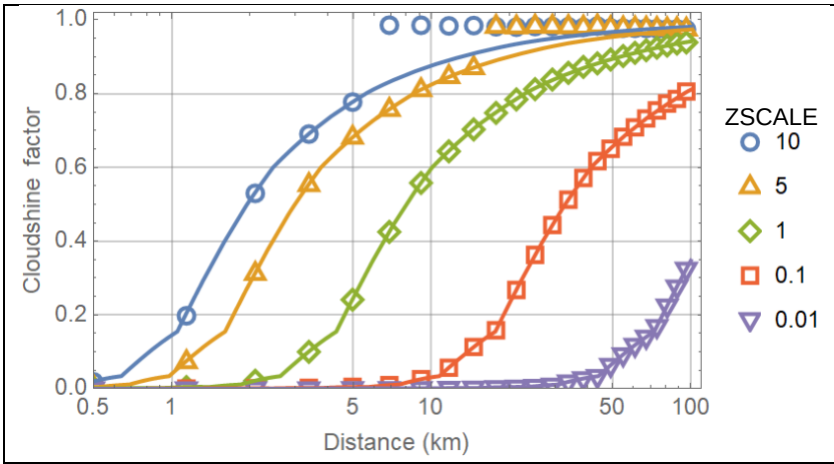

The symbols represent the MACCS cloudshine factor computed as described in Eq. (2-5). The solid curves were independently computed directly using the lookup table provided by the software developers.

The jump in the cases ZSCALE 5 and 10 in the MACCS data is possibly due to practical approximations in the MACCS interpolation algorithms for cases of large σ and small rrd.

Figure 2-6. Cloudshine factor versus downwind distance for additional ZSCALE cases.

The following test is associated with the computation of the mean concentration over a constant-radius arc in the MACCS polar grid. MACCS reports results in a polar coordinate grid. The Type C dose in the Model1.out file is the average dose along an arc of the MACCS grid. In the test problem, the 360° compass was divided into 16 sectors (NUMRAD=16), with each

sector of angular length equal to $\pi/8$ radians. An arc of the MACCS grid is a constant radius curve of angular length $\pi/8$ radians.

MACCS does not implement a strict transformation of polar (r, θ) to Cartesian (x, y) coordinates. Instead, MACCS adopts the following approximated mapping, which is accurate only for laterally narrow plumes (narrow angle approximation):

$$x \to r$$
$$y \to \theta\, r \tag{2-8}$$

The average Type C dose for the north sectors is computed in MACCS as the average dose computed over a constant-radius segment spanning from $-\pi/16$ to $\pi/16$ (angle measured with respect to the north direction). The average dose was independently computed by applying the following steps:

1. Select a downwind distance x and a central sector (north sector)

2. The corresponding arc of the grid is identified: constant radius arc $r = x$, spanning from $-\pi/16$ to $\pi/16$, angle measured with respect to the north direction

3. The average cloudshine factor was computed as a line integral along the arc, considering the MACCS narrow angle approximation in Eq. (2-8). The average equals the line integral divided by the arc length.

4. A low-precision average also was computed as an alternative approach, sampling six equidistant points along the arc, and computing the average of those six points

The average cloudshine factor divided by the cloudshine factor at $y=0$ (or $\theta = 0$, centerline cloudshine factor) must be equivalent to the ratio of the Type C mean dose to the Type 6 centerline dose. The comparison of the independently computed average to the MACCS outputs is displayed in Figure 2-7. The independent computations (solid curves in Figure 2-7) agree with the MACCS data (symbols in Figure 2-7). The jump in the cases ZSCALE 5 and 10 have the same explanation as jumps in Figure 2-6 (due to different interpolation approaches to compute the cloudshine factor in the case of large σ and small rrd). The independent computations matching the MACCS data for the cases ZSCALE 1, 5, and 10 considered a high-precision average based on a line integral. On the other hand, the independent computations matching the MACCS data for the cases ZSCALE 0.01 and 0.001 (vertically narrow plumes) considered a simple average computed with 7 equidistant points on the arc of north sectors. It appears that MACCS employs different mean algorithms in the computation of the Type C cloudshine mean dose depending on the plume spread. For narrow plume cases, a simplified average considering few points along an arc is used; for broad plumes a high-precision algorithm to compute means is employed.

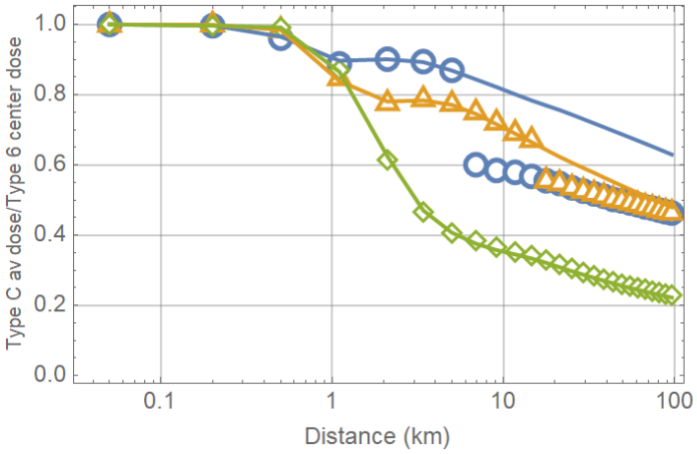

Comparison of the ratio of the Type C sector average dose to the Type 6 center dose (symbols, MACCS data) to the ratio of the mean cloudshine factor and the cloudshine factor at y=0 (solid curves, independent computations).

There is excellent agreement between MACCS data and the independent computations, considering an average based on a line integral in the independent computations. The jump for the cases ZSCALE 5 and 10 is due to same cause as the MACCS data jumps in Figure 2-6.

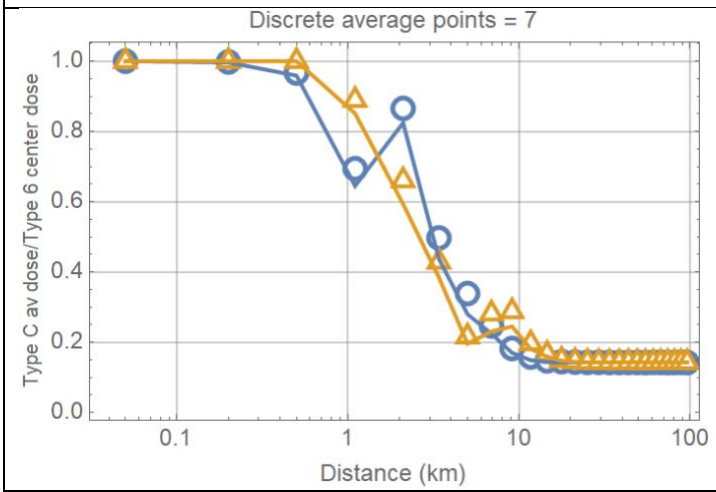

Comparison of the ratio of the Type C sector average dose to the Type 6 center dose (symbols, MACCS data) to the ratio of the mean cloudshine factor and the cloudshine factor at y=0 (solid curves, independent computations).

There is excellent agreement between the MACCS data and the independent computations, considering a discrete average with 7 equidistant points on the north sector arc.

Figure 2-7. Type C to Type 6 cloudshine dose ratio (symbols) versus the downwind distance compared to independent computations (solid curves).

2.1.4 Test Conclusions

Multiple aspects of the MACCS computations were tested; the MACCS ATMOS module passed the designed tests. The following aspects were verified to agree with descriptions in the MACCS Theory Manual:

- Computation of radionuclide concentrations in air, along the centerline and along the ground
- Computation of Gaussian dispersion coefficients according to power laws
- Computation of the Gaussian dispersion coefficients at x = 0, defined by the input parameters SIGYINIT and SIGZINIT
- Propagation of the plume, controlled by the windspeed
- Radioactive decay of the source

- Computation of the cloudshine pathway dose, accounting for the cloudshine factor
- Computation of an average cloudshine dose

A difference was noted in the computation of the cloudshine factor for broad plume cases (i.e., large σ) and small relative receptor distance, rrd (see Figure 2-6 and Figure 2-7) with respect to independent computations. Such difference is likely a practical conservative approach in MACCS interpolation algorithms.

2.2 Test 2.2: Wet Deposition, Long Plume Under Constant Rain

The objective of the set of tests is to verify the implementation of the wet deposition model. Wet deposition is modeled as a first order decay (Eq. 2-44 of the MACCS Theory Manual)

$$\frac{dQ}{dt} = -C_1 \left(\frac{I}{I_0}\right)^{C_2} \cdot Q \tag{2-9}$$

Q — airborne activity (Bq)
I — rain rate (mm/hr), BNDRAN=1 mm/hr in the test
I_o — reference rain rate (=1 mm/hr)
C_1 — linear wet deposition coefficient (1/s), CWASH1
C_2 — exponential wet deposition coefficient (dimensionless), CWASH2=0 in the test

For a case with constant rain and no dry deposition, the solution to Eq. (2-9) is an exponentially decaying function. A plume under rain deposits mass on the ground according to an exponentially decaying function.

The reader is referred to the MACCS Theory Manual for detailed equations. A qualitative derivation is provided in the following description. If ΔQ_j is the deposited inventory on the ground, then the average concentration along the centerline y=0 on the ground is defined as

$$GC(y=0)_j = \frac{\Delta Q_j}{\sqrt{2\pi}\,\sigma_y(x_j)\,L_j} \tag{2-10}$$

$GC(y=0)_j$ — centerline ground concentration for grid element j (Bq/m^2)
ΔQ_j — inventory deposited on the ground for grid element j (Bq)
$\sigma_y(x_j)$ — dispersion coefficient at the x position of grid element j (m)
L_j — length of the grid element j (m)

The MACCS Theory Manual introduces a term denoted as $f_{av,j}$ to account for the plume segment dimensions projected along the ground, and averaged in time. This factor is intended to constrain the amount of inventory carried by the plume available to wet deposition in a specific grid element j. For very long plume segments exceeding the dimensions of a plume element, the $f_{av,j}$ term is simply computed as

$$f_{av,j} = \frac{L_j}{2\,L_s} \tag{2-11}$$

L_j — length of the grid element j (m)
L_s — length of plume segment (m)

For a simple case of constant rain and constant wind direction and speed, the ground deposited inventory ΔQ_j is an exponentially decaying function of the elapsed time since the time of radionuclide release, i.e.,

$$\Delta Q_j = \Delta Q_o\, f_{av,j} \exp\left[-C_1 \left(\frac{I}{I_0}\right)^{C_2} (t - t_o)\right] = \Delta Q_o \frac{L_j}{2\,L_s} \exp\left[-C_1 \left(\frac{I}{I_0}\right)^{C_2} \frac{x_j}{u}\right] \tag{2-12}$$

ΔQ_o — reference ground inventory (Bq)
t_o — plume release time (s)

x_j — x-position of the grid element j (m)
u — wind speed (m/s)

Therefore, for a simple test problem of constant windspeed, long plume, and constant rain of long duration

$$GC(y=0)_j = \frac{\Delta Q_o}{2\ L_s} \frac{\exp\left[-C_1 \left(\frac{I}{I_0}\right)^{C_2} \frac{x_j}{u}\right]}{\sqrt{2\pi}\ \sigma_y(x_j)} \tag{2-13}$$

The ground concentration for grid element j is a Type 6 (centerline concentration) output in the file Model1.out. According to Eq. (2-13), the product $\sigma_y(x_j)\ GC(y=0)_j$ is proportional to $\exp\left[-C_1 \left(\frac{I}{I_0}\right)^{C_2} \frac{x_j}{u}\right]$. Thus, a plot of $\sqrt{2\pi}\ \sigma_y(x)\ GC(y=0)$ versus x should exhibit a linear decay (displayed as a straight line in a log-linear plot).

2.2.1 Test input

The inputs were identical to inputs in the ATMOS Test 2.1 with the following changes

- Weather, Constant or Boundary Conditions
  - BNDMXH (m) = 1000: plume ceiling
  - IBDSTB = 4: stability class
  - **BNDRAN (mm/hr) = 1: rain rate**
  - BNDWND (m/s) = 10: windspeed
- Deposition
  - Wet / Dry Deposition Flags
    - DRYDEP = FALSE for Cs and Ba
    - WETDEP = TRUE for Cs
  - Wet Deposition
    - CWASH1 (1/s) = 10^{-5} (reference value)
    - CWASH2 = 0: makes wet deposition to be independent of the precipitation

Output Controls

- Same output controls of Test 2.1.

2.2.2 Test procedure

Several runs of the MACCS code were executed with different values of CWASH1

- CWASH1 = 0 (0 × reference): case without wet deposition
- CWASH1 = 10^{-6} (0.1 × reference)
- CWASH1 = 10^{-5} (1 × reference)
- CWASH1 = 10^{-4} (10 × reference)
- CWASH1 = 10^{-3} (100 × reference)
- CWASH1 = 10^{-2} (1000 × reference)

Values of the Type 6 centerline concentration were extracted from Model1.out. Per Eq. (2-9) and for the simple system modeled (constant rain, constant windspeed), the air concentration exponentially decays with elapsed time and x distance away from the source. The centerline concentration is computed as

$$\chi_j(x, y = 0, z = 500\ m) = \chi_j^o(x) \exp[-C_1(t - t_o)] = \chi_j^o(x) \exp\left[-C_1 \frac{x}{u}\right] \quad (2\text{-}14)$$

$\chi_j(x, y = 0, z = 500\ m)$ — air concentration along the centerline (Bq-s/m^3)
$\chi_j^o(x)$ — air concentration along the centerline (Bq-s/m^3) for a case with no wet deposition
u — windspeed (m/s), BNDWND=10 m/s in the test

Equation (2-14) does not include any dependence on the rain rate, because it was assumed CWASH2=0. The centerline air concentration $\chi_j^o(x)$ can be computed with a MACCS simulation with C_1=CWASH1=0, or with the methods of the test in Section 2.1.

The test in Section 2.1 demonstrated that the time since the plume release and plume element travel distance x are simply related

$$x = u(t - t_o) \quad (2\text{-}15)$$

t_o — initial time of the release (s), PDELAY=18000 s in the test

The quantity $\chi_j(x, y = 0, z = 500\ m)/\chi_j^o(x)$ was computed using MACCS outputs [Type 6 centerline dose, label Centerline Air Concentration (Bq-s/m3)]. A plot of $\chi_j(x, y = 0, z = 500\ m)/\chi_j^o(x)$ versus x should exhibit exponential decay with a decay rate equal to CWASH1/u.

The quantity $\sigma_y(x)\ GC(y = 0)_j$ was computed using MACCS outputs in the file tbl_outStat.txt for the lateral dispersion coefficient and the ground concentration marked by the labels

- Plume Crosswind Dispersion (m)
- Centerline Air Concentration (Bq-s/m3)

A plot of $\sigma_y(x)\ GC(y = 0)_j$ versus x should exhibit exponential decay with a decay rate equal to CWASH1/u.

2.2.3 Test Results

Figure 2-8 shows $\chi_j(x, y = 0, z = 500\ m)/\chi_j^o(x)$ versus x for different cases of CWASH1. The case legend was the factor applied to the reference CWASH1 = 10^{-5} 1/s. The log-linear plot demonstrates the expected linear decay.

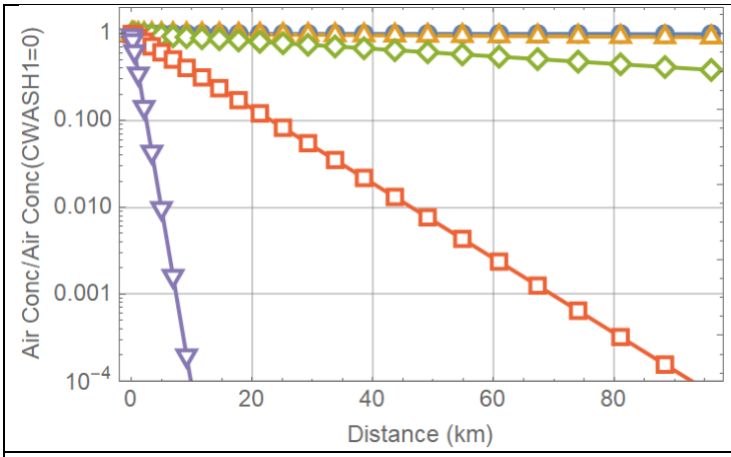

Plot of $\chi_j(x, y = 0, z = 500\ m)/\chi_j^o(x)$ versus downwind distance x for different cases of CWASH1. The case legend was the factor applied to the reference CWASH1 = 10^{-5} 1/s.

The log-linear plot demonstrates the expected exponential decay with distance. The decay rate equals CWASH1/wind speed, as expected.

	Fit	CWASH1 (1/s)	PDELAY (s)
CWASH1 (1/s) =1E-6	$0.0179992 - 9.99967 \times 10^{-7}$ t	9.99967×10^{-7}	17999.8
CWASH1 (1/s) =1E-5	$0.179985 - 9.99919 \times 10^{-6}$ t	9.99919×10^{-6}	18000.
CWASH1 (1/s) =1E-4	$1.79856 - 0.0000999201$ t	9.99201×10^{-5}	18000.
CWASH1 (1/s) =1E-3	$17.8594 - 0.000992183$ t	9.92183×10^{-4}	18000.1
CWASH1 (1/s) =1E-2	$174.047 - 0.0096556$ t	9.6556×10^{-3}	18025.5

The distance was transformed to a travel time using Eq. (2-15) with t_o=PDELAY=18000 s. Then the log of the vertical axis of the previous plot versus time was fit to a straight line, with results of the linear fit on the left table. The CWASH1 values computed from the fit well match the expected values of 10^{-6} 1/s, 10^{-5} 1/s, 10^{-4} 1/s, 10^{-3} 1/s, and 10^{-2} 1/s.

Figure 2-8. Ratio of Air concentration on the centerline to air concentration without wet deposition versus downwind distance, and results of a log-linear fit.

Figure 2-9 displays a plot of $\sqrt{2\,\pi}\,\sigma_y(x)\,GC(y=0)$ versus x for different cases of CWASH1. The case legend was the factor applied to the reference CWASH1 = 10^{-5} 1/s.

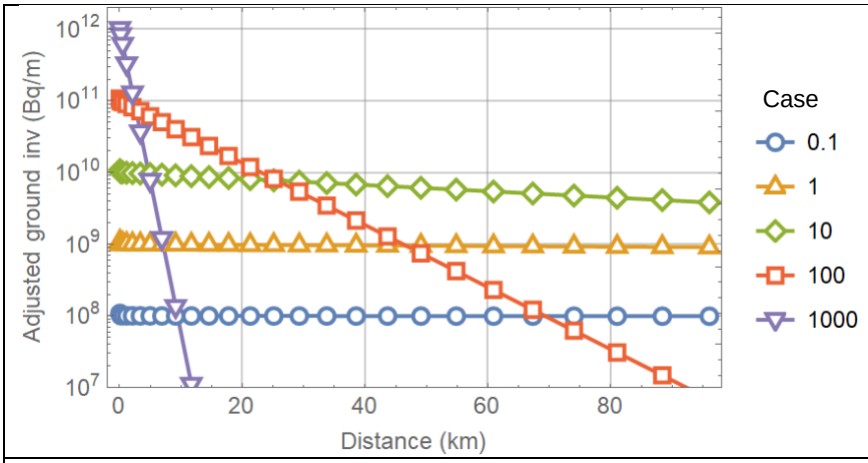

Plot of $\sqrt{2\,\pi}\,\sigma_y(x)\,GC(y=0)$ versus x for different cases of CWASH1. The case legend was the factor applied to the reference CWASH1 = 10^{-5} 1/s.

The log-linear plot demonstrates the expected exponential decay with distance.

The starting point of the different curves at x=0 is precisely spaced by factors of 10.

	Fit	CWASH1 (1/s)
CWASH1 (1/s) =1E-6	$18.4307 - 2.64633\times10^{-6}\,t$	2.64633×10^{-6}
CWASH1 (1/s) =1E-5	$20.7332 - 0.000011628\,t$	1.1628×10^{-5}
CWASH1 (1/s) =1E-4	$23.0358 - 0.000101598\,t$	1.01598×10^{-4}
CWASH1 (1/s) =1E-3	$25.3384 - 0.000998974\,t$	9.98974×10^{-4}
CWASH1 (1/s) =1E-2	$27.6904 - 0.00980354\,t$	9.80354×10^{-3}

The distance of the previous plot was divided by u=10 m/s to compute the elapsed time. Then a straight line was fit to the log of the vertical axis of the previous plot versus time, with results of the linear fit on the left table. The CWASH1 values computed from the fit match well with the expected values of 10^{-5} 1/s, 10^{-4} 1/s, 10^{-3} 1/s, and 10^{-2} 1/s. There is a sizable difference in the case CWASH1 = 10^{-6} 1/s because the corresponding slope is relatively flat, causing significant fitting uncertainty.

	Intercept $\frac{\Delta Q_o}{2\,L_s}$
CWASH1 (1/s) =1E-6	1.01012×10^{8}
CWASH1 (1/s) =1E-5	1.01002×10^{9}
CWASH1 (1/s) =1E-4	1.01×10^{10}
CWASH1 (1/s) =1E-3	1.00998×10^{11}
CWASH1 (1/s) =1E-2	1.06119×10^{12}

The intercepts of the plot at x=0 are spaced by factors of 10, as expected. The intercept equals Q_o CWASH1 u^{-1} (Q_o=plume segment inventory = 10^{15} Bq)

Figure 2-9. Adjusted ground concentration versus downwind distance, results of log-linear fits, and intercept values.

The results in Figure 2-9 and the embedded fit tables indicate that

$$\frac{\Delta Q_o}{2\,L_s} = C_1\left(\frac{I}{I_0}\right)^{C_2}\frac{Q_o}{u} \tag{2-16}$$

Q_o – plume segment inventory (Bq), CORINV=10^{15} Bq in the test
u – windspeed (m/s), BNDWND=10 m/s in the test

The intercept $\frac{\Delta Q_o}{2\ L_s}$ is the activity deposited at the ground per unit of length along the x-direction near the source (x = 0). Equation (2-16) can also be derived as a solution to Eq. (2-9), considering a total constant source Q_o at x=0. The right-hand side of Eq. (2-16) is independent of the plume length and the plume duration. As verification, another test was implemented by executing runs varying the plume length but keeping constant Q_o = 10^{15} Bq and keeping CWASH1 constant. It was verified that results (integrated air concentrations and ground concentrations) are independent of the plume duration (when the only quantity varied is the plume duration), as predicted by Eq. (2-16). Detailed results of that additional test are not included, for brevity.

2.2.4 Test Conclusions

Basic MACCS equations modeling wet deposition were tested, considering a simple case (single plume segment, constant wind speed of constant direction, no dry deposition, constant rain rate). Air concentrations exhibit an exponential decay with downwind distance x, with a decay rate controlled by the rate of wet deposition, as expected. Ground concentrations balance the airborne mass lost and also exhibit an exponential decay with downwind distance x, of the same decay rate as the airborne concentration, as expected.

The MACCS ATMOS module passed the designed tests.

2.3 Test 2.3: Wet Deposition, Variable Plume Duration

Test 2.2 examined a limit case of long-plume duration and constant rain. In that case, at any location the plume undergoes wet deposition. In Test 2.2 it was concluded that the extent of wet deposition was independent of the plume duration if the rain duration was longer than the plume duration.

In this test, a case is examined where the rain is of short duration, and the plume duration is variable (shorter or longer than the rain duration). Per the Test 2.2, wet deposition must be independent of the plume duration when

Rain duration > plume duration

In the other case, Rain duration < plume duration, only a fraction of the plume inventory (the fraction exposed to rain) is subject to wet deposition, and the extent of wet deposition is inversely proportional to the plume duration.

For a case of short rain and plume duration, Eq. (2-16) is modified as

$$\frac{\Delta Q_o}{2\,L_s} = C_1 \left(\frac{I}{I_0}\right)^{C_2} \frac{Q_o}{u} \frac{\min\left(t_p, t_R\right)}{t_p} \tag{2-17}$$

I — rain rate (mm/hr), HRRAIN=1 mm/hr in the test
I_o — reference rain rate (=1 mm/hr)
C_1 — linear wet deposition coefficient (1/s), CWASH1=10^{-3} 1/s in the test
C_2 — exponential wet deposition coefficient (dimensionless), CWASH2=0 in the test
Q_o — plume segment inventory (Bq), CORINV=10^{15} Bq in the test
u — windspeed (m/s), HRWNDV = 10 m/s in the test
t_p — plume duration (s), PLUDUR
t_R — rain duration (s), 1 hr in the test

Equation (2-17) is related to the centerline ground concentration at x=0 as

$$GC(x=0, y=0) = C_1 \left(\frac{I}{I_0}\right)^{C_2} \frac{Q_o}{u} \frac{\min\left(t_p, t_R\right)}{t_p} \frac{1}{\sqrt{2\pi}\,\sigma_y(x=0)} \tag{2-18}$$

$\sigma_y(x=0)$ — initial lateral, across wind, Gaussian dispersion coefficient at the source

2.3.1 Test input

The inputs were identical to inputs in Test 2.2 with the following changes.

General Properties

- WEATHER
  - METCOD=3: user supplied weather

Changes to Specific Input Parameters

- One plume segment: variables NUMREL, PDELAY, PLHITE, REFTIM, PLUDUR
  - PLHITE (m) = 500 m: plume release height (mid distance to ceiling)
  - PLUDUR (s): reference value 80000 s and decreased in factors of 10
  - PDELAY (s) = 0
- User-Supplied Weather
  - HRRAIN (mm/hr) = 1 for one hour, 0 after the first hour
  - HRWND (m/s) = 10 for 120 hours, windspeed
  - HRMXHT (m) = 1000 for 120 hours, plume ceiling
  - IHRSTB (-) = 4 for 120 hours, stability class 4
  - IHRDIR (-) = 1 for 120 hours, wind direction, 1=north direction
- Deposition
  - Wet Deposition
    - CWASH1 (1/s) = 10^{-3} (reference value)

Output Controls

- Same output controls of Test 2.1.

2.3.2 Test procedure

Four runs of the MACCS code were executed, varying the plume duration, PLUDUR. The reference duration was 80000 s, with different runs decreasing PLUDUR in factors of 10.

- PLUDUR = 80000 (1 × reference)
- PLUDUR = 8000 (0.1 × reference)
- PLUDUR = 800 (0.01 × reference), case with plume duration less than the rain duration
- PLUDUR = 80 (0.001 × reference), case with plume duration less than the rain duration

Values of the centerline concentration were extracted from tbl_outStat.txt. The following ratio was computed

$$\frac{\chi_j(x, y = 0, z = 500\ m)}{\chi_j^o(x)} \tag{2-19}$$

$\chi_j(x, y = 0, z = 500\ m)$ — air concentration along the centerline (Bq-s/m^3), from tbl_outStat.txt

$\chi_j^o(x)$ — air concentration along the centerline (Bq-s/m^3), assuming no wet deposition, computed using Eqs. (2-1) and (2-2) of Test 2.1.

According to Test 2.2, the ratio in Eq. (2-19) is an exponentially decaying function of the downwind position x for cases with rain duration longer than the plume duration (cases 0.01 and 0.001 in this test). Per Test 2.2, the decay rate with distance equals CWASH1/HRWNDV. The test was aimed at verifying this expected trend and the magnitude of the decay rate. Wet deposition is restricted to 1 hour (rain duration). After 1 hour, the plume travels 36 kilometers at a speed of 10 m/s. Past 36 km, there must not be any wet deposition (the rain would be over after the plume traveled 36 km).

In a second test, the following quantity was computed

$$\sqrt{2\,\pi}\;\sigma_y(x)\;GC(x, y=0) \tag{2-20}$$

$GC(x, y=0)$ — ground concentration along the centerline (Bq/m^2), from tbl_outStat.txt
$\sigma_y(x)$ — lateral, across wind, Gaussian dispersion coefficient (m), computed using the method described in Test 2.1.

The test focused in verifying that the quantity in Eq. (2-20) is consistent with Eq. (2-18) at x=0. The quantity $\sqrt{2\,\pi}\;\sigma_y(x=0)\;GC(x=0, y=0)$ is inversely proportional to the plume duration, if the plume lasts longer than the rain.

2.3.3 Test results

The results of the tests are presented in Figure 2-10. Expected trends and values were successfully verified. The agreement is reasonable, with differences due to different and detailed numerical integration algorithms implemented in MACCS. The verification computations are only simplified computations, not intended to reproduce the complexity and detail of the MACCS computations.

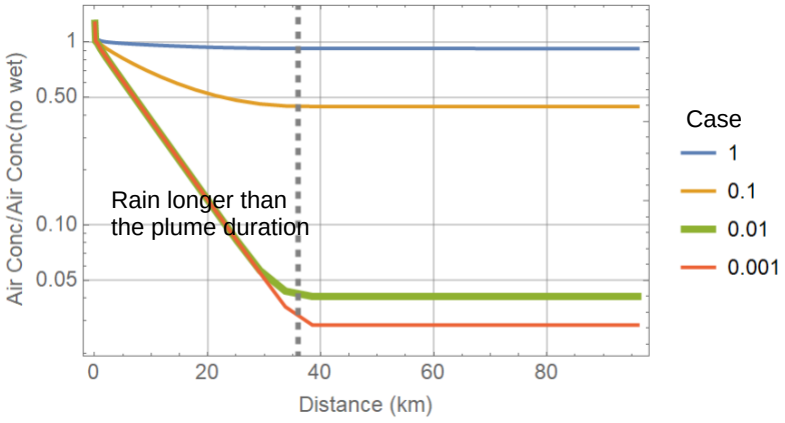

Plot of $\chi_j(x, y = 0, z = 500\ m)/\chi_j^0(x)$ versus x for different cases of the plume duration, PLUDUR. The case legend was the factor applied to the reference PLUDUR = 80,000 s.

The log-linear plot demonstrates the expected exponential decay, for the cases 0.01 and 0.001 (rain duration longer than the plume duration, green and red curves). The decay rate with x distance for those curves is CWASH1/HRWNDV=10^{-3} 1/s/10 m/s = 10^{-4} 1/m, as expected.

The curves become flat after 36 km, because rain only lasts 1 hour and 36 km is the distance traveled by the plume in 1 hour. The cases 1 and 0.1 do not exhibit exponential decay with distance because only a fraction of the plume intercepts the rain, with a fraction that is dependent on the downwind x location.

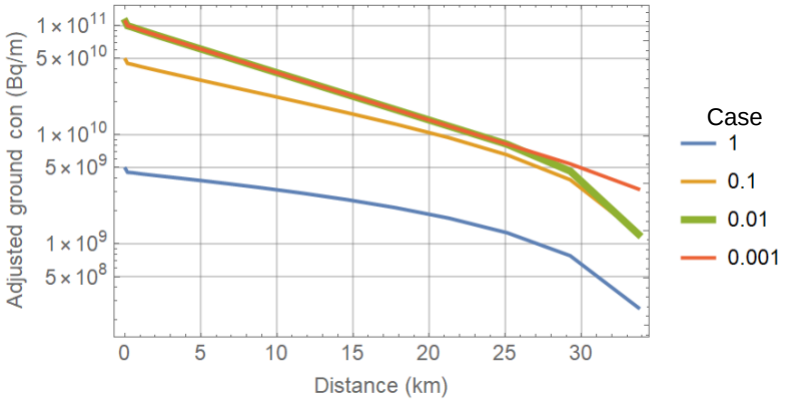

Adjusted ground concentration $\sqrt{2\,\pi}\,\sigma_y(x)\;GC(x, y = 0)$ versus x. For the cases 0.01 and 0.001 (rain duration longer than the plume duration, green and red curves), the curves exhibit exponential decay in most of the downwind distance domain as expected, with a decay rate equal to CWASH1/HRWNDV=10^{-4} 1/m.

The cases 1 and 0.1 do not exhibit exponential decay with distance because only a fraction of the plume intercepts the rain, with a fraction that is dependent on the sector x location.

Case	Intercept	Predicted
1	4.86232×10^9	4.5×10^9
0.1	4.85251×10^{10}	4.5×10^{10}
0.01	1.07687×10^{11}	$1. \times 10^{11}$
0.001	1.07687×10^{11}	$1. \times 10^{11}$

Intercept at x=0 of curves in the previous plot compared to predicted values based on Eq. (2-18). The agreement is reasonable, with differences due to different and detailed numerical integration algorithms implemented in MACCS. The simplified independent computations do not include the details of the MACCS computations.

The test verified that the intercept is inversely proportional to the plume duration for those cases where the plume lasts longer than the rain.

Figure 2-10. Ratio of Air concentration on the centerline to air concentration without wet deposition versus downwind distance; adjusted ground concentration versus downwind distance, and table with y-axis intercepts.

2.3.4 Test Conclusions

The test extended Test 2.2 to examine the effect of plume duration on the extent of ground deposition. Expected exponential decay rates were verified for derived quantities from the centerline air concentration and ground concentration, in the limit when the rain duration is longer than the plume duration. It was verified that the extent of wet deposition is inversely proportional to the plume duration.

The MACCS ATMOS module passed the designed tests.

2.4 Test 2.4: Wet Deposition, Variable Rain Duration

This test examined the effect of variable rain duration on wet deposition. Per Eq. (2-18), for cases with the plume duration longer than the rain, the wet deposition at x=0 is linearly proportional to the rain duration.

2.4.1 Test Input

The inputs were identical to inputs of Test 2.3, with the following changes

- One plume segment: variables NUMREL, PDELAY, PLHITE, REFTIM, PLUDUR
  - PLUDUR (s) = 86400 s (=24 hours)
  - PDELAY (s) = 0
- User-Supplied Weather
  - HRRAIN (mm/hr) = 1 for 1, 5, 10, 15, 25, and 30 hours

Output Controls

- Same output controls of Test 2.1.

2.4.2 Test procedure

Six runs of the MACCS code were executed, varying the rain duration using HRRAIN inputs in the user-supplied weather. The user-supplied weather requires 120 hourly inputs. The hourly inputs were modified to attain a target rain duration, considering 6 cases:

- 1 hour
- 5 hours
- 10 hours
- 15 hours
- 25 hours (plume duration < rain duration)
- 30 hours (plume duration < rain duration)

The ratio defined in Eq. (2-19) was computed from data in tbl_outStat.txt, and the air concentration along the centerline, assuming no wet deposition, using Eqs. (2-1) and (2-2) of Test 2.1. According to Test 2.2, the ratio in Eq. (2-19) is an exponentially decaying function of the downwind distance x for cases with rain duration longer than the plume duration (cases 25 and 30 hours in this test). Per Test 2.2, the decay rate with distance equals CWASH1/HRWNDV = 10^{-4} 1/m for the cases 25 and 30 hours. For other cases (cases 1 to 15 hours), the ratio in Eq. (2-19) is not an exponentially decaying function of x; however, an exponential decay should be a reasonable approximation, with a decay rate that is proportional to 10^{-4} 1/m and to the ratio (rain duration)/(plume duration).

A second test was performed, computing the adjusted concentration in Eq. (2-20) as a function of x. For cases with rain duration longer than the plume duration (cases 25 and 30 hours in this test), the adjusted concentration must be an exponentially decaying function of x with decay rate equal to CWASH1/HRWNDV = 10^{-4} 1/m.

Per Eq. (2-18) at x=0, the quantity $\sqrt{2\,\pi}\,\sigma_y(x=0)\,GC(x=0,y=0)$ is directly proportional to the rain duration when the rain duration is less than the plume duration. The Test 2.4 verified this proportionality.

2.4.3 Test results

Results of the tests are presented in Figure 2-11 and Figure 2-12.

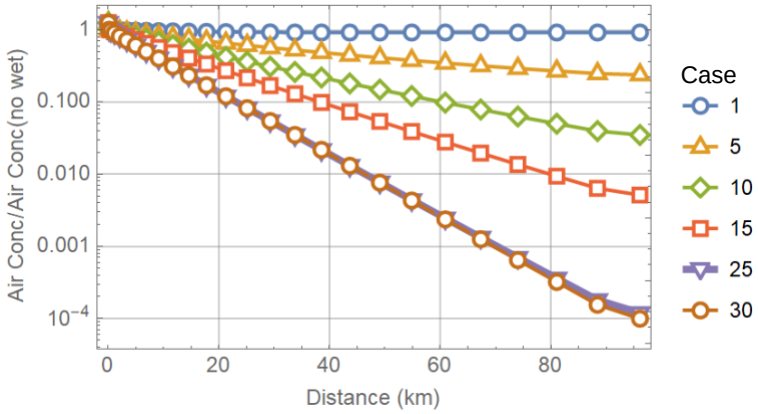

Plot of $\chi_j(x, y=0, z=500\,m)/\chi_j^o(x)$ versus x for different cases of the rain duration. The case legend was the rain duration in hours. The plume duration, PLUDUR, was 24 hours.

The log-linear plot demonstrates the expected exponential decay, for the cases 25 and 30 hours (rain duration longer than the plume duration). The decay rate with x distance for those bottom curves is CWASH1/HRWNDV=10^{-3} 1/s / 10 m/s = 10^{-4} 1/m, as expected.

The cases 1 to 15 hours can be well approximated with exponential decay. The computed decay rate is presented in the next entry.

Case	Decay rate (1/m)	Predicted
1	1.3×10^{-6}	4.2×10^{-6}
5	0.000016	0.000021
10	0.000037	0.000042
15	0.000057	0.000063
25	0.000097	0.0001
30	0.000099	0.0001

Decay rate computed as a log-linear fit, and decay rate predicted as

$$10^{-4}\ 1/\mathrm{m}\,\frac{\min(t_p, t_R)}{t_p}$$

with t_p = plume duration and t_R = rain duration. The agreement is reasonable given simplifications adopted in the test (the independent computations do not reproduce all details of the MACCS computations).

The test demonstrates that the rain duration is accounted for in the MACCS numerical integrals defining the span of active wet deposition.

Figure 2-11. Ratio of air concentration on the centerline to the air concentration without wet deposition versus downwind distance, and effective decay rate computed with a log-linear fit.

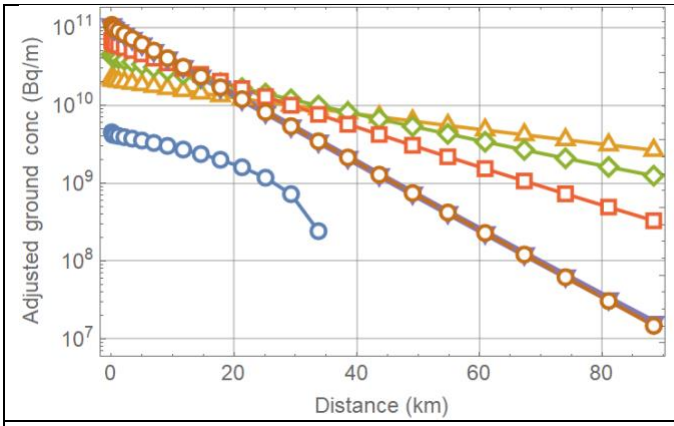

Adjusted ground concentration $\sqrt{2\,\pi}\,\sigma_y(x)\,GC(x, y=0)$ versus x. For the cases 25 and 30 hours (rain duration longer than the plume duration), the curves exhibit exponential decay with downwind distance, with an expected decay rate equal to CWASH1/HRWNDV=10^{-4} 1/m.

The other cases can be approximated as exponential decay functions, of decay rates identical to rates computed in the previous figure.

Case	Intercept (Bq/m)	Predicted
1	4.5×10^{9}	4.17×10^{9}
5	2.25×10^{10}	2.08×10^{10}
10	4.5×10^{10}	4.17×10^{10}
15	6.74×10^{10}	6.25×10^{10}
25	1.08×10^{11}	$1.\times10^{11}$
30	1.08×10^{11}	$1.\times10^{11}$

Intercept at x=0 of curves in the previous plot compared to predicted values based on Eq. (2-18). The agreement is reasonable, with differences due to different and detailed numerical integration algorithms implemented in MACCS. The verification computations are only simplified computations, not intended to reproduce the complexity and details of the MACCS computations.

The test verified that the intercept is proportional to the rain duration for those cases where the plume lasts longer than the rain.

Figure 2-12. Adjusted ground concentration versus downwind distance, results of log-linear fits, and table with y-intercept values.

2.4.4 Test Conclusions

The test extended Test 2.2 to examine the effect of rain duration on the extent of ground deposition. Expected exponential decay rates were verified for derived quantities from the centerline air concentration and ground concentration, in the limit when the rain duration is longer than the plume duration. It was verified that the extent of wet deposition is proportional to the rain duration when the plume lasts longer than the rain. The test demonstrated that the rain duration is accounted for in the MACCS numerical integrals defining the span of active wet deposition.

The MACCS ATMOS module passed the tests.

2.5 Test 2.5: Dry Deposition, Variable Speed

The objective of the test was to verify implementation of dry deposition equations, examining a simple case. For a single particle size, dry deposition is controlled by the equation 2-39 of the MACCS Theory Manual (Nosek, et al., 2021):

$$\frac{dQ}{dt} = -\frac{v_d}{\bar{z}(x)}\, Q \tag{2-21}$$

$$\frac{1}{\bar{z}(x)} = \frac{1}{\bar{z}(u\ t)} = \frac{\psi(x, z=0)}{\int_0^H \psi(x,z)\, dz} \tag{2-22}$$

Q — airborne activity (Bq)
v_d — vertical dry deposition velocity (m/s)
$\psi(x,z)$ — term defined by Eq. (2-2) (1/m)
$\bar{z}(x)$ — reference distance (m) [$1/\bar{z}(x)$ is a measurement of the plume spread along the vertical direction]
u — windspeed (m/s), HRWNDV = 10 m/s in the test
t — time measured since the plume release (s)
H — plume ceiling, maximum plume height (m), HRMXHT = 1000 m in the test

The general solution to Eq. (2-21) is

$$\frac{Q_1}{Q_o} = \exp\left[-v_d \int_0^t \frac{d\tau}{\bar{z}(u\ \tau)}\right] \tag{2-23}$$

Q_1 — airborne activity exiting a sector (Bq)
Q_o — airborne activity entering a sector (Bq)
t — relative time for a plume segment to cross a sector (s) (=sector length/u)

Equation (2-23) is a generalization of Eq. (2.40) of the MACCS Theory Manual. It is assumed in MACCS that dry deposition does not change the vertical distribution of the radioactive concentration. Therefore, Eq. (2-23) can be generalized for the computation of centerline concentrations (concentrations along the line y=0):

$$\frac{\chi_1(x = u\ t, y=0, z)}{\chi(x = u\ t, y=0, z)} = \exp\left[-v_d \int_0^t \frac{d\tau}{\bar{z}(u\ \tau)}\right] \tag{2-24}$$

$\chi_1(x,y,z)$ — integrated airborne concentration (Bq-s/m^3)
$\chi(x,y,z)$ — integrated airborne concentration (Bq-s/m^3) assuming no dry deposition, defined by Eqs. (2-1) and (2-2)
t — arbitrary time measured from the time of the plume release

The centerline ground concentration is computed as

$$GC(x = u\ t, y=0) = \chi_1(x = u\ t, y=0, z=0) v_d \tag{2-25}$$

$GC(x = u\ t, y=0)$ — centerline ground concentration (Bq/m^2)

The objective of the test was verifying that independently computed concentrations using Eqs. (2-24) and (2-25) agree with corresponding concentrations output in the file tbl_outStat.txt.

2.5.1 Test Input

Inputs were selected to simulate a single plume segment of constant speed (HRWNDV =10 m/s), constant wind direction (blowing north), only dry deposition (i.e., no wet deposition), one single long-lived radionuclide (Cs-137), and one particle size. The same input of Test 2.4 was used, with the following changes

- Deposition
    - Wet / Dry Deposition Flags
        - DRYDEP = TRUE for Cs
        - WETDEP = FALSE for Cs
    - Dry Deposition
        - VDEPOS (m/s) = 1 (reference value) for particle group 1, and 0 for other groups
- Release Description
    - Particle Size Distribution
        - PSDIST=1 for particle group 1, 0 for all other groups

- Weather / User-Supplied Weather
    - Constant weather for 120 hours
    - HRMXHT (m) = 1000
    - IHRSTB (-) = 4 (stability class 4 = D class, neutral class)
    - HRRAIN (mm/hr) = 0 (no rain)
    - HRWND (m/s) = 10
    - IHRDIR (-) = 1 (wind blowing in the north direction)

Output Controls

- Same output controls of Test 2.1.

2.5.2 Test Procedure

Individual runs of the MACCS code were executed varying only VDEPOS

- VDEPOS = 0 m/s
- VDEPOS = 0.01 m/s
- VDEPOS = 0.1 m/s
- VDEPOS = 0.3 m/s
- VDEPOS = 1 m/s
- VDEPOS = 10 m/s

The centerline air concentration, air concentration at the ground level, and ground concentration were extracted from the file tbl_outStat.txt, from outputs labeled

- Centerline Air Concentration (Bq-s/m3)
- Ground-Level Air Concentration (Bq-s/m3)
- Centerline Ground Concentration (Bq/m2)

The outputs were compared to results computed using Eqs. (2-24) and (2-25).

2.5.3 Test Results

Test results are presented in Figure 2-13.

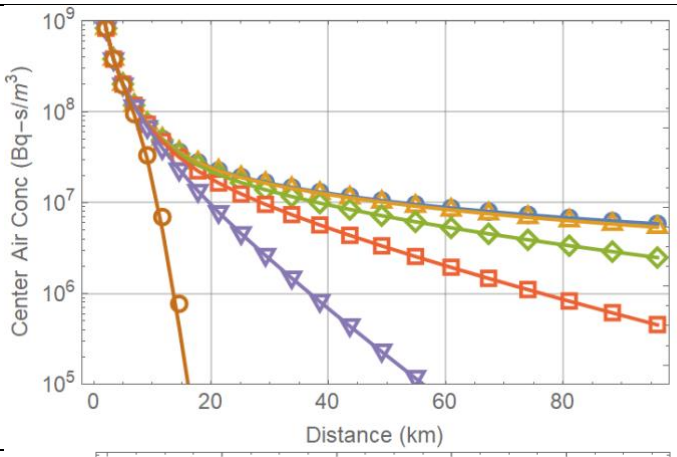

Plume centerline air concentration (z=500 m) versus downwind distance. The symbols represent MACCS data from the file tbl_outStat.txt, the solid curves were independently computed using Eq. (2-24) with z=500 m.

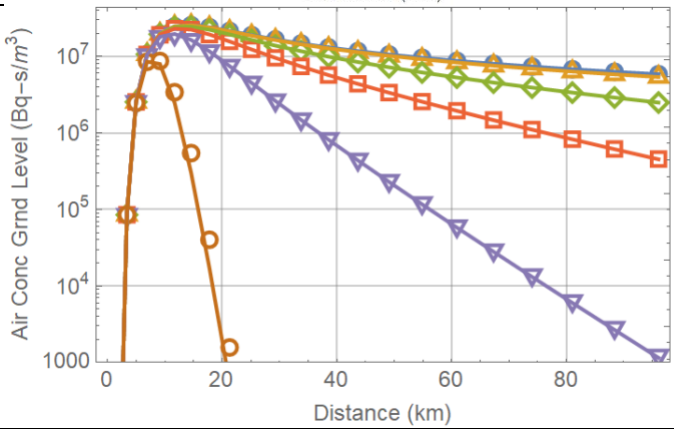

Centerline air concentration at the ground level (z=0 m) versus downwind distance. The symbols represent MACCS data from the file tbl_outStat.txt, the solid curves were independently computed using Eq. (2-24) z=0 m.

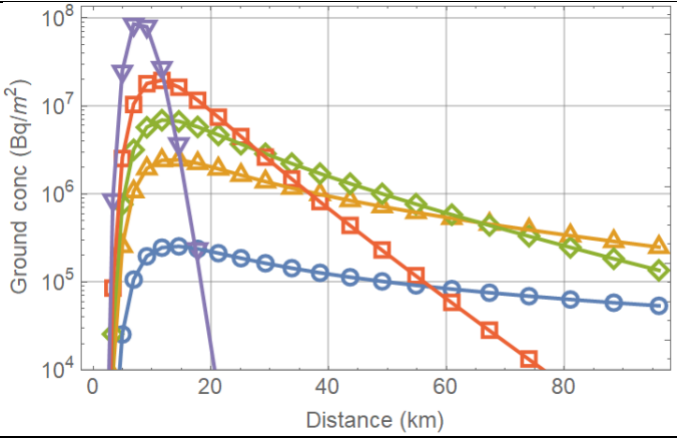

Ground concentration versus downwind distance. The symbols represent MACCS data from the file tbl_outStat.txt, the solid curves were independently computed using Eq. (2-25).

Figure 2-13. Centerline air concentration at y=500 m and at y=0 m, and centerline ground concentration versus downwind distance.

2.5.4 Test Conclusions

Concentrations independently computed successfully reproduced the MACCS concentrations under dry deposition.

3 EARLY MODULE

3.1 Test 3.1: Groundshine, Inhalation, Cloudshine, and Skin Dose

The objective of the test was to verify equations to compute individual doses from concentrations and given dose rate coefficients for simple cases. The simple case considered is summarized in the following bullets:

- One radionuclide, Cs-137
- One long-lasting plume segment, without plume rise
- Simple weather pattern: constant windspeed (10 m/s), north direction
- One cohort, non-evacuating and non-relocating

The groundshine, inhalation, cloudshine, and skin dose equations that were examined in the test are presented in the following paragraphs.

Groundshine dose (equation 3-10 of the MACCS Theory Manual):

$$GDR_k = \left(\sum_i DRCG_{ik}\ GC_i\ T_i \right) J\ SFG \tag{3-1}$$

GDR_k	—	sector average groundshine dose rate to organ k (Sv)
$DRCG_{ik}$	—	groundshine dose rate coefficient to organ k by radionuclide i (Sv-m^2/Bq-s)
GC_i	—	ground concentration along the plume centerline (Bq/m^2)
T_i	—	effective exposure time (s)
J	—	off-centerline factor to compute the sector average from the centerline dose
SFG	—	Groundshine shielding factor, specified by GSHFAC (=0 or 1 in the test runs)

The effective exposure time T_i accounts for linear buildup in time while the plume is passing, and radioactive decay while and after the plume passage. For the simple problem examined of a fast-moving plume, non-evacuating and non-relocating cohort, and a long-lived radionuclide, the effective exposure time is approximately equal to the duration of the early phase, specified by ENDEMP (=7 days in the test runs).

Inhalation dose (equation 3-12 of the MACCS Theory Manual):

$$DI_k = \left(\sum_i DCI_{ik}\ \chi_i(x, y = 0, z = 0) \right) BR\ J\ F\ SFI \tag{3-2}$$

DI_k	—	sector average inhalation dose to organ k from passage of a plume (Sv)
DCI_{ik}	—	inhalation dose coefficient to organ k from radionuclide i (Sv/Bq)
$\chi_i(x, y = 0, z = 0)$	—	integrated air concentration of radionuclide i at the ground level, along the plume centerline (Bq-s/m^3), Eq. (2-1) and (2-2)
BR	—	air breathing rate, specified by BRRATE (m^3/s) (BRRATE = 10^{-4} m^3/s in the test runs)

J	—	off-centerline factor to compute the sector average from the centerline dose
F	—	fraction of exposed time (=1 for non-evacuating and non-relocating cohort)
SFI	—	inhalation shielding factor, specified by PROTIN (=0 or 1 in the test runs

Cloudshine dose (equation 3-9 of the MACCS Theory Manual):

$$DC_k = \left[\sum_i DRCC_{\infty ik}\ \chi_i(x, y=0, z=h)\right] C(x,y)\ F\ SFC \tag{3-3}$$

DC_k	—	cloudshine centerline dose to organ k (Sv)
$DRCC_{\infty ik}$	—	semi-infinite cloudshine dose coefficient to organ k by radionuclide i (Sv-m^3/Bq-s)
$\chi_i(x, y=0, z=h)$	—	integrated air concentration of radionuclide i at the center level (y=h), along the plume centerline (Bq-s/m^3), Eq. (2-1) and (2-2)
$C(x,y)$	—	cloudshine factor at the location (x, y), which is a function of the plume height, h, and the dispersion coefficients $\sigma_y(x)$ and $\sigma_z(x)$
F	—	plume exposure time fraction (=1, for non-evacuating and non-relocating individuals)
SFC	—	cloudshine protection factor specified by CSFACT (=0 or 1 in the test runs)

Skin acute dose (derived from equations 3-15 and 3-16 of the MACCS Theory Manual, assuming a slow decay rate):

$$DS = T\ DRCS\ \ V_d\ J\ F\ SFS \sum_i \chi_i(x, y=0, z=0) \tag{3-4}$$

DS	—	sector average acute dose from skin deposition during passage of a plume (Sv)
T	—	exposure time, fixed to 8 hours = 28800 s in MACCS
$DRCS$	—	acute skin dose coefficient from deposition of radioactive contaminants on the skin, fixed to 5.4×10^{-14} Sv-m^2/Bq-s in MACCS, independently of the radionuclide
V_d	—	deposition velocity, fixed to 0.01 m/s in MACCS
J	—	off-centerline factor to compute the sector average from the centerline dose
F	—	fraction of the exposure duration during the plume passage, set to 1 in the test runs (due to no relocation and no evacuation assumptions)
SFS	—	skin shielding factor, specified by SKPFAC (=0 or 1 in the test runs)
$\chi_i(x, y=0, z=0)$	—	integrated air concentration of radionuclide i at the ground level, along the plume centerline (Bq-s/m^3), Eq. (2-1) and (2-2)

The MACCS computation of the air concentrations $\chi_i(x, y=0, z=h)$, $\chi_i(x, y=0, z=0)$, and centerline ground concentration GC_i were verified in the ATMOS module tests in Section 2. The same methods of Section 2 were applied to provide additional verification of concentration computations.

In the tests, doses were independently computed from Type 0 and Type D concentrations and compared to the Type 6 and Type C doses. The Type 0 and Type D concentrations were already verified for central sectors (sectors in the north direction in the tests) in Section 2 tests based on analytical steady-state Gaussian plume concentration equations, and equations to model dry and wet deposition.

3.1.1 Test Input

The input was similar to the Test 2.1 input with the following changes:

- One plume segment: variables NUMREL, PDELAY, PLHITE, REFTIM, PLUDUR
  - PLUDUR (s) = 86400 s (=24 hours)
  - PDELAY (s) = 0
- Deposition
  - Wet / Dry Deposition Flags
    - DRYDEP = TRUE for Cs
    - WETDEP = FALSE for Cs
  - Dry Deposition
    - VDEPOS (m/s) = 0.3 m/s for particle group 1, and 0 for other groups
- Release Description
  - Particle Size Distribution
    - PSDIST=1 for particle group 1, 0 for all other groups

Output Controls

Same outputs Test 2.1 were used, with the following additional outputs:

- Type D (NUMD) Average Sector Concentrations
  - I1DISD = 26 (outer radial interval)
  - NUCLIDE = Cs-137
  - ELEVCONC (Bq/m^2) = 0 (threshold value, all sectors are reported when 0)
  - PRINT_FLAG_D = True
  - Report Options = REPORT

For the skin acute dose tests, additional outputs were generated with the following settings:

- Type 6 (NUM6) Centerline Dose
  - ORGNAM = A-SKIN (acute skin dose)
  - PATHNM = TOT ACU
  - I1D1S6 = 1
  - I2DIS6 = 26
  - Report Options = NONE
- Type A (NUMA) Peak Dose
  - NAME = A-SKIN
  - I1DISA = 1
  - I2DISA = 26
  - Report Options = NONE
- Type C (NUMC) Land Area Exceeding Dose
  - ORGNAM = A-SKIN
  - ELEVDOSE (Sv) = 0

- PRINT_FLAG_C = True
- Report Options = NONE

For the groundshine, inhalation, and cloudshine dose tests, the extracted doses from the MACCS output files corresponded to ORGNAM = L-ICRP60ED. For the skin acute dose test, the dose extracted from the MACCS output files corresponded to ORGNAM = A-SKIN.

3.1.2 Test Procedure

Multiple runs of the MACCS code were executed with the following selections of the Gaussian dispersion coefficient factors:

- YSCALE = ZSCALE = 0.1
- YSCALE = ZSCALE = 0.5
- YSCALE = ZSCALE = 1
- YSCALE = ZSCALE = 2

The shielding and exposure factors were set to output groundshine dose only (GSHFAC=1, other shielding factors = 0), inhalation dose only (PROTIN=1, other shielding factors = 0), cloudshine dose only (CSFACT=1, other shielding factors = 0), or skin dose only (SKPFAC=1, other shielding factors = 0).

A total of 16 runs (= 4 dispersion coefficient factors × 4 shielding factor selections) were executed. Different runs with a specific value of the dispersion coefficient factor correspond to cases with identical air and ground concentrations (the only difference of runs with the same dispersion coefficient is the type of dose tracked in the output files). A total of 4 runs for each dispersion coefficient factor were executed to itemize the different pathway doses (groundshine, inhalation, cloudshine, or skin) in the MACCS outputs.

Air and ground concentrations were extracted from the file tbl_outStat.txt and compared to independently computed concentrations using closed-form analytical equations from Section 2. In addition, those concentrations were compared to

- Type 0 concentrations, air and ground concentrations along the centerline
- Type D concentrations, sector average air concentration at the ground level and sector average ground concentration

The off-centerline factor *J* was verified by computing the ratio Type D concentration/Type 0 concentration (= *J* factor), and comparing the ratio to independently computed values of *J* computed based on line integrals along constant radius arcs.

Multiplying appropriate dose coefficient and exposure factors by the Type 0 and Type D concentrations, alternative dose estimates were computed, which were compared to the Type 6 dose (centerline dose) and Type C dose (sector average dose).

In addition, the Type A dose (peak dose) was compared to the Type 6 dose (centerline dose). The following inequality must be true

$$\text{Type A dose} < \text{Type 6 dose}$$

Violation of that inequality reveals artefacts in the MACCS computations. In initial testing with MACCS Version 4.0, it was found that the inequality was violated for broad plume cases. In discussing with MACCS software developers, it was concluded that the anomalous result was due to failing to constrain the lateral plume domain to $\pm 2.15\ \sigma_y$ around the plume centerline. In MACCS Version 4.1, the appropriate lateral constraints were implemented and, in addition, runs with extremely large values of σ_y are not permitted. These changes fixed anomalies identified in testing of MACCS Version 4.0.

3.1.3 Test Results

Figure 3-1 shows MACCS concentrations from the tbl_outStat.txt output files (symbols), compared to concentrations computed using Eqs. (2-1), (2-2), and (2-24) with $N=20$ in the series in Eq. (2-2) (solid curves). The agreement between the MACCS outputs and the independently computed concentrations was excellent. The legends represent the value input for YSCALE = ZSCALE (scale factor for the Gaussian dispersion coefficients). This test provides additional verification of air and ground concentration computations, based on steady-state Gaussian plume concentration equations and equations to model dry deposition, complementing Test 2.5.

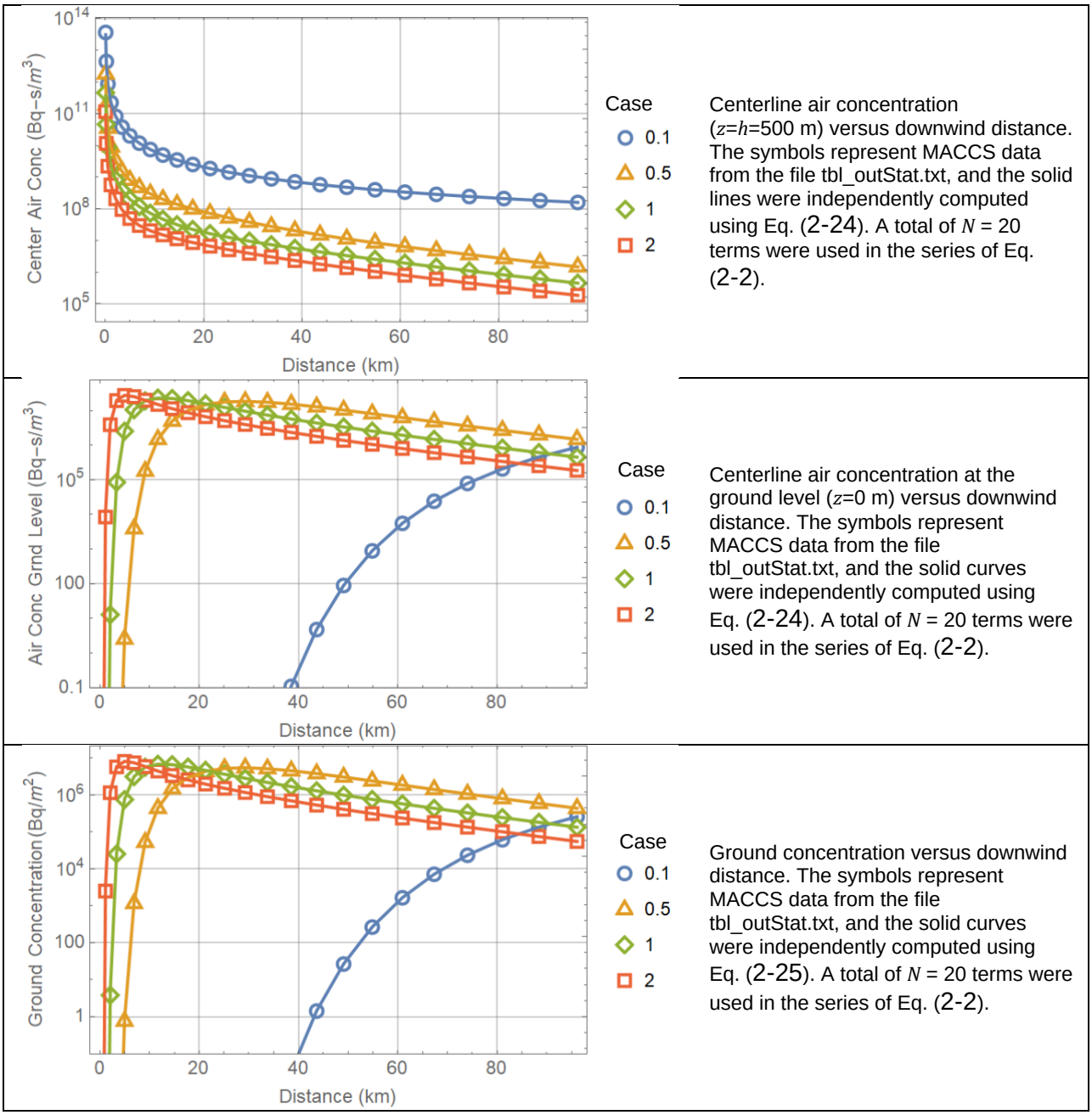

Figure 3-1. Centerline air concentration at a height, z=500 m and at z=0 m (ground level), and centerline ground concentration versus downwind distance; comparison of MACCS outputs to independent computations. Four cases were considered: YSCALE = ZSCALE = 0.1, 0.5, 1, and 2.

Figure 3-2 compares concentrations in the output file tbl_outStat.txt (symbols) to Type 0 concentrations in Model1.out output file. The concentrations in both output files are identical, as expected.

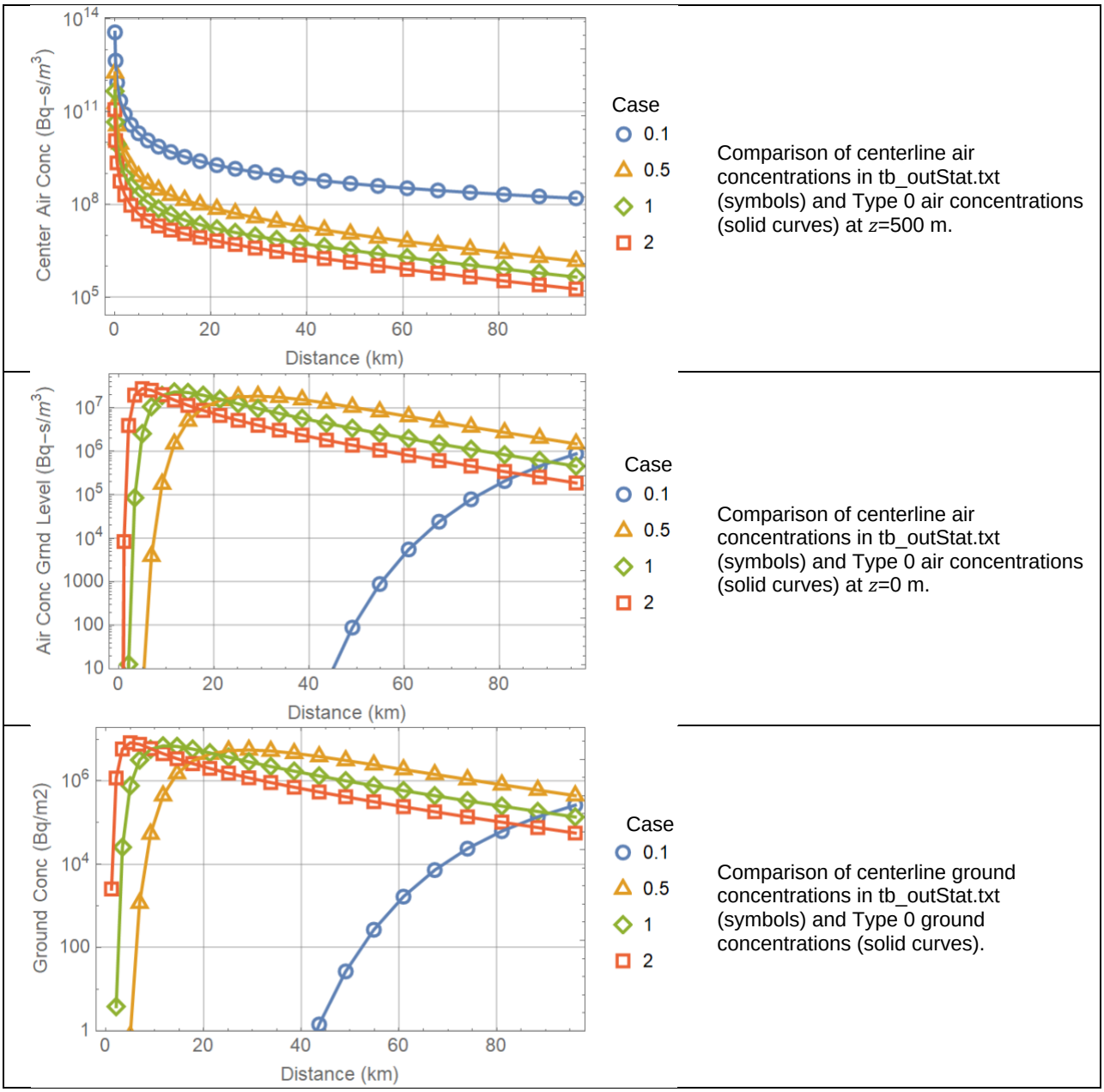

Figure 3-2. Centerline air concentration at a height, z=500 m and at z=0 m (ground level), and centerline ground concentration versus downwind distance; comparison of MACCS outputs in tbl_outStat.txt to Type 0 outputs in Model1.out. Four cases were considered: YSCALE = ZSCALE = 0.1, 0.5, 1, and 2.

Figure 3-3 compares Type 0 centerline air and ground concentrations (solid curves), to Type D sector average air and ground concentrations (dashed curves). As expected, Type D (sector average) < Type 0 (centerline). The ratio Type D/Type 0 is equivalent to the off-centerline factor J of the central grid sector. The off-centerline factor was independently computed as the average of the normal distribution function of 0 mean and $\sigma_y(r)$ standard deviation, over an arc of constant radius r spanning an angle θ from $-\pi/16$ to $\pi/16$ (the angle θ

is measured with respect to the north direction), divided by the center value of the normal distribution (i.e., normal distribution evaluated at y=0 or angle θ=0). The small-angle approximation in Eq. (2-8) was adopted to transform Cartesian coordinates to polar coordinates. In Figure 3-3, the independently computed value of the off-centerline factor as a function of the downwind distance is in excellent agreement with the Type D/Type 0 concentration ratio.

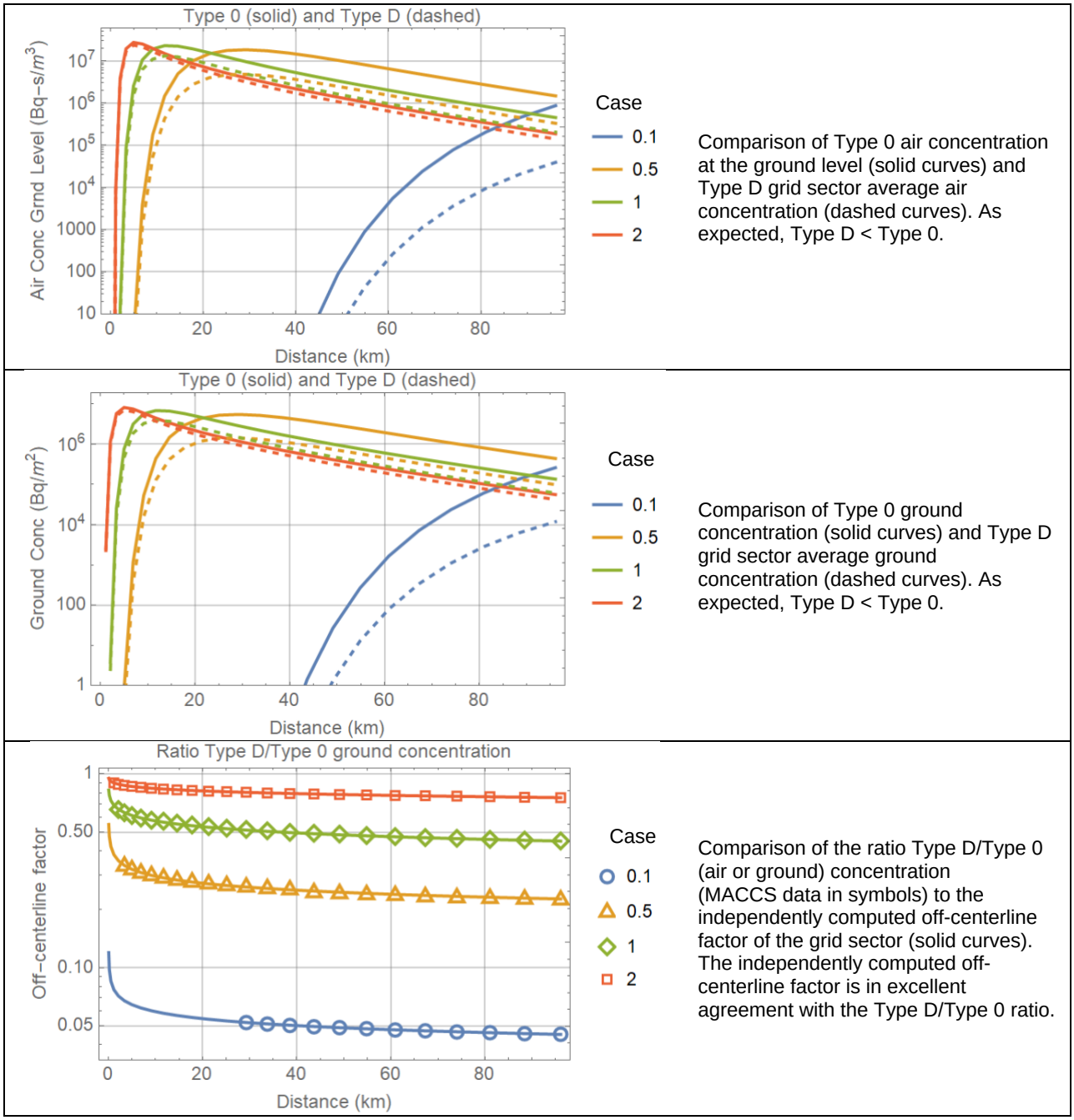

Figure 3-3. Comparison of Type 0 (solid curves) to Type D sector average concentrations (dashed curves), including centerline air concentration at the ground level (z=0) and centerline ground concentration. The bottom plot is the off-centerline factor *J* (MACCS data in symbols, independent computations in solid curves) versus the downwind distance.

The following tests verify dose outputs. A specific dose pathway output (groundshine, inhalation, cloudshine, or skin) was produced by a MACCS run by setting the appropriate shielding factor to 1 (GSHFAC, PROTIN, CSFACT, SKPFAC) and the complementary factors set to zero.

Groundshine Dose

The test verified that the groundshine dose is computed by MACCS according to Eq. (3-1). In Figure 3-4, groundshine doses (Type 6 centerline and Type C average) were compared to doses independently computed from ground concentrations (Type 0 and Type D), the Cs-137 dose coefficient for groundshine ($DRCG_{ik} = 2.99 \times 10^{-18}$ Sv-m^3/Bq-s), and $T_i \approx 6.048 \times 10^5$ seconds ignoring radioactive decay (=7 days —assumed duration of the EARLY emergency response period). The MACCS groundshine dose outputs were in excellent agreement with the independently computed groundshine doses.

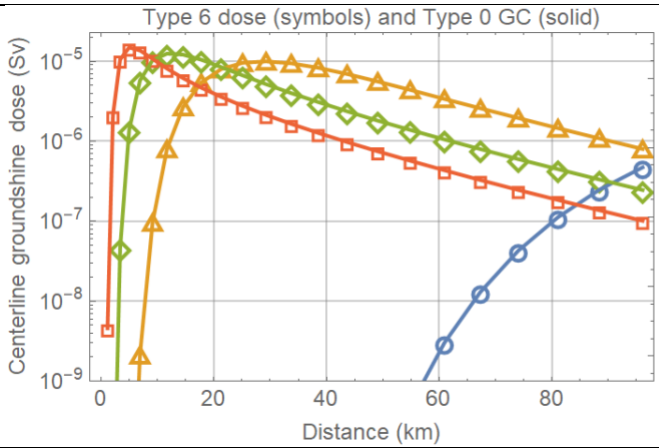

Comparison of Type 6 centerline groundshine dose (symbols) to independently computed doses using the Type 0 centerline ground concentration (solid curves).

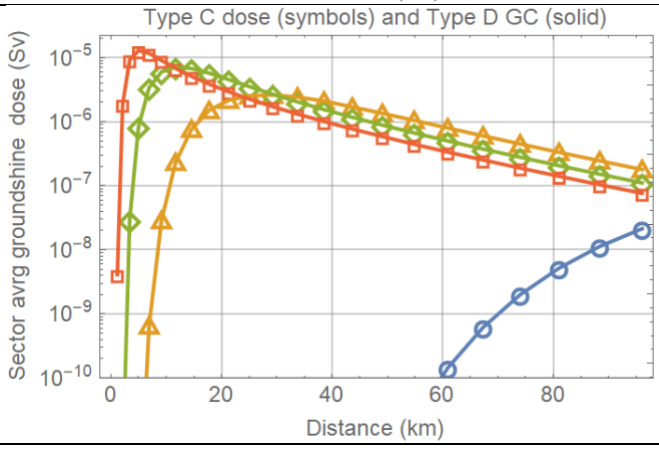

Comparison of Type C grid sector average (north sectors) groundshine dose (symbols) to independently computed doses using the Type D sector average ground concentration of north sectors (solid curves).

Figure 3-4. Centerline groundshine dose, and sector-average groundshine dose (north sector) versus downwind distance.

The Type 6 centerline groundshine dose was compared to the Type A grid sector maximum groundshine dose. It is expected that

Type A groundshine dose ≤ Type 6 centerline dose

The Type A groundshine dose and the Type 6 centerline dose should differ by the off-centerline factor, which is approximately equal to 1 for well spread plume cases (e.g., cases 1 and 2). The comparison is displayed in Figure 3-5. As expected, the Type A doses are below Type 6 doses. For the Case 2, the solid and dashed curves almost overlap in Figure 3-5.

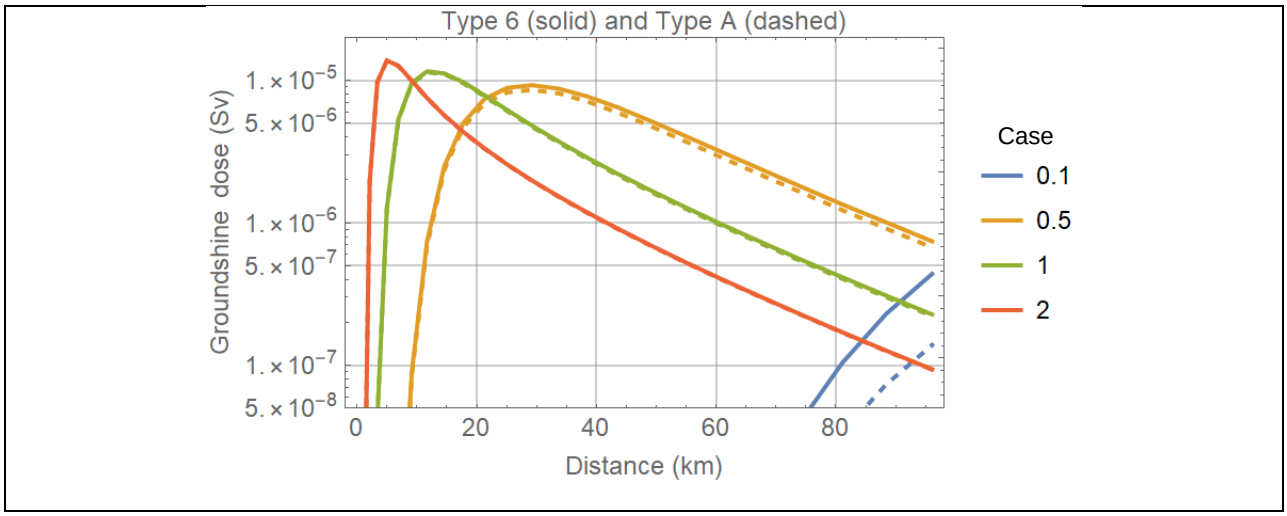

Figure 3-5. Comparison of the Type 6 centerline groundshine dose (solid curves) to the Type A maximum dose (dashed curves).

Inhalation Dose

The test verified that the inhalation dose is computed by MACCS according to Eq. (3-2). Inhalation doses (Type 6 and Type C) were compared to doses independently computed from air concentrations at the ground level (Type 0 and Type D), the Cs-137 dose coefficient for inhalation ($DCI_{ik} = 4.88 \times 10^{-9}$ Sv/Bq), and the input breathing rate BRRATE $= BR = 10^{-4}$ m^3/s. Figure 3-6 shows that MACCS inhalation dose outputs were in excellent agreement with the independently computed inhalation doses.

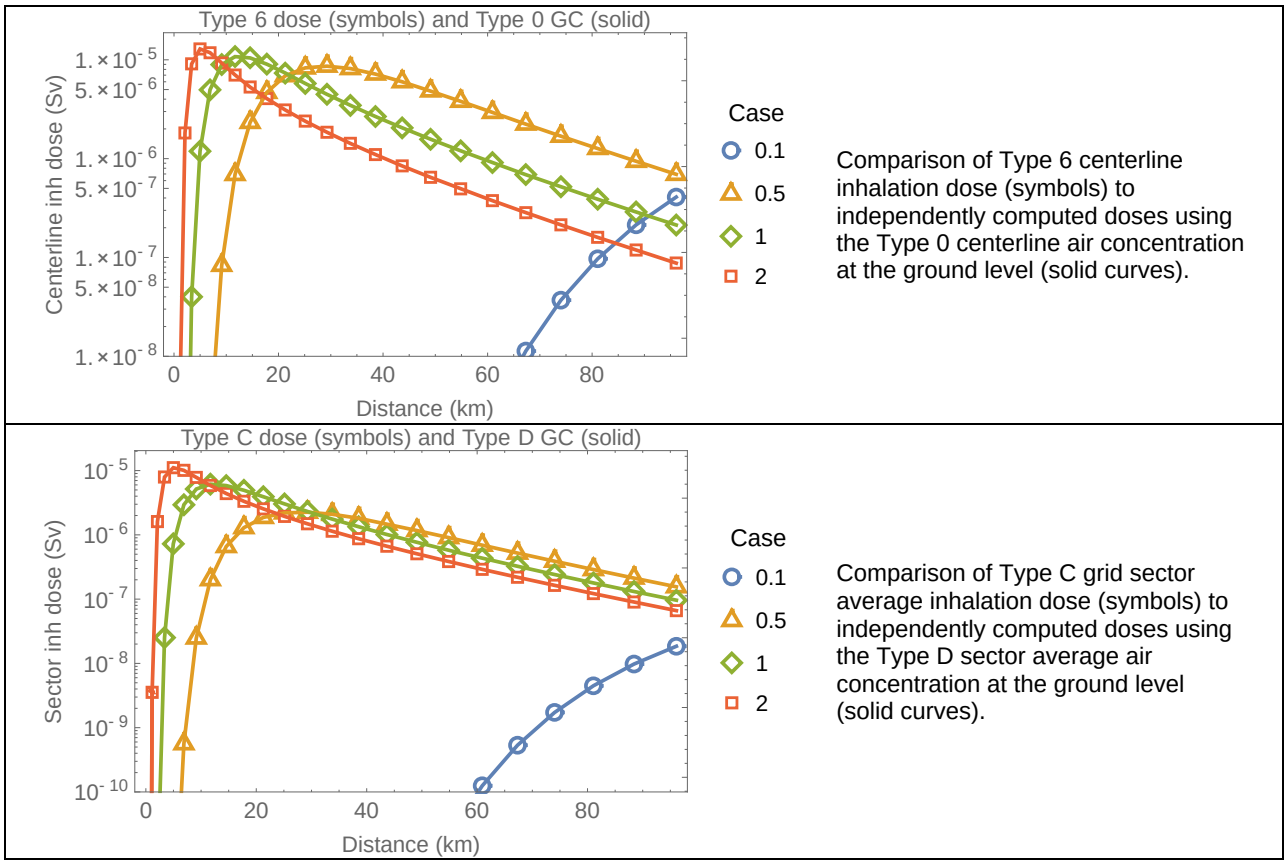

Figure 3-6. Centerline inhalation dose, and sector-average inhalation dose (north sector) versus downwind distance.

The Type 6 centerline inhalation dose was compared to the Type A grid sector maximum inhalation dose in Figure 3-7. The test verified that

$$\text{Type A inhalation dose} \leq \text{Type 6 centerline dose}$$

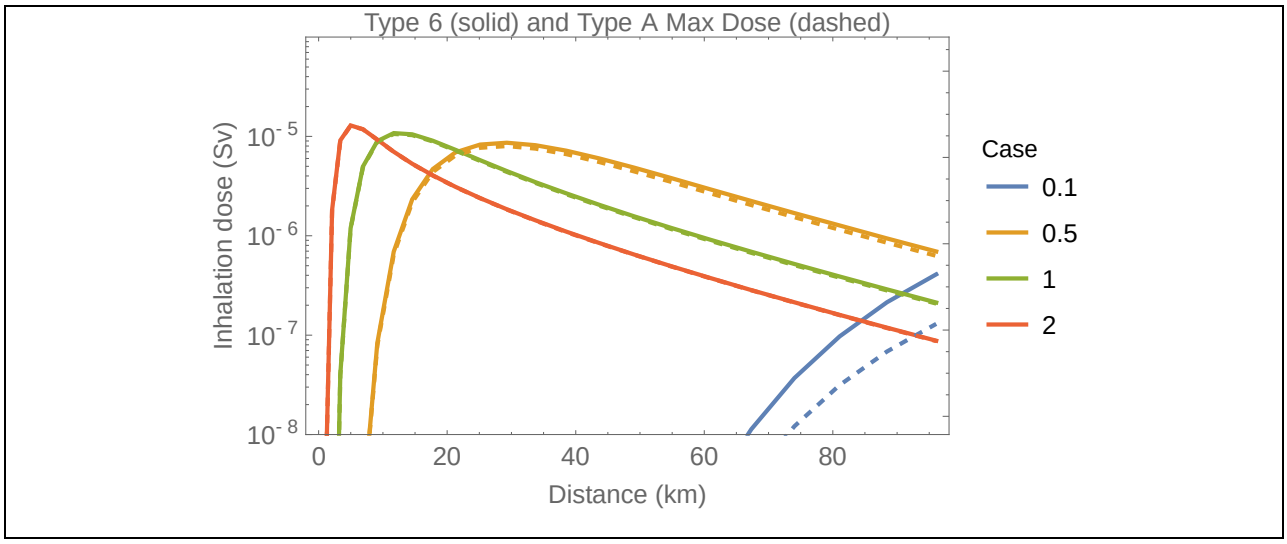

Figure 3-7. Comparison of Type 6 centerline inhalation dose (solid curves) to the Type A sector maximum inhalation dose (dashed curves).

Cloudshine Dose

The approach to verify the cloudshine dose computation is summarized as follows. From Eq. (3-3), the cloudshine factor C can be computed from the Type 6 cloudshine dose (DC_k) and the Type 0 centerline air concentration [$\chi_i(x, y = 0, z = h)$] as the ratio

$$C = \frac{DC_k}{DRCC_{\infty ik}\ \chi_i(x, y = 0, z = h)} \tag{3-5}$$

The Cs-137 dose coefficient for cloudshine in the test is $DRCC_{\infty ik} = 9.28 \times 10^{-17}$ Sv-m^3/Bq-s. The value of C computed with the MACCS outputs was compared to the cloudshine factor directly computed by linear interpolation from a lookup table supplied by the MACCS software developers. The results of the test are presented in Figure 3-8. The MACCS data are in excellent agreement with the independent computations. A jump is noted in the MACCS data for the Case 2 (YSCALE = ZSCALE = 2), which has the same explanation than similar jumps in Figure 2-6. The jump is due to a practical approach to compute the cloudshine factor in cases with large effective plume size and small relative receptor distance. Figure 3-8 also compares the MACCS Type 6 centerline cloudshine dose (symbols) to independent computations based on Eq. (3-3) and Type 0 MACCS centerline concentrations (solid curves). The agreement between the independent computations and the MACCS data is excellent.

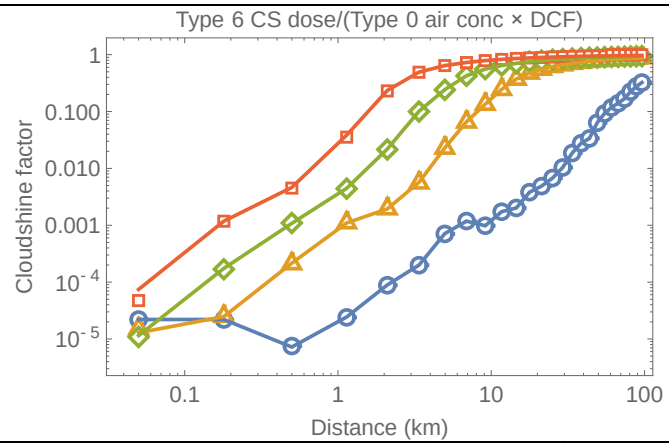

Comparison (in logarithmic scale) of the cloudshine factor computed based on Eq. (3-5) and Type 6 centerline dose and Type 0 centerline air concentration (symbols), to the cloudshine factor directly computed by linear interpolation from a lookup table supplied by MACCS software developers (solid curves).

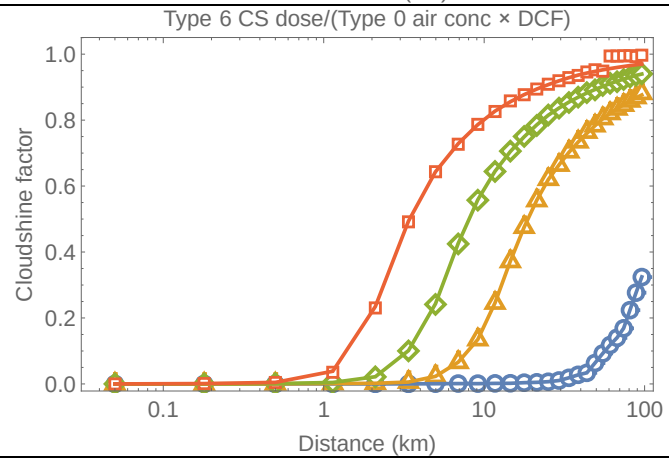

Same as the previous plot, but with the vertical axis in linear scale. The small jump in the Case 2 has the same explanation than similar jumps in Figure 2-6.

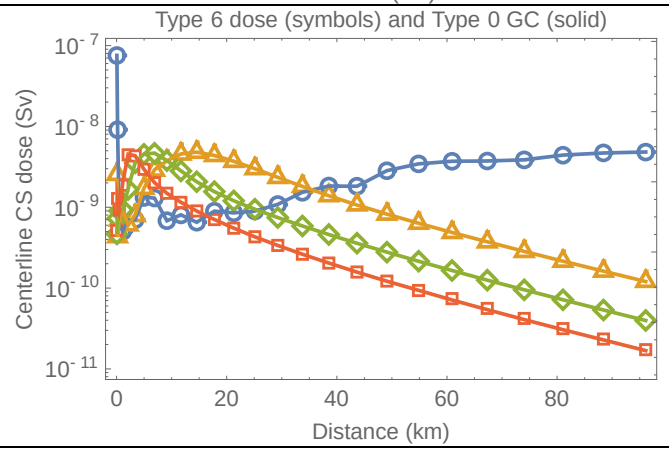

Type 6 centerline cloudshine dose MACCS outputs (symbols) compared to independent computations based on Eq. (3-3) and Type 0 air concentration MACCS outputs at the plume center (solid curves).

Figure 3-8. Cloudshine factor in logarithmic and linear scale displays, and centerline cloudshine dose versus downwind distance.

The relationship of the Type 6 centerline dose to the Type C sector average dose was examined. The Type 6 and Type C MACCS outputs are compared in Figure 3-9. As expected, the Type 6 centerline cloudshine dose (solid curve) is greater than the Type C sector average dose (dashed curve). The ratio Type C/Type 6 is equivalent to the average cloudshine factor computed along a constant radius arc (arc of angular length $\pi/8$ radians) divided by the cloushine factor at the arc center. See the Figure 2-7 of Test 2.1 for a detailed description of the computation of the arc average of the cloudshine factor, accounting for Eq. (2-8) to transform Cartesian to polar coordinates. The cloudshine factor arc average was computed considering a

line integral, and using a simple average from seven equidistant points along the arc. A comparison of the ratio Type C/Type 6 (symbols) to the independent computations (solid curves) is also displayed in Figure 3-9. The Type C/Type 6 MACCS output ratio compares well to the independent computations. The computations considering a line integral average matched the MACCS Type C/Type 6 ratio for the Cases 1 and 2 (broad plumes, ZSCALE=YSCALE=1 and ZSCALE=YSCALE=2). On the other hand, the computations considering a simple seven-point average matched the Type C/Type 6 ratio for the Cases 0.1 and 0.5 (narrow plumes). This result is consistent with the result in Figure 2-7 of Test 2.1, indicating that MACCS implements different algorithms to compute the Type C cloudshine dose average depending on the relative plume size. The MACCS data in the middle plot of Figure 3-9 exhibit a jump for the Case 2. The jump has the same explanation than similar jumps in Figure 2-7 and Figure 3-8. The jump is due to practical approximations in MACCS interpolation algorithms to compute the cloudshine factor for cases of large effective plume size and small relative receptor distance.

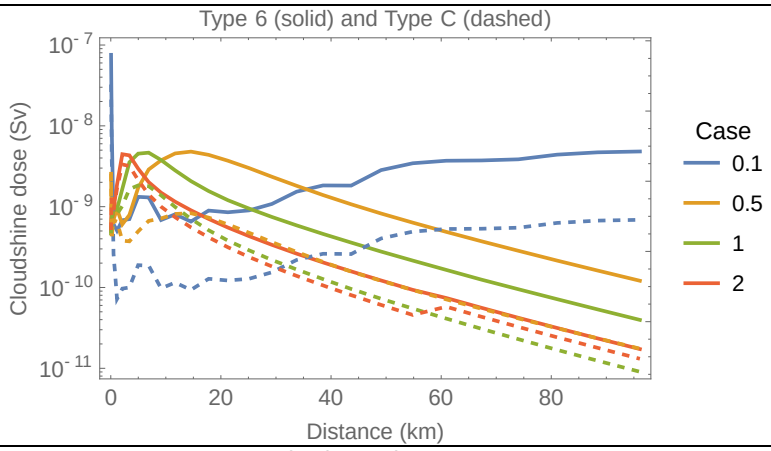

Comparison of the Type 6 centerline dose to the Type C sector average dose. As expected, Type 6 > Type C.

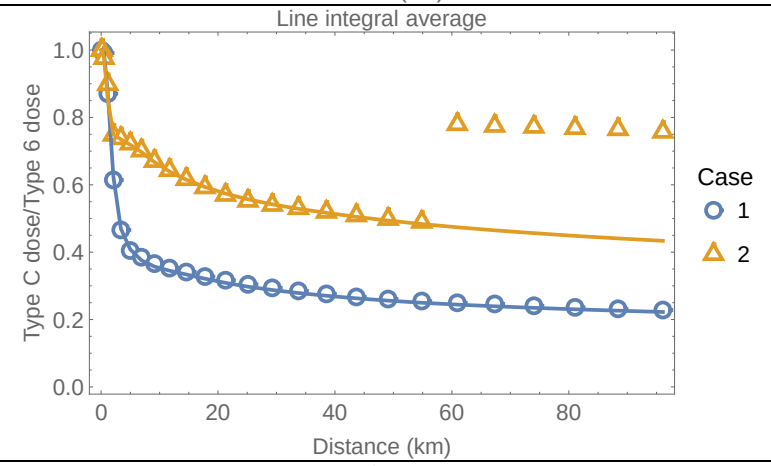

Type C/Type 6 MACCS output ratio (symbols) compared to the average cloudshine factor divided by the cloudshine factor at the arc center (solid curves). The arc average was computed based on line integration.

The jump for the Case 2 is due to practical approximations in MACCS interpolation algorithms to compute the cloudshine factor. See the explanation of similar jumps in Figure 2-7.

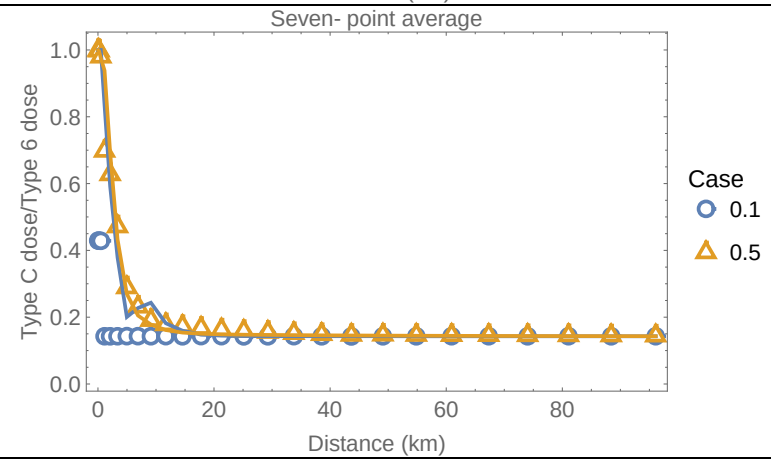

Type C/Type 6 MACCS output ratio (symbols) compared to the average cloudshine factor divided by the cloudshine factor at the arc center (solid curves). The arc average was computed based on a simple seven-point average.

Figure 3-9. Comparison of Type 6 centerline dose to the Type C sector (north sectors) average dose, and Type C/Type 6 ratio versus downwind distance.

Type 6 centerline cloudshine dose was compared to the Type A grid sector maximum cloudshine dose in Figure 3-10. It is expected that

Type A maximum cloudshine dose = Type 6 centerline dose

The off-centerline *J* factor concept is not used in the cloudshine dose, for that reason, the Type A and Type 6 doses should be identical. The test verified that the Type A and Type 6 doses are strictly identical.

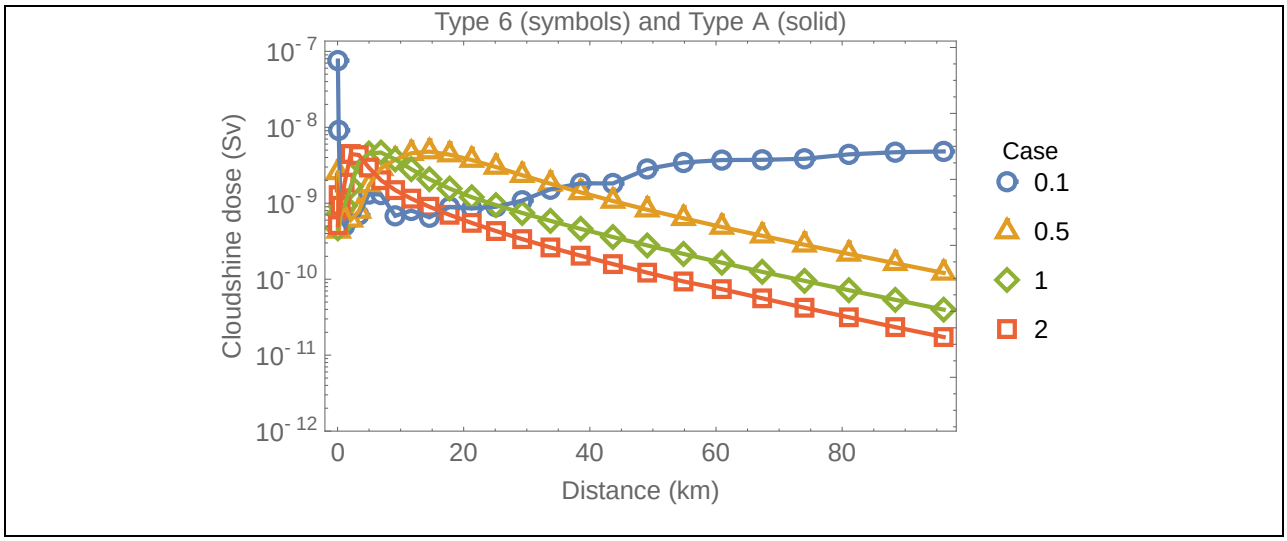

Figure 3-10. Comparison of Type 6 centerline groundshine dose (symbols) to the Type A maximum dose (solid curves).

Skin Acute Dose

It was verified that the skin acute dose is computed by MACCS according to Eq. (3-4). Figure 3-11 displays the skin acute doses (Type 6 and Type C) compared to doses independently computed based on air concentrations at the ground level (Type 0 and Type D) and Eq. (3-4). The MACCS skin dose outputs were in excellent agreement with the independently computed skin acute doses.

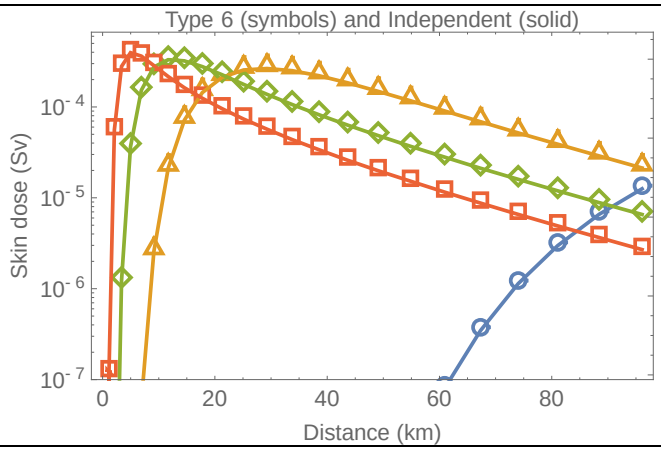

Comparison of Type 6 centerline skin acute dose (symbols) to independently computed skin doses based on the Type 0 centerline air concentration at the ground level (solid curves).

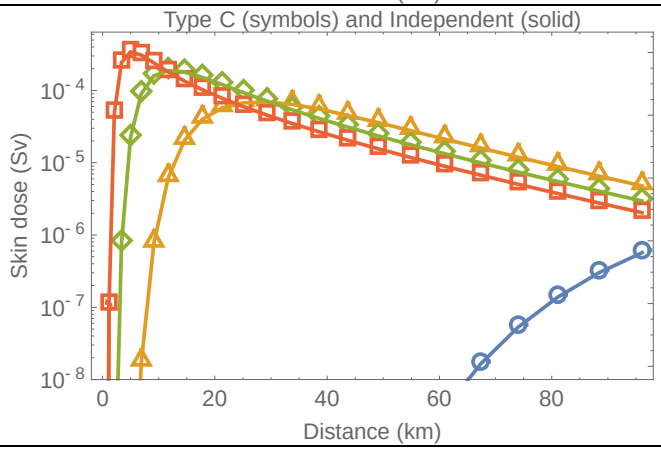

Comparison of Type C grid sector average skin dose (symbols) to independently computed doses based on the Type D sector average air concentration at the ground level (solid curves).

Figure 3-11. Centerline skin acute dose, and sector-average skin acute dose (north sector) versus downwind distance.

Figure 3-12 compares the Type 6 centerline dose to the Type A maximum dose. The test verified that the Type 6 is greater than the Type A dose.

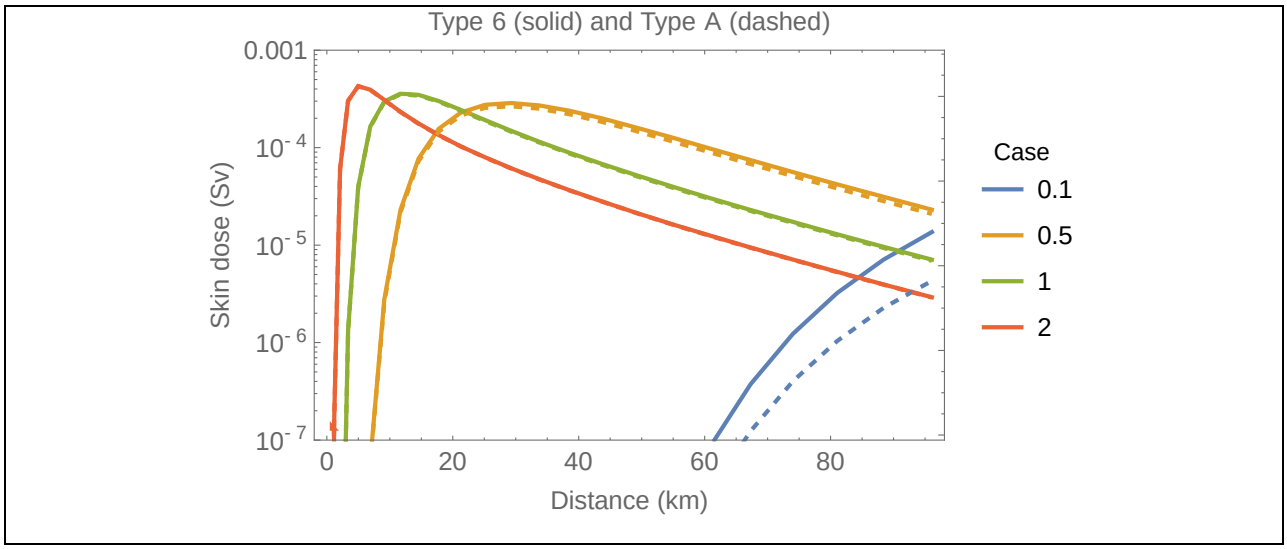

Figure 3-12. Comparison of Type 6 centerline skin dose (solid curves) to the Type A maximum dose (dashed curves).

3.1.4 Test Conclusions

The computations of groundshine, inhalation, cloudshine, and skin doses were verified for a simple case based on independent computations of air concentrations along the plume center, air concentrations at the ground level, and ground concentrations. The approaches to compute sector average concentrations and doses were also verified. MACCS successfully passed the designed tests.

3.2 Test 3.2: Population Dose

In this test the approach to compute the population dose was examined. For simple cases of non-evacuating and non-relocating cohorts, the population dose for a MACCS sector equals the average individual dose for the sector times the number of people residing in the sector. The population dose is a Type 5 output of the EARLY module. The average dose per sector is a Type C output of the EARLY module.

3.2.1 Test Input

The MACCS input was identical to the Test 3.1.

Output Controls

Same outputs Test 2.1 with the following addition:

- Type 5 (NUM5) Population Dose per 360° Grid Ring
  - NAME = L-ICRP60ED
  - I1DIS5 = 1 to 26
  - I2DIS5 = 1 to 26
  - Report Options = NONE

The specified Type 5 inputs cause the EARLY module to itemize population doses for each of the 26 rings of the test problem.

3.2.2 Test Procedure

Multiple runs of the MACCS code were executed with the following selections of the Gaussian dispersion coefficient factors:

- YSCALE = ZSCALE = 0.1
- YSCALE = ZSCALE = 1
- YSCALE = ZSCALE = 2
- YSCALE = ZSCALE = 2.6[1]

The shielding and exposure factors were set to output the inhalation dose only (PROTIN=1, other shielding factors = 0), groundshine dose only (GSHFAC=1, other shielding factors = 0), or cloudshine dose only (CSFACT=1, other shielding factors = 0).

A total of 12 runs (= 4 dispersion coefficient factors × 3 shielding factor selections) were executed. Different runs with a specific value of the dispersion coefficient factor correspond to a single case with identical air and ground concentrations. The runs only differ in the outputs, itemizing different pathway doses. A total of 3 runs for each dispersion coefficient factor were executed to manually itemize the different pathway doses (groundshine, inhalation, or cloudshine) in the Type C dose MACCS outputs.

[1]Testing of MACCS Version 4.0 identified issues related to the inadvertent lack of constraints on the lateral spread of plumes. The issue was fixed in Version 4.1. For example, a value YSCALE = 2.7 triggers an error message requesting the user to adjust the lateral spread of the plume, and MACCS is aborted. The largest YSCALE value with one decimal point not triggering the error message in this test was 2.6.

The population dose for each MACCS sector was independently computed as

Number of people in a sector × Type C average sector dose

The number of people in a sector was computed as the sector area times the population density (POPDEN = 10 people/km^2). The independently computed population dose (inhalation, groundshine, cloudshine), aggregated over 360° rings, was compared to the Type 5 population dose.

3.2.3 Test Results

Inhalation Dose (PROTIN=1, other shielding factors = 0)

The Type C average sector inhalation dose (left plots) and the independently computed population doses per sector (right plots) are presented in Figure 3-13. The color scheme is based on a logarithmic scale. The plots display only the sectors with non-zero doses. With increasing values of the dispersion coefficient factor, more sectors exhibit non-zero doses. For every case of specific dispersion coefficient values (e.g., case YSCALE = ZSCALE=2.6), there is consistency in the sectors with non-zero individual and population doses.

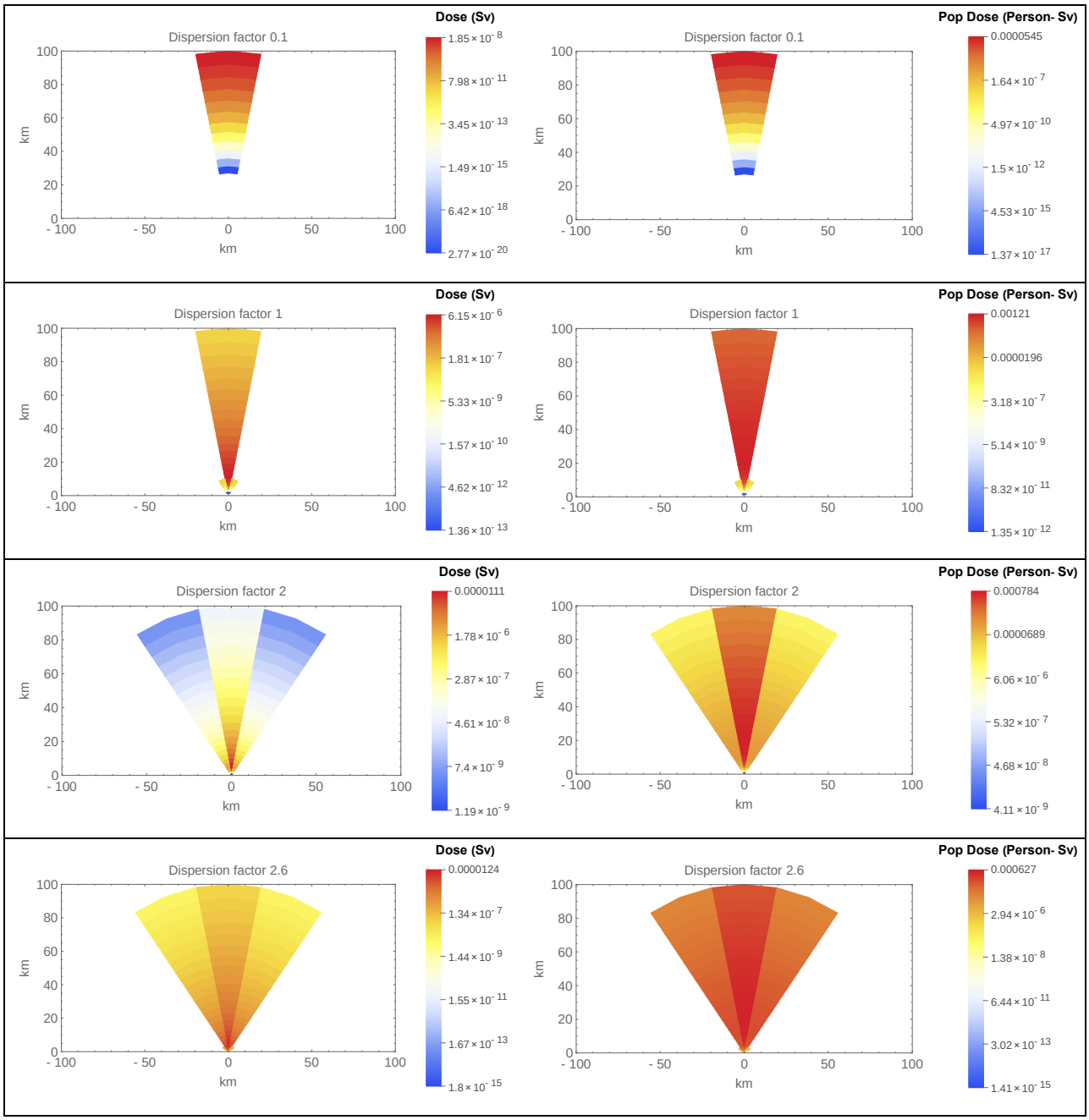

Figure 3-13. Sector plots of Type C inhalation dose and Type 5 population dose, with a color scheme representing a log-scale in the dose and population dose.

The independently computed population dose was aggregated over 360° concentric rings for direct comparison to the Type 5 population dose. The comparison is presented in Figure 3-14. There is excellent agreement between the MACCS Type 5 population dose and the independent computations.

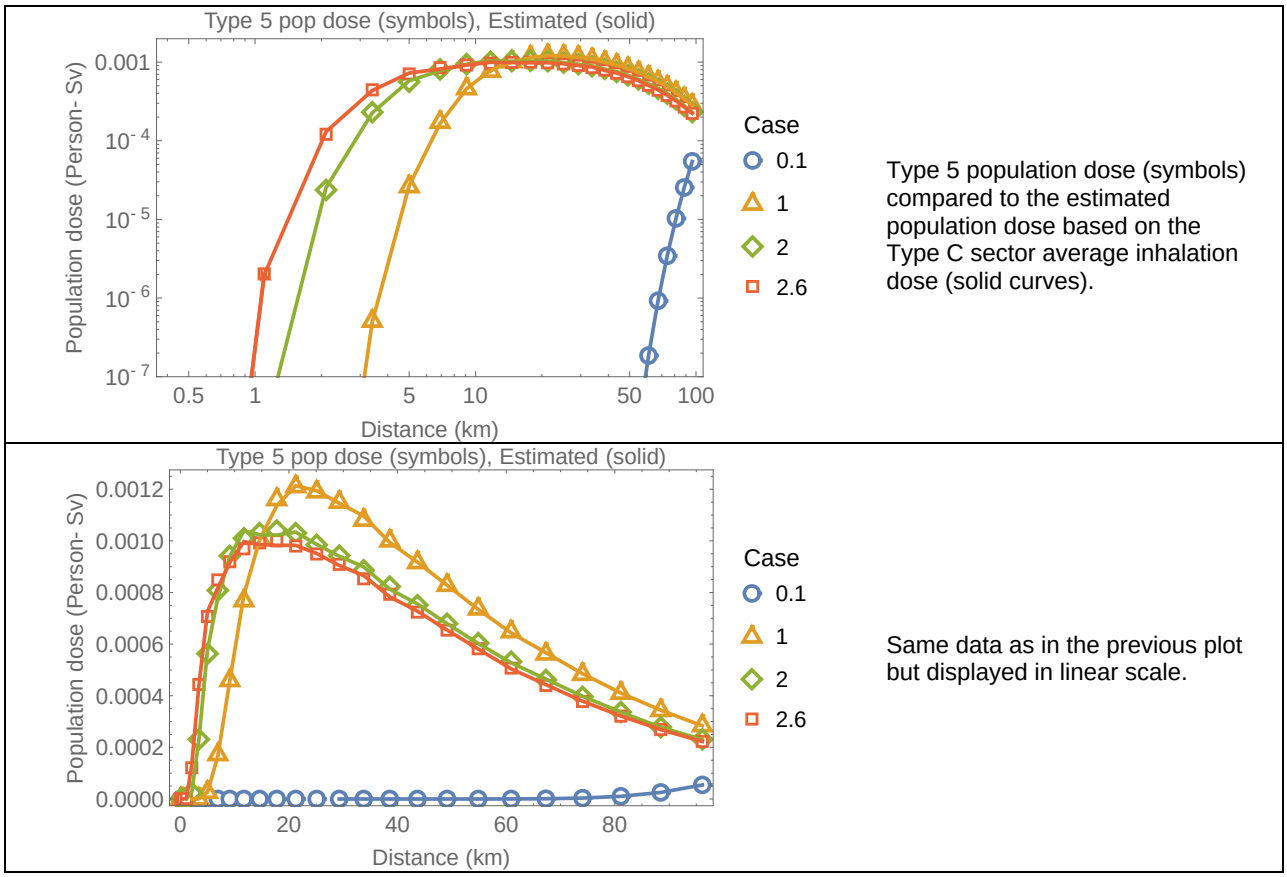

Figure 3-14. Population dose (inhalation) versus distance.

Groundshine Dose (GSHFAC=1, other shielding factors = 0)

The population dose was computed based on the Type C sector average groundshine dose, following the same approach described previously (inhalation dose example). Sector plots of groundshine dose and population dose are similar to the corresponding plots based on the inhalation dose, and not presented in this report for brevity. The independently computed population dose was aggregated over concentric rings for direct comparison to the Type 5 population dose. The comparison is presented in Figure 3-15.

The results are very similar to the inhalation dose results (because the example examined only considered dry deposition, and the ground concentration is proportional to the air concentration at the ground level).

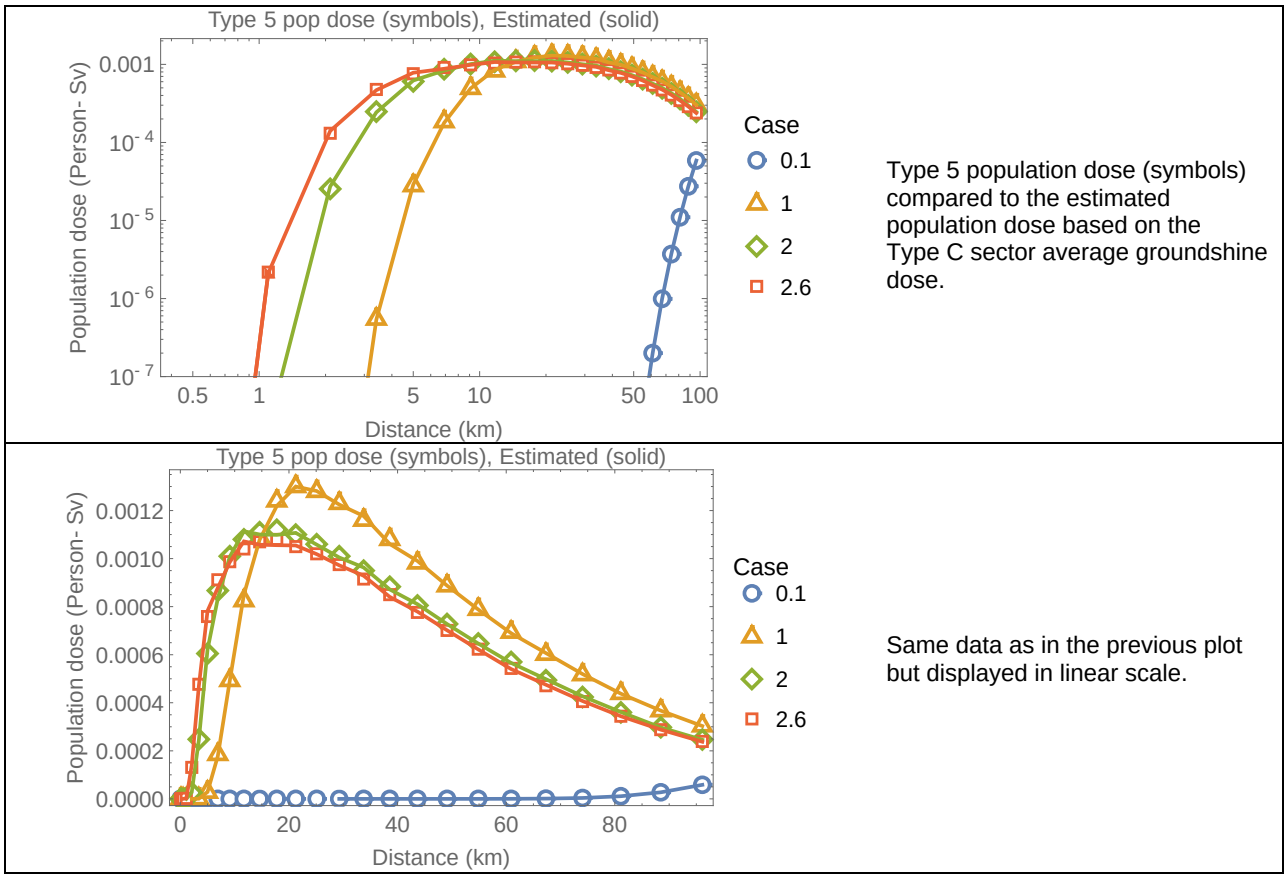

Figure 3-15. Population dose (groundshine) versus distance.

Cloudshine Dose (CSFACT=1, other shielding factors = 0)

The Type C average sector cloudshine dose (left plots) and the independently computed population doses per sector (right plots) are presented in Figure 3-16. The color scheme is based on a logarithmic scale. The plots display only the sectors with non-zero doses. With increasing values of the dispersion coefficient factor, more sectors exhibit non-zero doses.

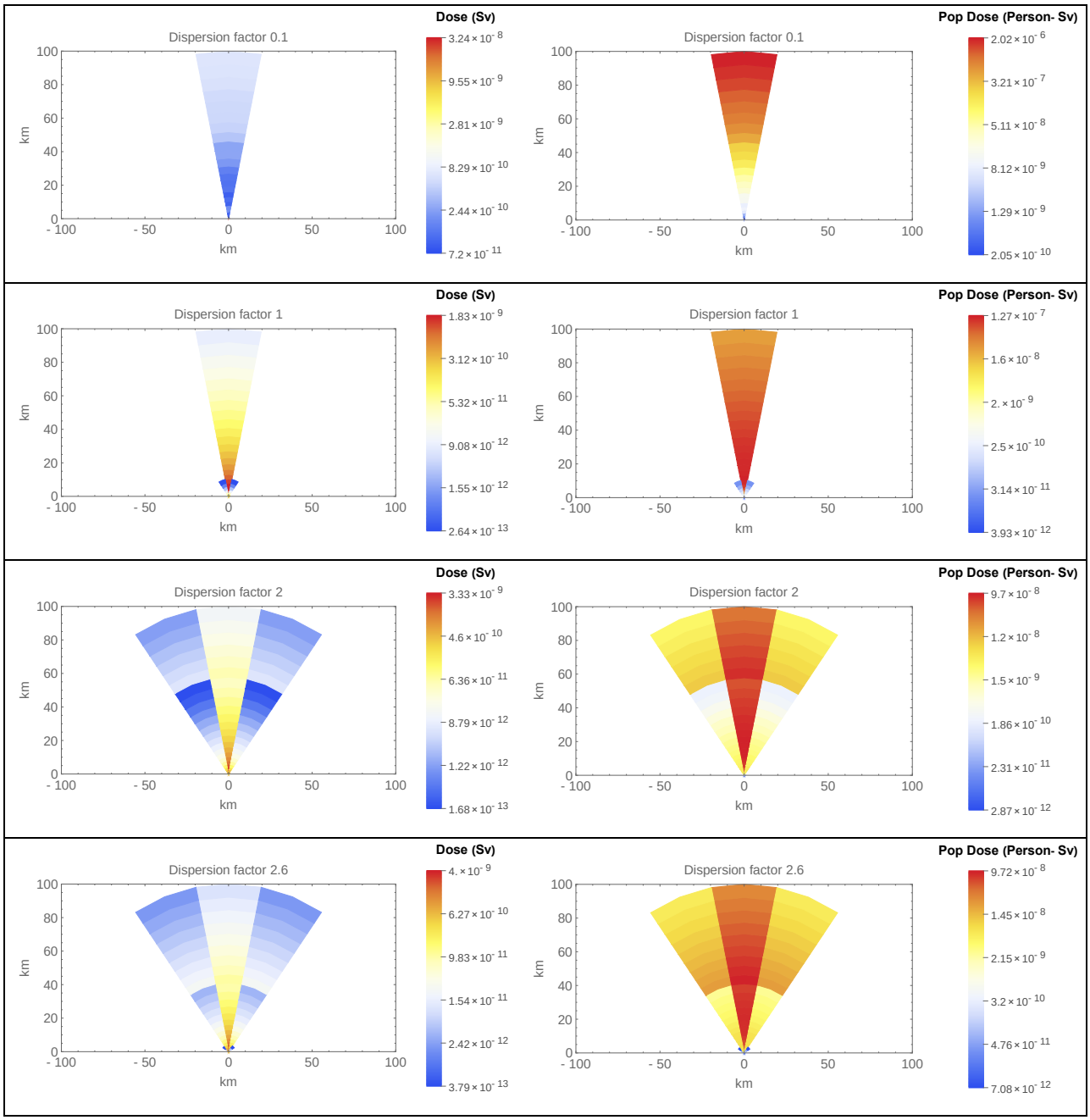

Figure 3-16. Sector plots of Type C cloudshine dose and Type 5 population dose, with a color scheme representing a log-scale in the dose and population dose.

The independently computed population dose was aggregated over 360° concentric rings for direct comparison to the Type 5 population dose. The comparison is presented in Figure 3-17.

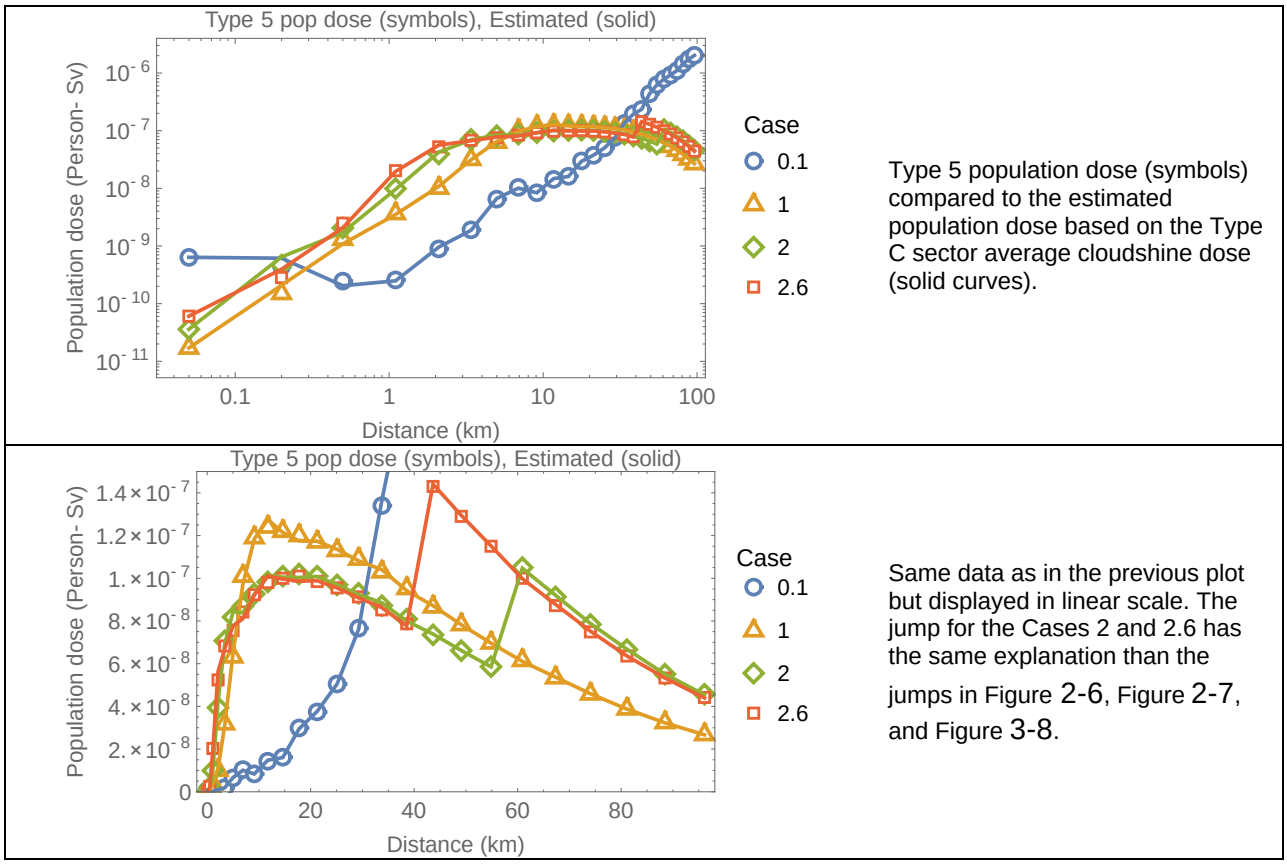

Figure 3-17. Population dose (cloudshine) versus distance.

There is excellent agreement between the MACCS Type 5 population dose and the independent computations. The jump for the Cases 2 and 2.6 in Figure 3-14 is of the same nature than similar jumps in other tests, for example the jump on Figure 2-7 of Test 2.1. The jump is due to simplifications in MACCS interpolation algorithms for the computation of the cloudshine dose in case of large effective plume size and small relative receptor distance.

3.2.4 Test Conclusions

Population doses were independently computed based on Type C sector average individual doses. The independently computed population doses agree with the Type 5 population doses. MACCS successfully passed the designed tests.

3.3 Test 3.3: Early Health Effects and Stochastic Health Effects

This test was aimed at computations of the expected number of people to experience non-lethal injuries during the early period due to acute doses, and stochastic health effects (cancer fatalities and non-fatal cancer — referred to as cancer *injuries*) due to latent doses incurred due to the plume passage.

The equation to compute the number of early injuries due to acute doses is the following (equation 6-1 of the MACCS Theory Manual)

$$N_k = f_k \, POP \left[1 - e^{-H_k(D_k)}\right] \tag{3-6}$$

N_k — number of injured people (early health effect k) in a sector due to an acute dose
POP — number of people residing in a sector
f_k — fraction of people susceptible to early health effect k, specified by EISUSC (=1 in this test)
$H_k(D_k)$ — Hazard function for early health effect k as a function of the acute dose D_k

The hazard function is defined as follows (equation 6-4 of the MACCS Theory Manual)

$$H_k(D_k) = \begin{cases} 0 & D_k < D_{T,k} \\ \left(\dfrac{D_k}{D_{50,k}}\right)^{\beta_k} \ln(2) & D_k \geq D_{T,k} \end{cases} \tag{3-7}$$

D_k — acute dose to a target organ inducing health effect k (Gy)
$D_{T,k}$ — threshold acute dose for the onset of health effect k, specified by EITHRE
$D_{50,k}$ — dose causing half of the population to experience early health effect k (Gy), specified by EIFACA
β_k — shape parameter, specified by EIFACB

For a small dose D_k and assuming $D_{T,k} = 0$, Eq. (3-6) simplifies to (after applying a first order Taylor expansion to the exponential function)

$$N_k = f_k \, POP \left(\frac{D_k}{D_{50,k}}\right)^{\beta_k} \ln(2) \tag{3-8}$$

If the shape factor β_k is one, then the number of early injuries is linearly related to the acute dose D_k.

The individual risk of cancer fatality or cancer injury in the long term due to a lifetime dose arising from the plume passage is computed as (based on equations 6-5 and 6-6 of the MACCS Theory Manual)

$$r_k^E = \begin{cases} f_k \, RC_k \, D_k^E & D_k^E \geq D_\alpha \\ f_k \, RC_k \dfrac{D_k^E}{\alpha_k} & D_k^E < D_\alpha \end{cases} \tag{3-9}$$

r_k^E — risk of an individual to experience health effect k, due to a lifetime early dose D_k^E

f_k — fraction of people susceptible to health effect k, specified by ACSUSC (=1 in the test runs)
RC_k — lifetime risk factor early health effect k (Gy), specified by CFRISK for cancer fatalities or CIRISK for cancer injuries (1/Sv)
D_k^E — lifetime dose associated with the early period causing the health effect k in a sector (Sv)
α_k — dose and dose rate effectivity factor, specified by DDREFA
D_α — threshold dose (Sv), specified by DDTHRE

To compute the number of people in a sector that would experience the health effect k, r_k^E is multiplied by the number of people residing in a sector of the spatial grid.

The test was aimed at computing the number of people with early injuries, and late fatalities and cancer injuries (Type 1 output) based on sector average acute and lifetime doses (Type C output).

3.3.1 Test Input

The input was identical to the Test 3.1, with the following changes

- Shielding and Exposure
  - PROTIN = 1, inhalation dose pathway
  - BRRATE = 1 m^3/s, exaggerated breathing rate to cause sizable risk
  - CSFACT (cloudshine) = SKPFAC (skin dose) = GSHFAC (ground dose) = 0
- Early Injury Parameters
  - EINAME = HYPOTHYROIDISM
  - ORGAN = A-THYROID
  - EITHRE (Gy) = 0 Gy, zero threshold dose
  - EIFACA (Gy) = 1 Gy
  - EIFACB = 1, selection to make the risk linearly dependent on the acute dose, per Eq. (3-8)
- Latent Cancer Parameters
  - ACNAME = LUNG
  - ORGNAM = L-LUNGS
  - ACSUSC = 1 (fraction of people affected)
  - CFRISK (1/Sv) = 0.026 1/Sv
  - CIRISK (1/Sv) = 0 1/Sv (no long-term injury)
  - DDREFA = 1 (no risk reduction)

  - ACNAME = THYROID
  - ORGNAM = L-THYROID
  - ACSUSC = 1
  - CFRISK (1/Sv) = 6.34×10^{-4} 1/Sv
  - DDREFA = 1 (no risk reduction)

Output Controls

The same outputs used for Test 3.2 were selected with the following addition:

- Type 1 (NUM1) Health-Effect Cases
  - NAME = ERL INJ/HYPOTHIROIDISM (early hypothyroidism due to acute dose

A-THYROID)
    - I1DIS1 = 1 to 26
    - I2DIS1 = 1 to 26
    - Report Options = NONE

    - NAME = CAN FAT/LUNG (lung cancer fatality due to lifetime dose L-LUNGS during the early period)
    - I1DIS1 = 1 to 26
    - I2DIS1 = 1 to 26
    - Report Options = NONE

    - NAME = CAN INJ/THYROID (lung cancer injury due to lifetime dose L-THYROID during the early period)
    - I1DIS1 = 1 to 26
    - I2DIS1 = 1 to 26
    - Report Options = NONE
- Type 4 (NUM4) Average Individual Risk
    - NAME = ERL INJ/HYPOTHIROIDISM
    - IDIS4 = 1 to 26
    - Report Options = NONE

    - NAME = CAN FAT/LUNG
    - I1DIS4 = 1 to 26
    - Report Options = NONE

    - Note: an error was produced when trying to add more outputs, such as CAN INJ/THYROID
- Type 8 (NUM8) Population-Weighted Individual Risk
    - NAME = ERL INJ/HYPOTHIROIDISM
    - I1DIS1 = 1 to 26
    - I2DIS1 = 1 to 26
    - Report Options = NONE

    - NAME = CAN FAT/LUNG
    - I1DIS1 = 1 to 26
    - I2DIS1 = 1 to 26
    - Report Options = NONE
- Type C (NUMC) Average Sector Dose
    - ORGNAM = L-ICRP60ED
    - ELEVDOSE (Sv) = 0: outputs all grid elements with dose > 0 Sv
    - PRINT_FLAG_C = True: outputs information for all grid elements

    - ORGNAM = A-LUNGS
    - ELEVDOSE (Sv) = 0: outputs all grid elements with dose > 0 Sv
    - PRINT_FLAG_C = True: outputs information for all grid elements

    - ORGNAM = L-LUNGS
    - ELEVDOSE (Sv) = 0: outputs all grid elements with dose > 0 Sv
    - PRINT_FLAG_C = True: outputs information for all grid elements

    - ORGNAM = A-THYROID

- ELEVDOSE (Sv) = 0: outputs all grid elements with dose > 0 Sv
- PRINT_FLAG_C = True: outputs information for all grid elements

- ORGNAM = L-THYROID
- ELEVDOSE (Sv) = 0: outputs all grid elements with dose > 0 Sv
- PRINT_FLAG_C = True: outputs information for all grid elements

3.3.2 Test Procedure

Six runs of the MACCS code were executed with the following selections of the Gaussian dispersion coefficient factors:

- YSCALE = ZSCALE = 0.1
- YSCALE = ZSCALE = 0.5
- YSCALE = ZSCALE = 1
- YSCALE = ZSCALE = 2
- YSCALE = ZSCALE = 2.6

The shielding and exposure factors were set to output the inhalation dose only (PROTIN=1, other shielding factors = 0).

The expected number of people with early injuries (hypothyroidism) due to an acute dose (A-THYROID) was independently computed using Eq. (3-6) and the Type C average sector dose (A-THYROID). The number of people in a sector (POP) was computed as the sector area times the population density (POPDEN = 10 people/km^2).

The risk of cancer fatalities and injuries due to lifetime doses to the lungs (L-LUNGS) or to the thyroid (L-THYROID) was independently computed using the corresponding Type C sector average dose (L-LUNGS or L-THYROID) and Eq. (3-9). The expected number of affected people per sector was computed by multiplying the computed risk number and the number of people in a sector (in this test problem it was assumed a constant population density, POPDEN = 10 people/km^2).

The independently computed number of health effects (e.g., early injury, cancer fatalities and injuries), aggregated over 360° rings, were compared to the Type 1 health-effect cases.

The average individual risk (early injury risk, cancer fatality risk, cancer injury risk) in a MACCS grid ring was computed as the average of 16 risk values (one independently computed risk value for each of the 16 sectors in a 360° ring). The average individual risk per grid ring was compared to Type 4 outputs of the EARLY module.

The test did not evaluate early fatality risk. In the test runs, the early fatalities were zero. Although the early fatality results were not explicitly tested, the early injury computations are identical to the early fatality computations.

3.3.3 Test Results

The independently computed individual risk of early injury (hypothyroidism) from acute doses to the thyroidal gland was compared to the corresponding Type 4 MACCS output in Figure 3-18. The MACCS outputs are in excellent agreement with the independent computations. Particularly noteworthy is that the Type 4 risk considers sectors located upwind from the source

(i.e., sectors south of the source in the test problem), with zero dose, in the computation of the average risk. Figure 3-18 also compares the Type 1 MACCS population risk output to the independently computed number of people affected by hypothyroidism, showing complete agreement. Finally, Figure 3-18 includes a comparison of Type 8 population-weighted individual risk to Type 4 average individual risk (in the form of a ratio of Type 8/Type 4 versus distance). As expected, Type 8 and Type 4 are identical due to the consideration of uniform population density in the test problem.

The independently computed individual lung cancer fatality risk (based on the Type C sector average lifetime lung dose, L-LUNGS) was compared to the corresponding Type 4 MACCS output in Figure 3-19. Figure 3-19 also includes the independently computed number of people with fatal lung cancer compared to the corresponding Type 1 output, as well as a comparison of Type 8 population-weighted individual risk to Type 4 average individual risk (in the form of a ratio of Type 8/Type 4 versus distance). As expected, Type 8 MACCS outputs are identical to Type 4 MACCS outputs, due to the assumption of uniformly distributed population.

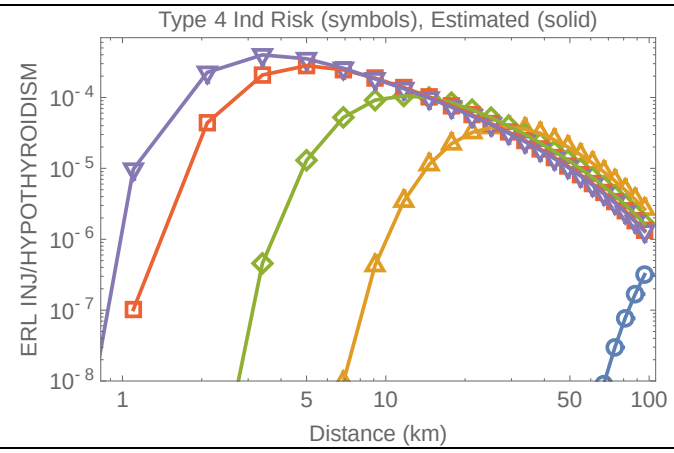

Type 4 average individual risk (symbols, early injury, hypothyroidism) compared to the independently computed average risk based on the Type C sector average inhalation A-THYROID dose (solid curves).

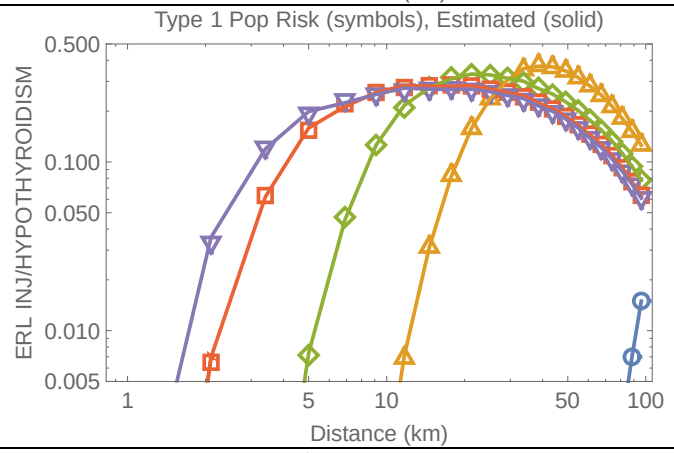

Type 1 population risk (symbols, early injury, hypothyroidism) compared to the independently computed average risk based on the Type C sector average inhalation A-THYROID dose (solid curves).

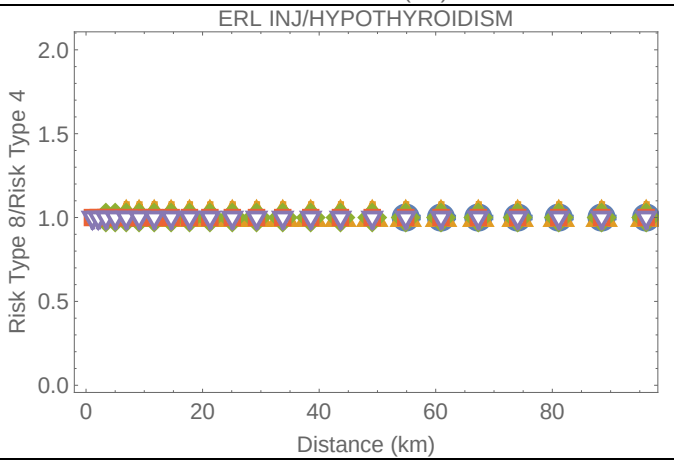

Comparison of Type 8 population-weighted individual risk and Type 4 average individual risk of early injury (hypothyroidism), presented as a ratio Type 8/Type 4.

As expected, Type 4 and Type 8 results are strictly identical due to the use of a uniform population density in the test.

Figure 3-18. Individual average risk (Type 4 output) and population risk (Type 1 output) from acute doses to the thyroidal gland versus radial distance from the source. The third plot is a ratio comparison of Type 4 and Type 8 MACCS outputs (the results are strictly identical).

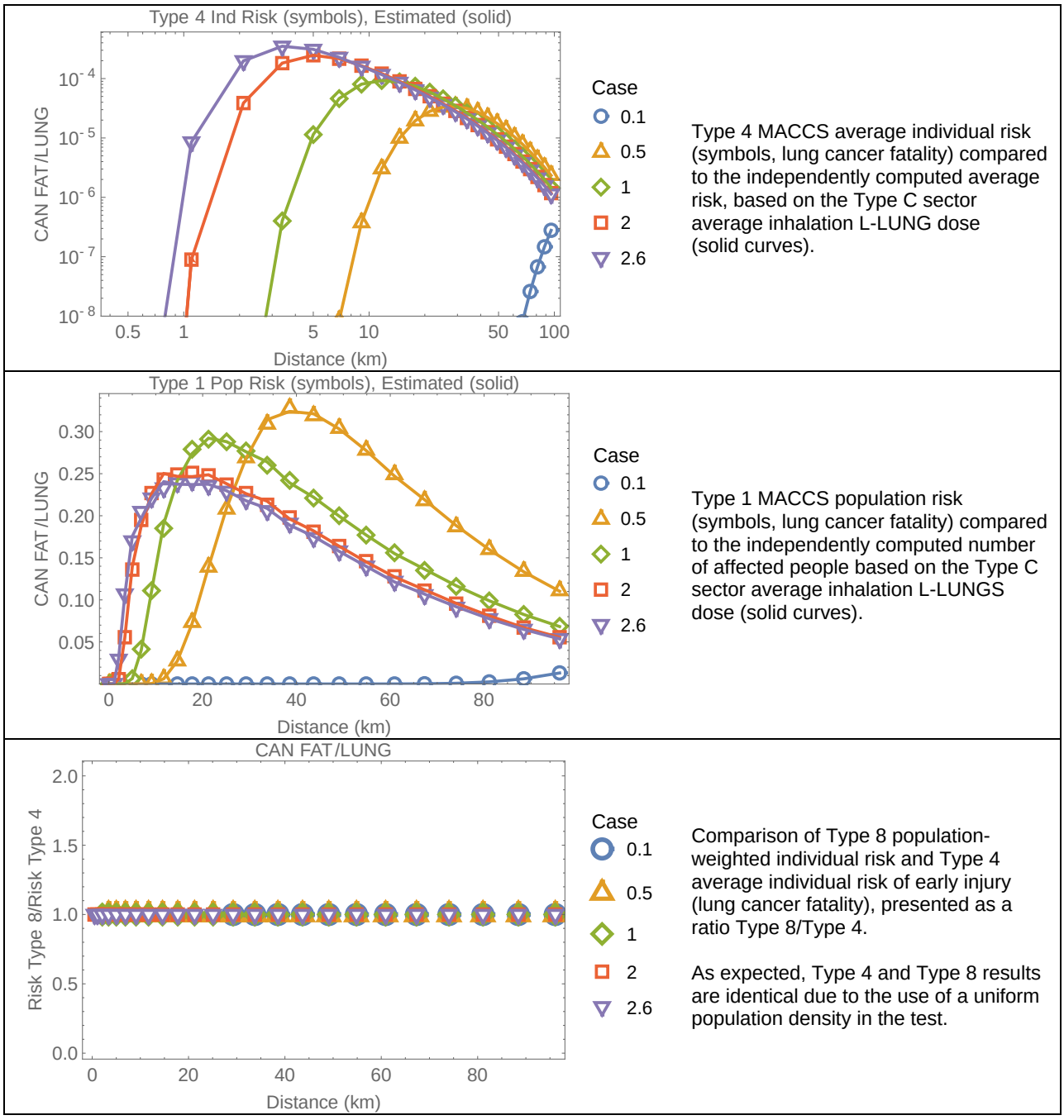

Figure 3-19. Average individual risk (Type 4 output) and population risk (Type 1 output) from long-term lung doses from inhalation of radioactivity carried by the plume, versus radial distance from the source. The third plot is a ratio comparison of Type 4 and Type 8 MACCS outputs (the results are strictly identical).

The independently computed number of people affected by thyroidal cancer (based on the Type C sector average lifetime thyroidal dose, L-THYROID) was compared to the corresponding Type 1 output in Figure 3-20. The MACCS outputs are in excellent agreement with the independent computations.

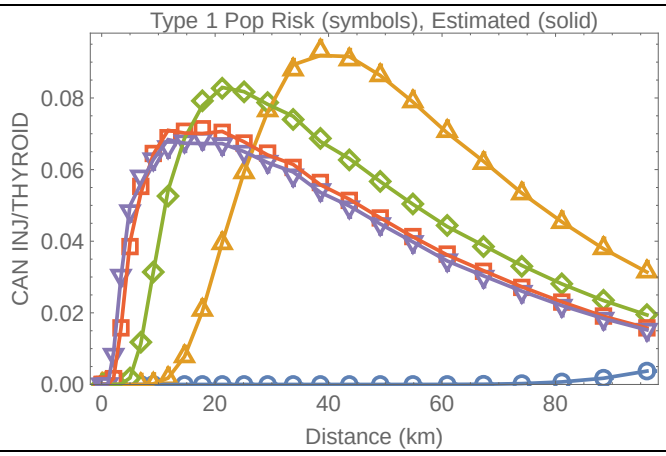

Type 1 population risk (symbols, thyroidal cancer injury) compared to the independently computed number of affected people by thyroidal cancer based on the Type C sector average inhalation L-THYROID dose (solid curves).

Figure 3-20. Population risk (from long-term doses to the thyroid from inhalation of radioactivity carried by the plume) versus radial distance from the source.

3.3.4 Test Conclusions

The test verified the MACCS algorithms to compute individual risk and the number of people exhibiting specific health effects due to acute doses of lifetime doses incurred during the early phase. Independent computations verified the computation of risk indices and the number of affected people. MACCS successfully passed the designed tests.

3.4 Test 3.4: Dependence of Results on Lateral Dispersion σ_y

Tests 3.1, 3.2, and 3.3 with MACCS Version 4.0 identified anomalies related to lack of numerical constraints on the spread of plumes. Test 3.4 was originally designed as a complementary test, to identify whether anomalies in Version 4.0 were related to scenarios with large values of vertical or lateral Gaussian dispersion coefficients. The causes of the identified anomalies in the referred tests were already addressed in MACCS Version 4.1, but the Test 3.4 with Version 4.1 is documented herein for the sake of completeness.

In Tests 3.1, 3.2, and 3.3, the vertical and lateral dispersion coefficients were adjusted through the factors YSCALE and ZSCALE. In all those previous tests, YSCALE = ZSCALE. In the current Test 3.4, the effect of lateral dispersion was independently examined by setting ZSCALE=1 and varying YSCALE. Similarly, vertical dispersion effects were examined by setting YSCALE=1 and varying ZSCALE. Anomalies in MACCS Version 4.0 were related to lateral dispersion (acrosswind direction) and numerical artefacts in the computation of concentrations, doses, and health effects on non-central grid sectors. As previously stated, those anomalies do not exist in MACCS Version 4.1, given the constraints on the allowed extent of lateral spread of plumes.

3.4.1 Test Input

Identical inputs and outputs than Test 3.3 were used.

3.4.2 Test Procedure

Five runs of the MACCS code were executed with ZSCALE=1 and the following selections of the lateral Gaussian dispersion coefficient factors:

- YSCALE = 0.1
- YSCALE = 1
- YSCALE = 2
- YSCALE = 2.6

In addition, four runs of the MACCS code were executed with YSCALE=1 and the following selections of the vertical Gaussian dispersion coefficient factors:

- ZSCALE = 0.1
- ZSCALE = 1
- ZSCALE = 10
- ZSCALE = 100

Tests exhibiting anomalous results using MACCS Version 4.0 were repeated, following procedures in Tests 3.1, 3.2, and 3.3.

3.4.3 Test Results

ZSCALE = 1 and variable YSCALE

The Type A maximum dose and Type 6 centerline inhalation dose were compared in Figure 3-21. Figure 3-22 includes multiple plots of MACCS outputs (symbols) to independent

computations (solid curves), with excellent agreement and no anomalies. Note that population doses and health effects in Figure 3-22 were aggregated over 360° rings. The aggregated results are almost independent of the lateral plume spread.

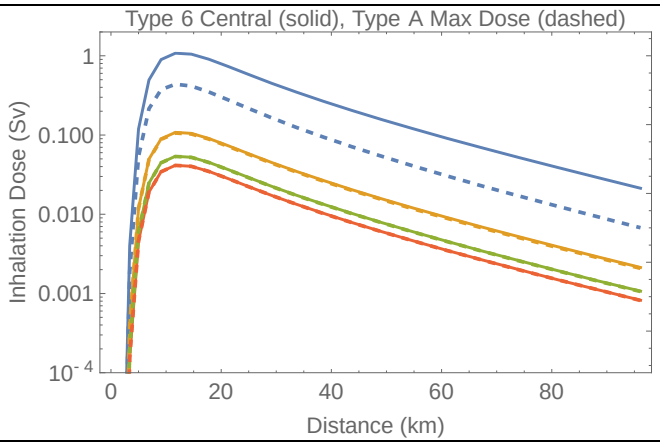

Comparison of the Type 6 centerline dose (solid curves) and Type A maximum dose (dashed curves). As expected, the comparison indicates that Type A ≤ Type 6, with differences increasing with decreasing values of YSCALE.

Figure 3-21. Comparison of Type 6 centerline inhalation dose (solid curves) to the Type A maximum dose (dashed curves).

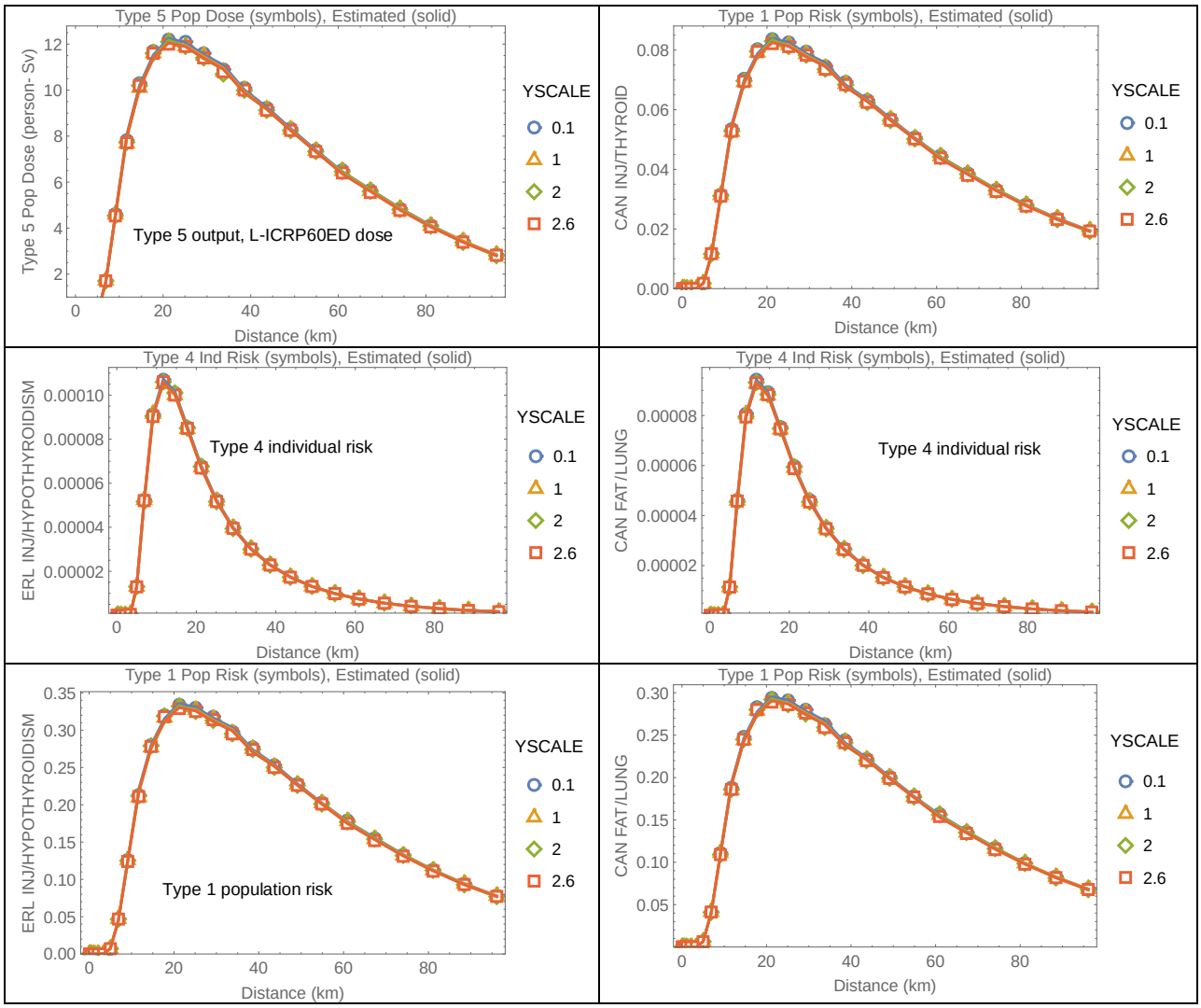

Figure 3-22. Comparison of several MACCS outputs (symbols) to independent computations (solid curves). Health effects arise from acute and long-term lung and thyroid doses from inhalation of radioactive material carried in the plume. Results are combined over 360° rings.

Figure 3-23 shows sector plots of the air concentration on the left column (air concentration of Cs-137 at the ground level extracted from Type D outputs) and individual inhalation dose on the right column (L-ICRP60ED inhalation dose extracted from Type C outputs). The concentration plots are visually identical to the dose plots because the inhalation dose is proportional to the air concentration at ground level.

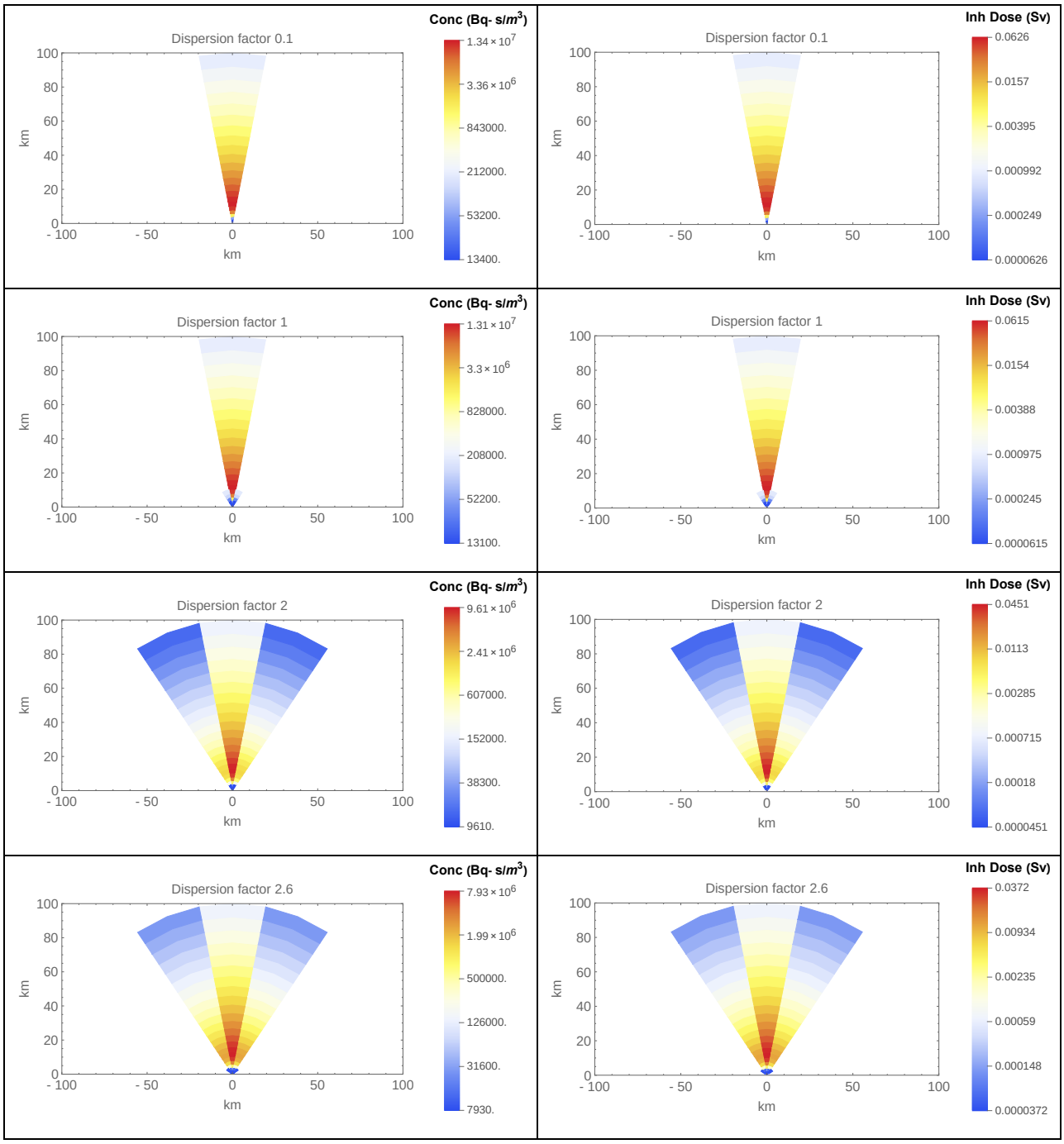

Figure 3-23. Sector plots of Type D average air concentration at the ground level and Type C average inhalation dose, with a color scheme representing a log-scale in the dose and population dose and truncated to span 3 orders of magnitude.

Figure 3-24 is an alternative visual display of the same data shown in Figure 3-23: the air concentration and inhalation dose were plotted versus the sector angle, for the different radial distances of the sector centers. Each curve in each plot in Figure 3-24 represents information of sectors on a single ring of the MACCS spatial grid (i.e., sectors located at the same radial distance from the source). The color scale represents the ring radius (blue is for a small radius

close to the source, red is for a radius far from the source). The angle was measured with respect to the east direction: i.e., east = 0°, north = 90°, west = 180°. The air concentration plots (left hand side plots) and the inhalation dose plots (right hand side plots) are visually identical because the inhalation dose is proportional to the air concentration at the ground level. The expected shape of a concentration or dose versus angle curve is a bell shape: a value that is maximal in the central sectors (90°) and with smaller values for angles farther away from the central angle. There are no visual anomalies in the MACCS outputs.

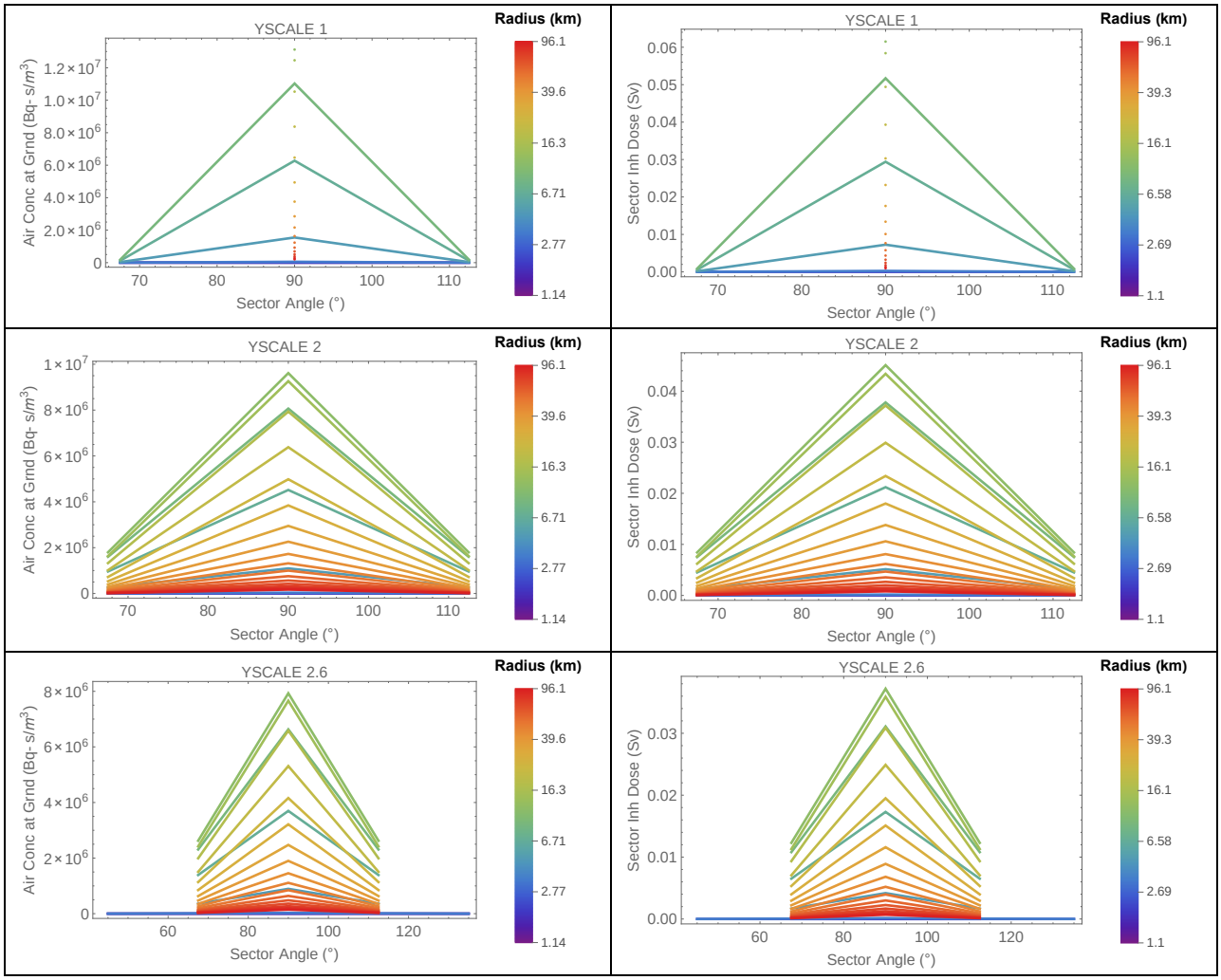

Figure 3-24. Sector average air concentration at the ground level (Type D output) and sector average inhalation dose (Type C output) versus sector angle and radial distance to the source. The color scheme represents radial distances in a log-scale (blue for near distances and red for far distances).

YSCALE = 1 and variable ZSCALE

A final test was implemented to independently examine variation of vertical dispersion. The following figure compares the Type A maximum dose to the Type 6 centerline dose.

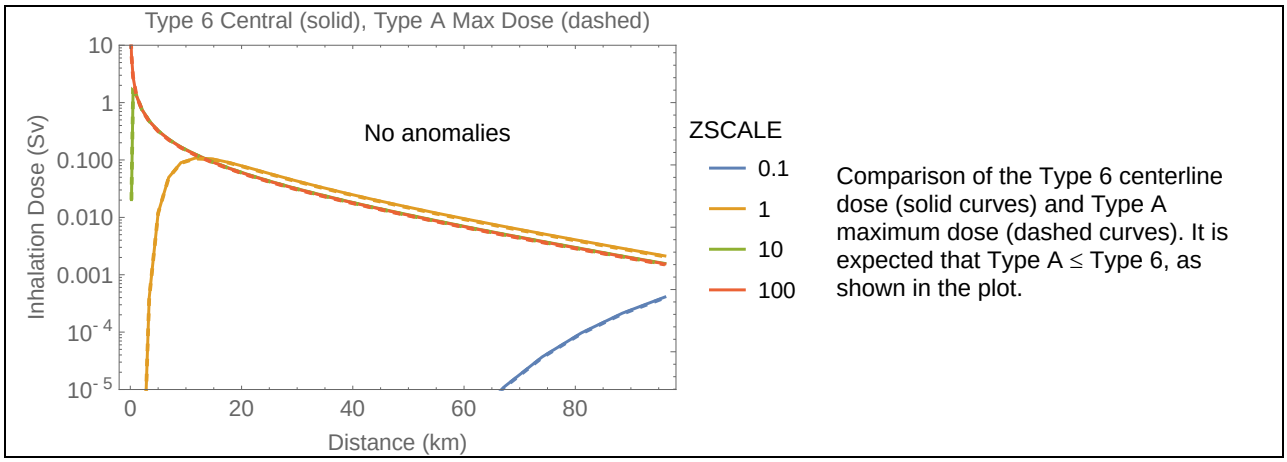

Figure 3-25. Comparison of Type centerline inhalation dose (solid curves) to the Type A maximum dose (dashed curves).

Figure 3-26 shows no anomalies in the population dose and health effects. The plots compare the MACCS outputs (symbols) to independent computations (solid curves). The MACCS outputs agree with the expected results. For the case ZSCALE = 0.1, the plume is narrow and the inhalation dose is small (source height = 500 m). Other cases correspond to wider plumes, causing greater Cs-137 air concentration at the ground level. The cases ZSCALE = 10 and ZSCALE = 100 correspond to well spread plumes along the vertical direction, and the results are nearly identical. There were no anomalies in the results.

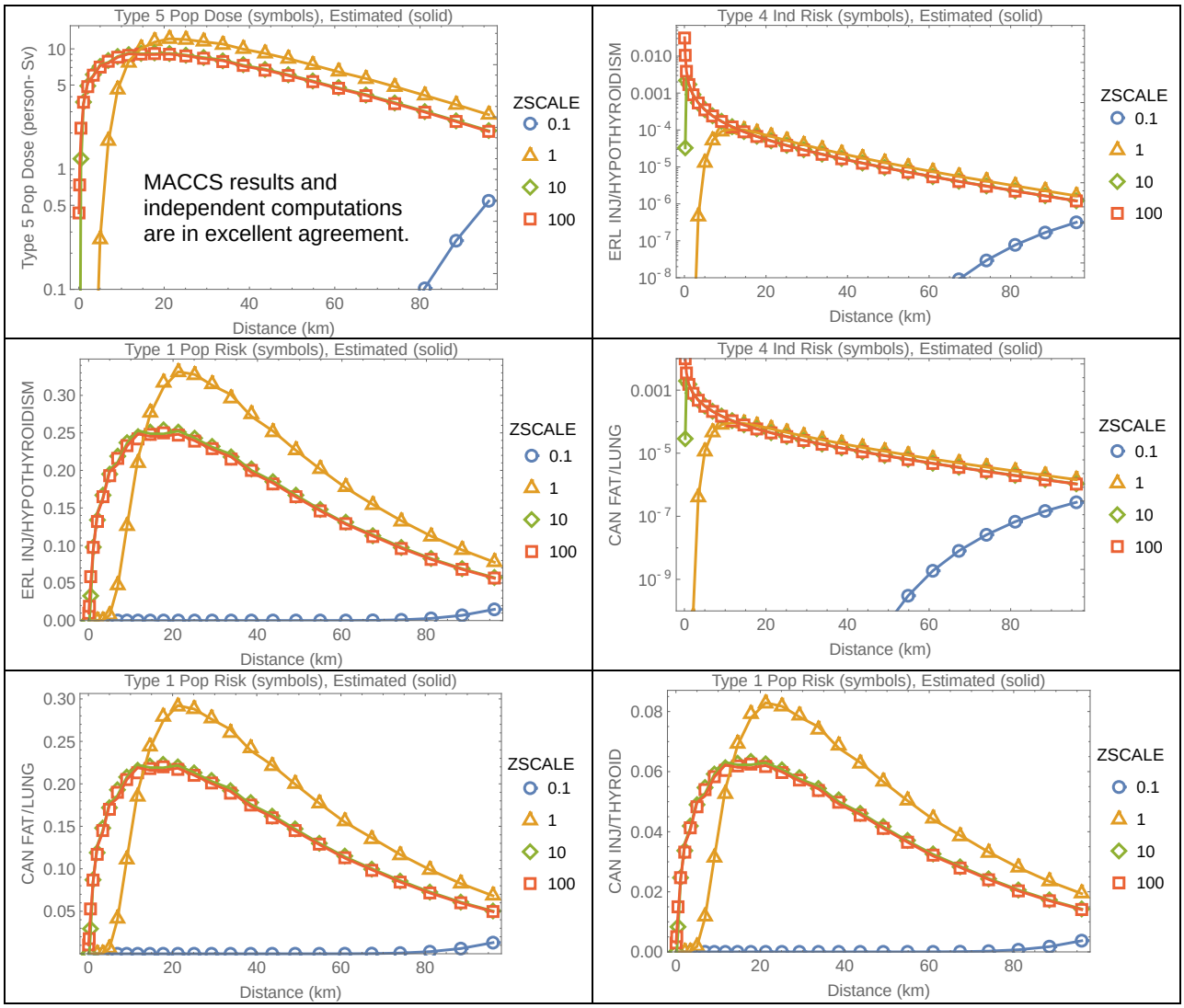

Figure 3-26. Comparison of Type 5 population dose, Type 4 average individual risk, and Type 1 population health effects (from inhalation of radioactivity in a plume) to independent computations. The MACCS outputs are in excellent agreement with the independent computations.

3.4.4 Test Conclusions

MACCS Version 4.1 successfully passed the designed tests. There were no anomalies in the MACCS outputs.

3.5 Test 3.5: Off-Center Sector Air Concentrations and Cloudshine Doses

The EARLY module considers fine grid concentrations/doses to compute a coarse sector representative concentration/dose, as an average of the fine grid concentrations/doses. The computation of coarse sector averages was examined in Tests 2.1 and 3.1, but focusing only on central sectors (i.e., north sectors in the test runs). In this test, the examination is extended to concentrations in non-central sectors (i.e., other sectors than the north sectors).

If dry and wet deposition is ignored and radioactive decay is negligible, air concentrations at an arbitrary 3D location (x, y, z) can be computed using Eqs. (2-1) and (2-2). However, MACCS tracks results in a cylindrical grid; thus, MACCS requires transformation of cylindrical to Cartesian coordinates to use Gaussian steady-state concentration functions expressed in Cartesian coordinates. If (r, θ, z) are the equivalent cylindrical coordinates of a point (x, y, z), with the radial distance r measured with respect to source location, and the angle θ measured with respect to the east direction, the integrated air concentration at a point (r, θ, z) should be computed as

$$\chi(r\sin\theta\,, r\cos\theta\,, z) \tag{3-10}$$

$\chi(x,y,z)$	—	integrated air concentration defined by Eq. (2-1), Bq-s/m^3
r	—	radial distance to the source, m
θ	—	angle measured with respect to the east direction
z	—	vertical distance, m

However, MACCS does not implement a strict cylindrical to Cartesian coordinates conversion. Instead, MACCS adopts a narrow plume approximation, which does not require trigonometric functions:

$$\begin{aligned} x &\approx r \\ y &\approx \left(\theta - \frac{\pi}{2}\right) r \end{aligned} \tag{3-11}$$

This approximation is valid for θ angles close to $\pi/2$ and becomes inaccurate for angles far from $\pi/2$. See Figure 3-27 for a graphical representation of the approximation, and how the narrow plume approximation diverges for sectors towards the east or west directions. MACCS computes the integrated air concentration at an arbitrary location (r, θ, z) as

$$\chi\left(r, r\,\theta - r\frac{\pi}{2}, z\right) \tag{3-12}$$

which, again, is a good approximation to Eq. (3-10) for θ angles close to $\pi/2$.

The objective of the test was to examine the use of Eq. (3-12) to compute representative or average air concentrations of sectors. Average concentrations were independently computed and compared to Type D outputs. The test was extended to include the cloudshine dose. Per Eq. (3-3), the cloudshine dose at any receptor location (located on the ground) of Cartesian coordinates (x, y) is computed based on the plume centerline air concentration $\chi(x, y = 0, z = h)$ (h is the source height, 500 m in the test runs), and the cloudshine factor computed at the location (x, y). The cloudshine factor, $C(\sigma, rrd)$, is computed by linear interpolation from a lookup table as a function of two independent variables, the effective plume size σ and the

relative receptor distance, rrd, defined as

$$\sigma(x) = \sqrt{\sigma_y(x)\,\sigma_z(x)}$$
$$rrd(x,y) = \frac{\sqrt{h^2+y^2}}{\sigma(x)} = \sqrt{\frac{h^2+y^2}{\sigma_y(x)\,\sigma_z(x)}} \quad (3\text{-}13)$$

$\sigma_y(x)$ — lateral, acrosswind, Gaussian dispersion coefficient, m
$\sigma_z(x)$ — vertical Gaussian dispersion coefficient, m
h — source height, m
(x,y) — receptor coordinates on the ground, m

The cloudshine dose at an arbitrary location (x, y) is proportional to the factor

$$\chi(x,0,h)\;C[\sigma(x), rrd(x,y)] \quad (3\text{-}14)$$

MACCS implements the narrow plume approximation of Eq. (3-11) in the computation of the cloudshine dose to transform polar to Cartesian coordinates. Specifically, the cloudshine dose at a position on the ground of polar coordinates (r,θ) is computed in MACCS as

$$DC_k(r,\theta) = DRCC_{\infty k}\;\chi(r,0,h)\;C\left[\sigma(r), rrd(r, r\,\theta - r\frac{\pi}{2})\right]\;F\;SFC \quad (3\text{-}15)$$

$DC_k(r,\theta)$ — cloudshine dose to organ k at the location (r,θ) (Sv)
$DRCC_{\infty k}$ — semi-infinite cloudshine dose coefficient to organ k for a specific radionuclide (Sv-m^3/Bq-s) (=9.28×10^{-17} S-m^3/Bq-s for Cs-137 in the test problem)
$\chi(r,0,h)$— integrated air concentration at the plume centerline (Bq-s/m^3), Eqs. (2-1) and (2-2)
$C[\cdots]$ — cloudshine factor computed at the position $x = r, y = r\,\theta - r\frac{\pi}{2}$
F — fraction of the exposure time (=1, for non-evacuating and non-relocating individuals)
SFC — cloudshine protection factor specified by CSFACT (CSFACT = 1 in the test runs)

The test examined the MACCS implementation of Eq. (3-15) to compute the cloudshine dose in non-central sectors (i.e., sectors at other orientations than π/2 or 90°).

3.5.1 Test Input

The input was identical to the Test 3.3, with the following changes:

ATMOS
- Deposition / Wet/Dry Depos Flags
  - DRYDEP=WETDEP=False for Cs-137 (no wet deposition, no dry deposition)
- Dispersion / Scaling Factors
  - YSCALE = 1, 2, 2.6
  - ZSCALE = 1

EARLY

- Shielding and Exposure (**Set 1**)
  - PROTIN = 1, inhalation dose pathway only
  - BRRATE = 1 m^3/s, exaggerated breathing rate to cause sizable risk
  - CSFACT (cloudshine) = SKPFAC (skin dose) = GSHFAC (ground dose) = 0
- Shielding and Exposure **(Set 2**)
  - CSFACT = 1, cloudshine pathway only
  - PROTIN (inhalation) = SKPFAC (skin dose) = GSHFAC (ground dose) = 0

Identical outputs than Test 3.3 were used.

3.5.2 Test Procedure

The MACCS code was executed to simulate a case of

- Wind blowing in the north direction at constant speed (10 m/s)
- No dry/wet deposition
- Release and transport of Cs-137 only (long-lived radionuclide)
- One plume segment

Several runs of the MACCS code with variable lateral dispersion coefficient were executed with the following inputs, ZSCALE = 1 (vertical Gaussian dispersion coefficient factor) and

- YSCALE = 1
- YSCALE = 2
- YSCALE = 2.6

Two sets of runs were executed, in the Set 1, the shielding and exposure flags were set to output only inhalation doses, and in the Set 2, the shielding and exposure flags were set to output only cloudshine doses.

An alternative method was designed to compute representative average concentrations and cloudshine doses of coarse spatial sectors. Points were sampled within a coarse sector (e.g., north-north-east, NNE, sector), exemplified by the red points in Figure 3-27. The red dots in Figure 3-27 are located along an arc of constant radius passing through the center of each of the three sectors and at equidistant angles. The sector average concentration/cloudshine dose was defined as the average of the air concentrations/cloudshine doses computed at the red points falling within a sector. To increase accuracy of the mean, the average was computed based on a numerical line integral determined by trapezoidal integration. The average so computed must be equivalent to Type D sector average concentrations output by the EARLY module in the case of air concentrations, and to Type C sector average doses in the case of cloudshine doses. The objective of the test was verifying that Type D sector average concentrations and Type C sector average cloudshine doses are equivalent to concentrations/doses computed with the independent average method, accounting for the MACCS narrow plume approximation, Eq. (3-12). An additional test was designed to consider accurate polar to Cartesian coordinate transformation, to evaluate the effect of the MACCS narrow plume approximation. Figure 3-27 displays points located on a horizontal line (constant x). Those points are the true locations where concentrations and doses are computed, using the MACCS narrow plume approximation in the north-north-east (NNE) and north-east (NE) sectors.

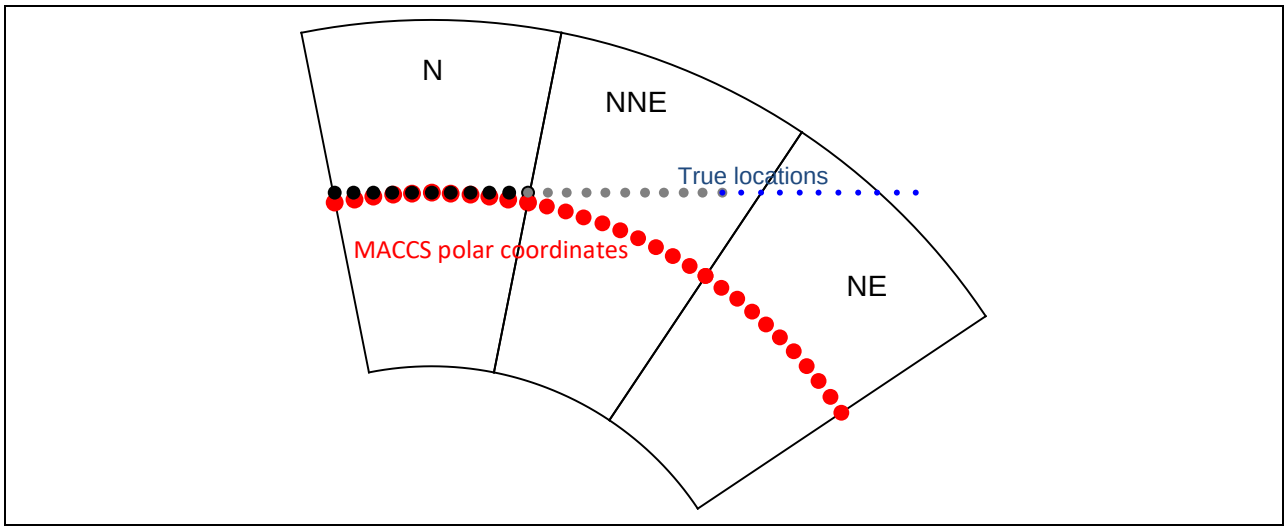

Figure 3-27. Example of red points sampled within three sectors (N, NNE, NE) to compute average concentrations or cloudshine doses. The red points fall along a constant radius arc passing through the center of each sector and are located at equidistant angles.

3.5.3 Test Results

Air Concentrations at the Ground Level, Set 1 Runs

Figure 3-28 displays sector plots prepared with Type D MACCS outputs, air concentration at the ground level. The color scheme represents concentrations in log-scale (red for high concentration, blue for low concentration). Each plot corresponds to a different value of the dispersion coefficient factor YSCALE. The dashed lines in each plot enclose a region ± 2.15 $\sigma_y(x)$ around the center, with a distance 2.15 $\sigma_y(x)$ measured along constant-radius arcs (r=x). The boundaries define the point at which the concentration becomes a factor of 10 lower than the central concentration. The ± 2.15 $\sigma_y(x)$ boundaries are practical boundaries in MACCS to define sectors with non-zero concentrations and to avoid numerical underflow. Figure 3-28 verifies that the sectors farthest away from the center with non-zero concentrations are the sectors intercepting the ± 2.15 $\sigma_y(x)$ boundaries, as expected.

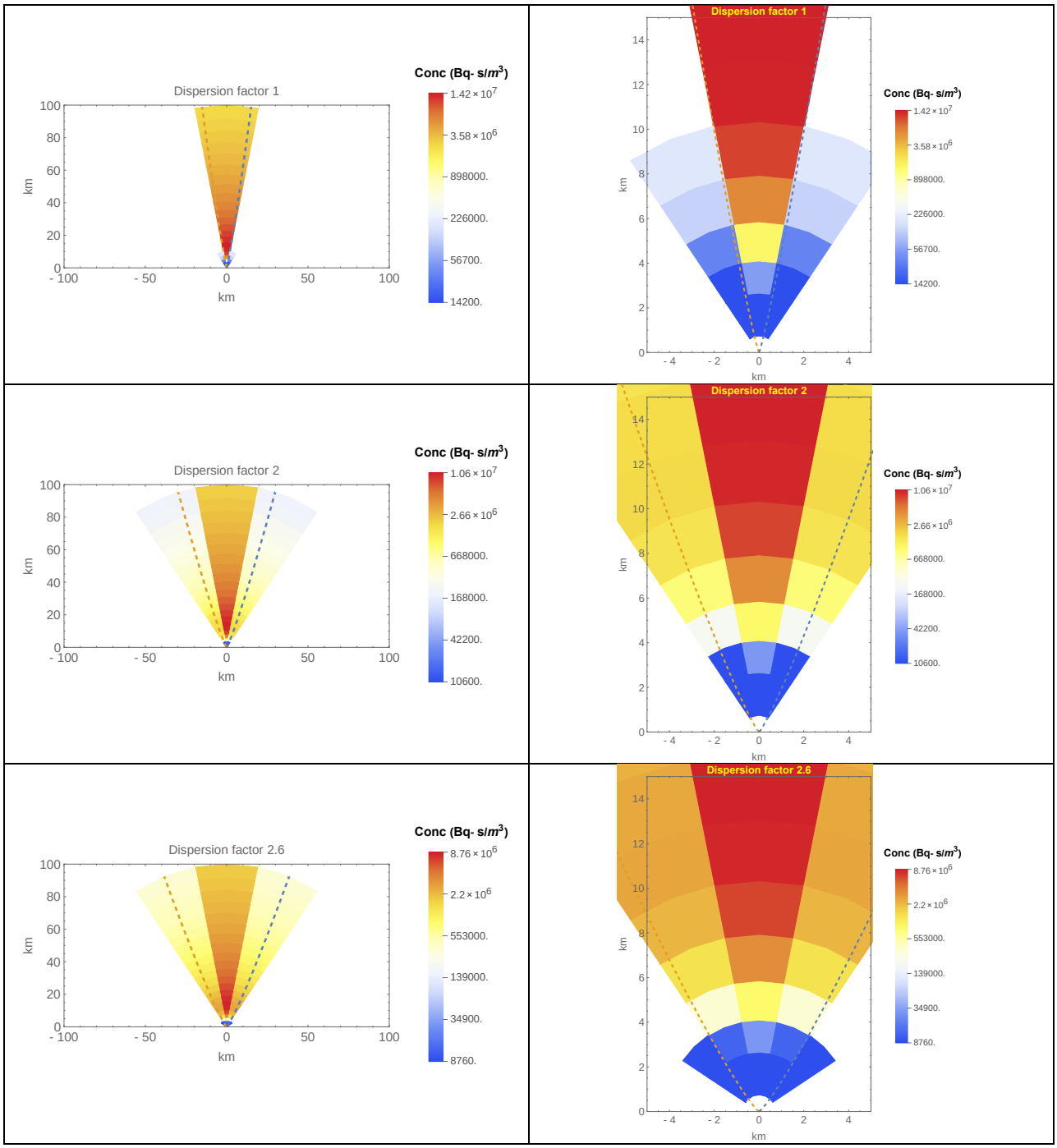

Figure 3-28. MACCS Type D sector average air concentrations at the ground level for different cases of YSCALE. Plots on the right are amplified scale plots. The dashed curves represent the ± 2.15 $\sigma_y(x)$ boundaries.

Plots in Figure 3-29 compare the MACCS outputs to average concentrations independently computed. The plots display the sector average air concentration at the ground level versus the radial distance (distance measured with respect to the source), for the different runs (different cases of YSCALE dispersion factor). MACCS outputs are represented by symbols and the independent computations by the solid curves. The different plots correspond to different sector sets oriented at specific angles (90°, 67.5°, and 45°).

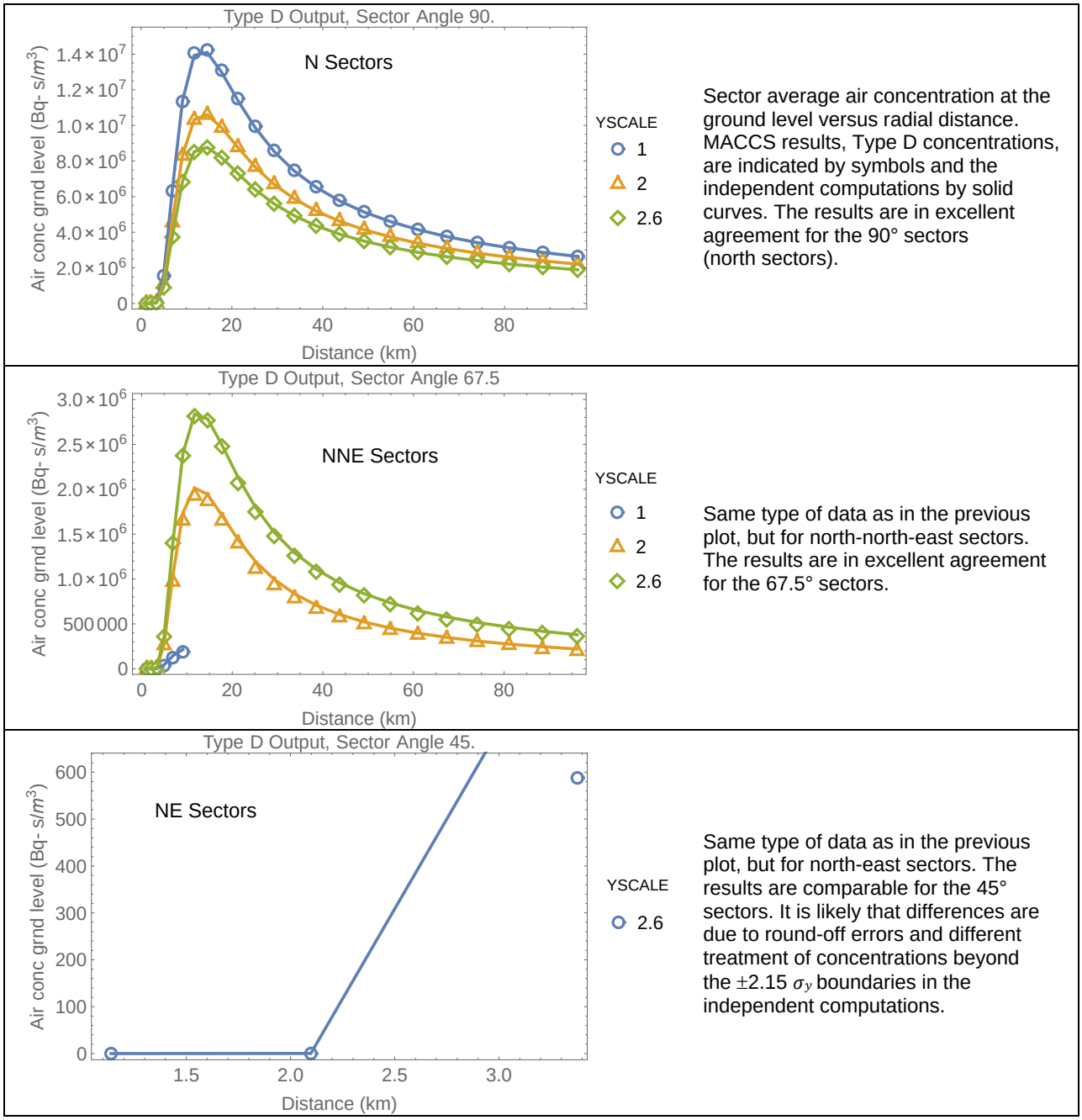

Figure 3-29. Type D sector average air concentration (symbols) versus radial distance for sectors of different orientation compared to independently computed average air concentrations (solid curves).

Figure 3-29 shows reasonable agreement between the MACCS Type D concentrations and the independent computations. There are differences in the concentrations in the north-east (45°) sectors, most likely due to round-off error and the different treatment of concentrations beyond the ± 2.15 $\sigma_y(x)$ boundaries in the independent computations. Figure 3-30 presents similar information, in the form of concentration versus the sector angle. Each plot corresponds to different values of the dispersion factor YSCALE. The color code is based on the radial distance (blue for short distance, red for far distance) in logarithmic scale. The plots indicate there is excellent agreement between the MACCS results (symbols) and the independent computations (solid lines). The last plot, with points at 45°, makes evident that differences in Figure 3-29 correspond to very small air concentrations.

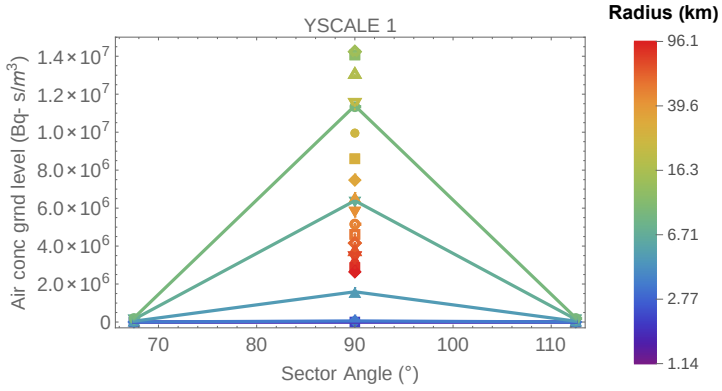

Sector average air concentration at the ground level versus sector angle for YSCALE = 1 case. MACCS Type D concentrations are indicated by symbols and the independent computations by solid curves.

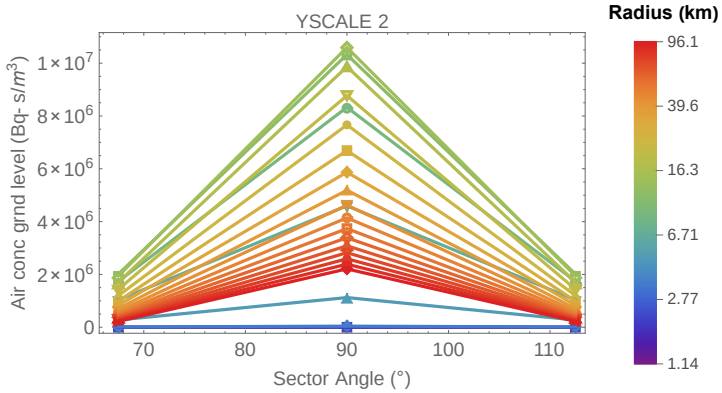

Same data type as in the previous plot, for YSCALE=2 case.

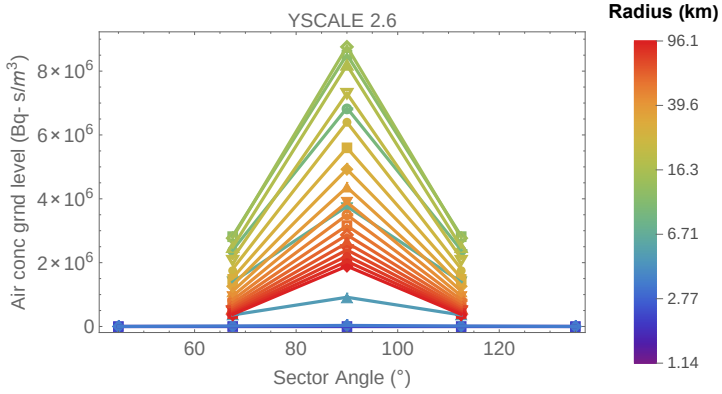

Same data type as in the previous plot, for YSCALE=2.6 case.

Figure 3-30. Comparison of Type D sector average air concentrations (symbols) versus sector angle to independent computations (solid lines) for different cases of YSCALE.

It is highlighted that the independent computations also adopted the MACCS narrow plume approximation to transform polar coordinates to Cartesian coordinates, Eq. (3-11). The approximation becomes inaccurate for sectors away from north. For example, the points along a horizontal (constant x) line in Figure 3-27, represent the true locations where concentrations and doses are effectively computed by MACCS to define averages on the polar grid. Only in the north sector are the true locations close to the red point locations in Figure 3-27. The MACCS polar locations (red dots in Figure 3-27) increasingly deviate from the true locations in north-north-east and north-east sectors. The MACCS narrow plume approximation should be kept in mind when using MACCS for consequence assessments, because it could lead to non-intuitive results especially when examining consequences of radionuclide releases under atmospheric conditions of low stability (leading to the formation of broad plumes). To explore the effect of the MACCS narrow plume approximation, an additional test was performed adopting a strict polar to Cartesian coordinate conversion, i.e.,

$$x = r \sin\theta$$
$$y = r \cos\theta \tag{3-16}$$

Concentrations and average concentrations computed along constant radius arcs were computed and compared to the MACCS outputs, following the described approaches, and using the Eq. (3-16) transformation. The results are displayed in Figure 3-31. In the north sectors, the MACCS Type D outputs are in excellent agreement with the independent computations accounting for precise polar to Cartesian conversions, as expected. For non-central sectors, the MACCS Type D outputs tend to be greater than the independently computed average concentrations. However, the independent results are still relatively close to the MACCS outputs for the NNE sectors. In testing performed with MACCS Version 4.0, which allowed laterally broader plumes, there were differences that increased in sectors away the north sector (i.e., increasing differences in the sector sequence NNE, NE, ENE, E), and always with MACCS Type D outputs greater than the independently computed values considering precise polar to Cartesian coordinate conversions. Those differences are constrained in MACCS Version 4.1 by limiting the allowed values of lateral Gaussian dispersion coefficients. In the tests, no examples were found with outputs beyond the 45° or NE sectors.

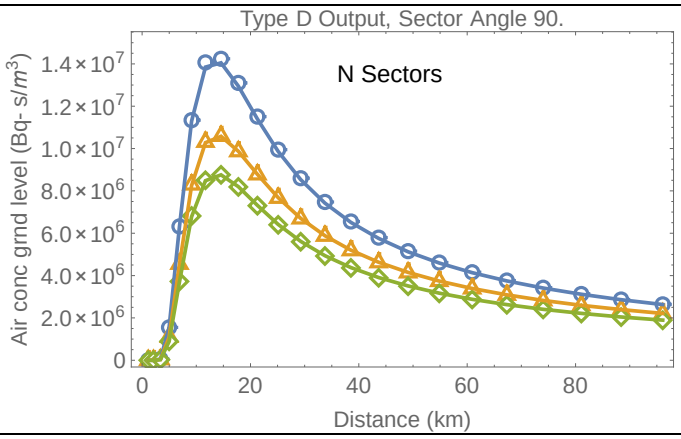

Sector average air concentration at the ground level versus radial distance. MACCS results, Type D concentrations, are indicated by symbols and the independent computations by solid curves. The results are in excellent agreement for the 90° sectors (north sectors).

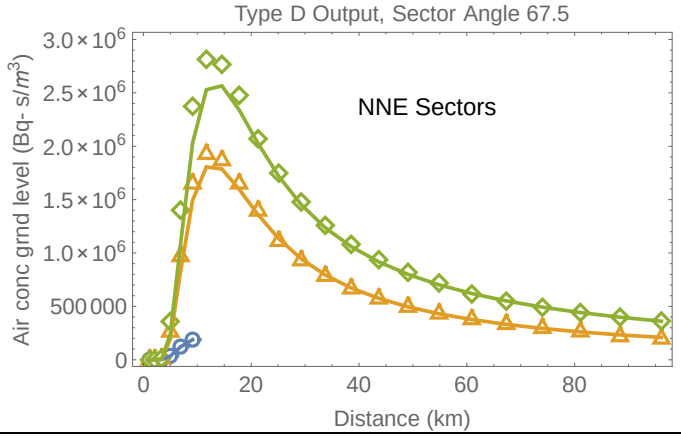

Same type of data as in the previous plot, but for north-north-east sectors. The independent computations (solid curves) with accurate polar to Cartesian coordinate conversion tend to be below the MACCS outputs.

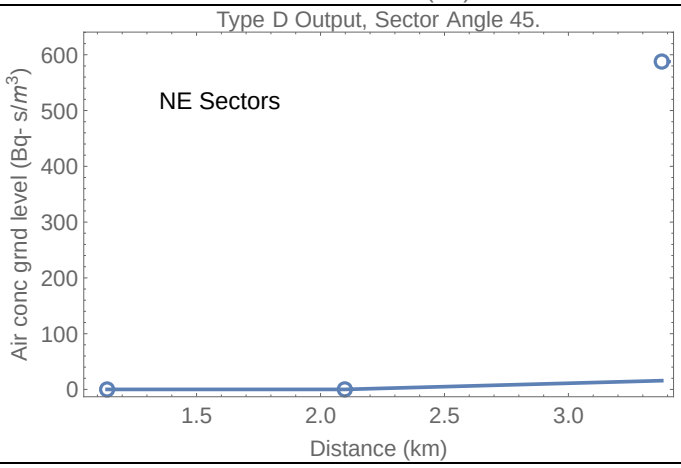

Same type of data as in the previous plot, but for north-east sectors. The independent computations (solid curves) with accurate polar to Cartesian coordinate conversion are below the MACCS outputs.

Figure 3-31. Type D sector average air concentration (symbols) versus radial distance for sectors of different orientation compared to independently computed average air concentrations (solid curves) using accurate polar to Cartesian coordinate conversion.

Cloudshine Dose, Set 2 Runs

Figure 3-32 compares the Type 6 MACCS centerline cloudshine doses (symbols) to independently computed cloudshine doses (solid curves) based on Eq. (3-15) with angle $\theta=90°=\pi/2$ radians. The Type 6 centerline doses are in excellent agreement with the independent computations. Figure 3-33 compares the Type C sector average doses (L-ICRP60 cloudshine dose, symbols) to independently computed average doses (solid curves) based on the method described in Section 3.5.2.

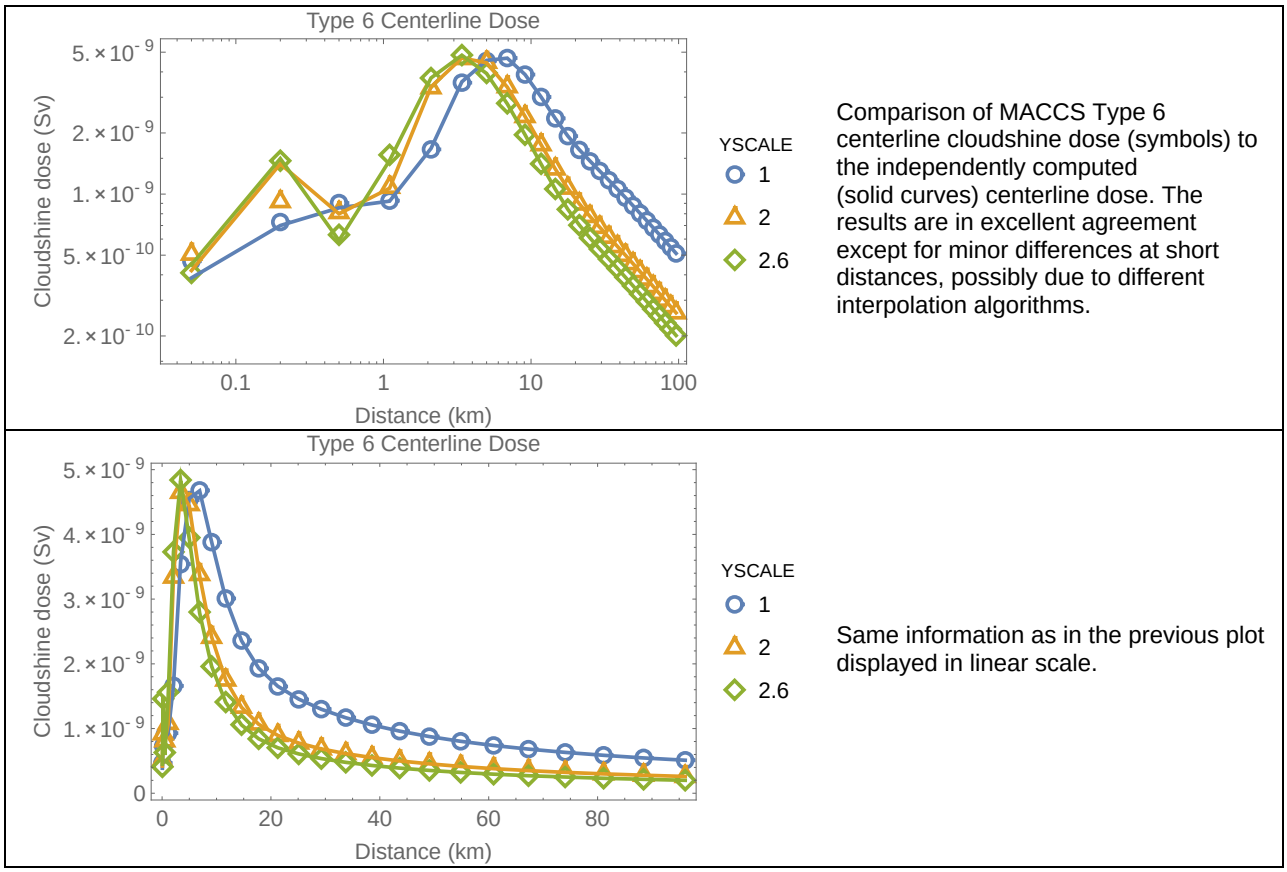

Figure 3-32. Comparison of Type 6 centerline dose outputs (symbols) to independent computations (solid curves) in logarithmic and linear scales.

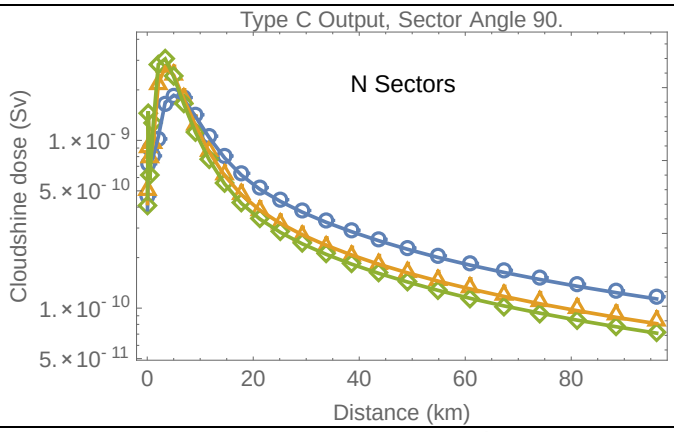

YSCALE
1
2
2.6

Comparison of MACCS Type C cloudshine dose (symbols, L-ICRP60ED) to the independent computations (solid curves) for north sectors. The results are in excellent agreement.

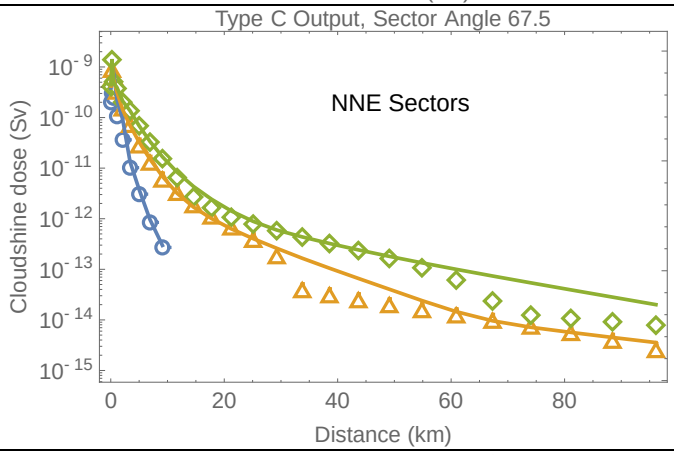

YSCALE
1
2
2.6

Same data type as in the previous plot, for north-north-east sectors. The results are in excellent agreement, except at far distances for the cases YSCALE = 2 and 2.6. Those differences are very likely due to differences in interpolation algorithms to compute the cloudshine factor for cases of large effective plume size and small relative receptor distance. Those differences may be related to jumps noted in other tests of the Type C cloudshine dose (e.g., Figure 2-6, Figure 2-7, Figure 3-8, Figure 3-9, and Figure 3-17)

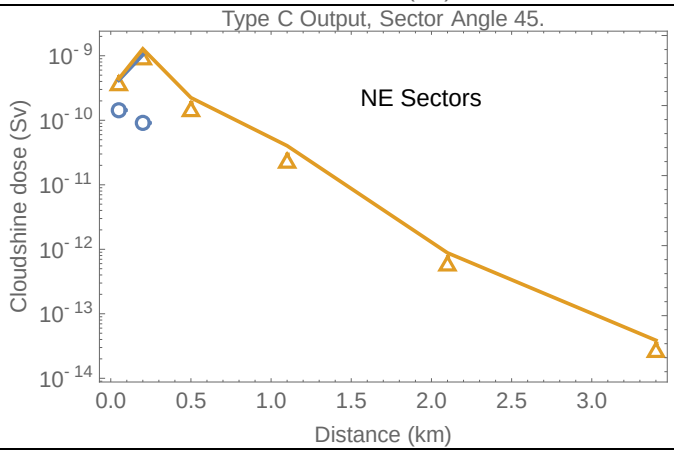

YSCALE
2
2.6

Same data type as in the previous plot, for north-east sectors. The results are in reasonable agreement, with differences possibly due to different interpolation algorithms to compute the cloudshine factor.

Figure 3-33. Type C sector average cloudshine dose versus radial distance for different sectors (symbols), compared to independent computations (solid curves) using the MACCS narrow plume approximation, Eq. (3-11).

There is reasonable agreement between the MACCS Type C outputs and the independently computed doses in Figure 3-33, with differences possibly due to different interpolation algorithms to compute the cloudshine factor. The differences in the middle plot of Figure 3-33 are likely related to jumps noted in other tests of the Type C cloudshine dose (e.g., Figure 2-6, Figure 2-7, Figure 3-8, Figure 3-9, and Figure 3-17), and explained due to differences in interpolation algorithms to compute the cloudshine factor for cases of large effective plume size, σ, and small relative receptor distance, rrd.

To complete the test, additional independent computations were implemented considering the accurate polar to Cartesian coordinate conversion, Eq. (3-16), in the computation of the cloudshine dose and the Type C average cloudshine dose. The independent computations (solid curves) and the corresponding Type C MACCS outputs (symbols) are displayed in Figure 3-34.

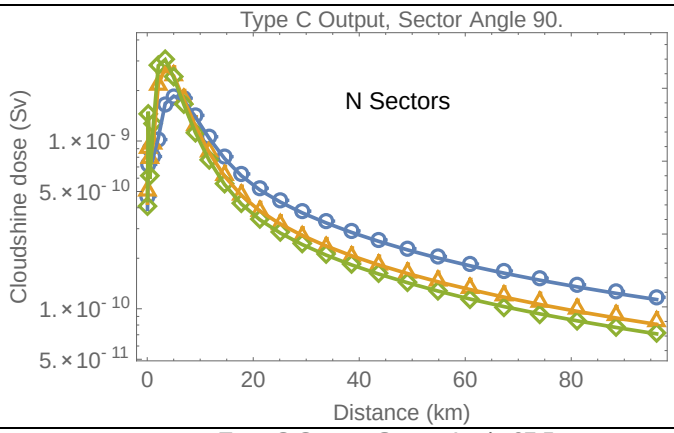

YSCALE
1
2
2.6

Comparison of MACCS Type C cloudshine dose (symbols, L-ICRP60ED) to the independent computations (solid curves) for north sectors. The results are in excellent agreement.

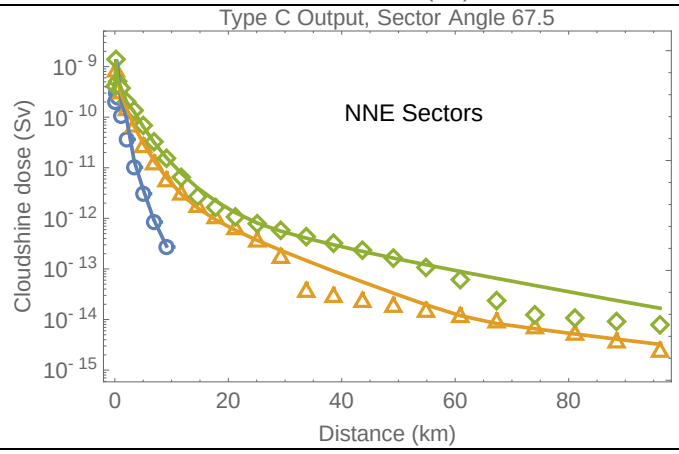

YSCALE
1
2
2.6

Same data type as in the previous plot, for north-north-east sectors. The results are in excellent agreement, except at far distances for the cases YSCALE = 2 and 2.6. Those differences are very likely due to differences in interpolation algorithms to compute the cloudshine factor for cases of large effective plume size and small relative receptor distance. Those differences may be related to jumps noted in other tests of the Type C cloudshine dose (e.g., Figure 2-6, Figure 2-7, Figure 3-8, Figure 3-9, and Figure 3-17)

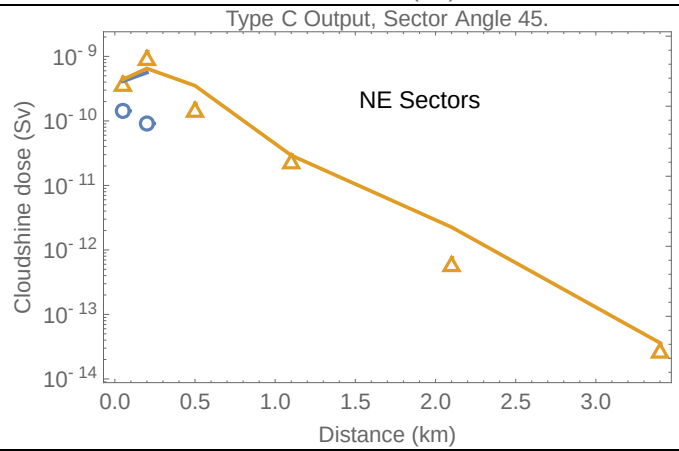

YSCALE
2
2.6

Same data type as in the previous plot, for north-east sectors. The results are in reasonable agreement, with differences possibly due to different interpolation algorithms to compute the cloudshine factor

Figure 3-34. Type C sector average cloudshine dose versus radial distance for different sectors (symbols), compared to independent computations (solid curves) using the accurate polar to Cartesian coordinate conversion, Eq.(3-16).

The results of the independent computations in Figure 3-34, using the accurate polar to Cartesian coordinate conversion, Eq.(3-16), are very similar to results in Figure 3-33, using the MACCS narrow plume approximation to transform polar to Cartesian coordinates, Eq. (3-11), with the greatest differences exhibited in the north-east sector (45° sector). It may be concluded that that extending the narrow plume approximation to sectors other than the central sectors does not seem to significantly degrade the results, although caution is recommended to generalize this conclusion for any situation. In the tests, no examples were found with outputs beyond the 45° or north-north-east sectors. For example, increasing YSCALE from 2.6 to 2.7 triggers an error message in MACCS Version 4.1 and the run is aborted. The user is requested by MACCS to reduce the extent of lateral dispersion for the run to proceed.

3.5.4 Test Conclusions

The MACCS Type D air concentrations and Type C cloudshine doses in off-center sectors agreed with independently computed values. The following aspects of the MACCS computations were verified:

- MACCS adopts a narrow plume approximation to transform polar coordinates to Cartesian coordinates in the computation of time-integrated concentrations and cloudshine doses, in the central sector and any other sector.

- MACCS applies a criterion based on a ± 2.15 $\sigma_y(x)$ arc distance around a centerline to identify sectors that are output in result files with non-zero concentrations.

- Averages based on numerical line integrals along constant-radius arcs well reproduced the MACCS Type D average time-integrated air concentrations and the Type C average cloudshine doses.

There were some differences, associated with very small concentrations, in the Type D MACCS results with respect to the designed benchmarks possibly due to the different treatment of concentrations beyond the 2.15 $\sigma_y(x)$ limits in the independent computations. Also, there were some differences in the Type C cloudshine doses possibly due to different interpolation algorithms to compute the cloudshine factor. Those differences are not considered to be errors of the MACCS code. They reflect the fact that the independent computations were not intended to precisely incorporate all the details of the MACCS computations. Minor differences with respect to the designed benchmarks were expected.

It is highlighted that the MACCS narrow plume approximation to translate polar coordinates to Cartesian coordinates tends to overestimate Type D concentrations, when generalized to laterally broader plumes. MACCS Version 4.1 introduced limits to avoid simulations with very broad plumes. For example, in the test problems, simulations with YSCALE=2.6 were allowed, but simulations with YSCALE=2.7 were aborted, by MACCS Version 4.1. The farthest sectors with non-zero concentrations were the 45° or north-north-east sectors in the tests. Although the MACCS narrow plume approximation tends to overestimate the Type D average concentrations, the results are still comparable to detailed simulations using accurate polar to Cartesian coordinate conversions. Similarly, independent computations using accurate polar to Cartesian coordinate conversions to compute Type C cloudshine doses produced results very similar to computations based on the MACCS narrow plume approximation. The comparison of results using the narrow plume approximation to results relying on accurate polar to Cartesian coordinate conversions suggests that errors caused by the narrow plume approximation in

non-central sectors are not significant. Only a few examples were examined, however, so caution is recommended in generalizing this conclusion to any scenario.

3.6 Test 3.6: Potassium Iodide Ingestion Model

The objective of this test was examining the implementation of the potassium-iodide (KI) ingestion model. The ingestion of KI pills to mitigate the effect of inhalation of radioactive isotopes of iodine is simulated in MACCS as an adjustment factor to the dose (equation 4-4 of the MACCS Theory Manual):

$$DP_{I,thyroid} = (1 - \varepsilon_{KI})\, DB_{I,thyroid} \tag{3-17}$$

$DP_{I,thyroid}$ — thyroid dose from inhalation of radioiodine considering ingestion of KI pills (Sv)

$DB_{I,thyroid}$ — thyroid dose from inhalation of radioiodine without any mitigation effects by the ingestion of KI pills (Sv)

ε_{KI} — Efficacy factor to reduce the radioiodine (1 = 100% effectivity, 0 = no effectivity), specified by EFFACY

In addition, the MACCS code includes another factor, POPFRAC, to define the fraction of people taking KI pills. To simplify computations, MACCS computes individual inhalation doses as a weighted average of the dose by individuals taking KI pills and those not taking any KI pills:

$$\overline{DP}_{I,thyroid} = POPFRAC\ (1 - \varepsilon_{KI})\, DB_{I,thyroid} + (1 - POPFRAC)\, DB_{I,thyroid} \tag{3-18}$$

$\overline{DP}_{I,thyroid}$ — average thyroid dose from inhalation of radioiodine considering ingestion of KI pills, and the fraction of the population taking and not taking KI pills (Sv)

Note that when ε_{KI} = EFFACY = 1, Eq. (3-18) reduces to

$$\overline{DP}_{I,thyroid} = (1 - POPFRAC)\, DB_{I,thyroid} \tag{3-19}$$

And when POPFRAC=1, Eq. Eq. (3-18) becomes

$$\overline{DP}_{I,thyroid} = (1 - \varepsilon_{KI})\, DB_{I,thyroid} \tag{3-20}$$

Both Eqs. (3-19) and (3-20) are identical. Therefore, a run with EFFACY = 1 and POPFRAC = 0.25 must yield identical inhalations doses to a run with POPFRAC = 1 and EFFACY = 0.25. Such test was implemented herein, as well as a test of the linearity of Eqs. (3-19) and (3-20).

3.6.1 Test Input

The input was identical to the Test 3.3, with the following changes:

General Properties

- DOSE
  - Linear No Threshold
  - Activate KI Model: TRUE

Changes to specific input parameters

ATMOS

- Radionuclides/Pseudostable Radionuclides
  - Remove I-129 from list
- Radionuclides/Radionuclides
  - Add I-129 to list
- Release Description/Release Fractions
  - RELFRC
    - I = 1
    - Other elements = 0
- Deposition, Wet/Dry Depos Flags
  - DRYDEP = WETDEP = False for I-129
- Dispersion/Scaling Factors
  - YSCALE = ZSCALE = 1
- Output Control
  - NUCOUT = I-129

EARLY

- Emergency Cohort One/KI Ingestion Linear No Threshold
  - POPFRAC = 1, EFFACY = 0, 0.25, 0.5, 0.75, 1.0
  - POPFRAC = 0, 0.25, 0.5, 0.75, 1.0, EFFACY = 1
- Shielding and Exposure
  - PROTIN = 1, inhalation dose pathway
  - BRRATE = 1 m^3/s, exaggerated breathing rate to cause sizable risk
  - CSFACT (cloudshine) = SKPFAC (skin dose) = GSHFAC (ground dose) = 0

Output Controls

- The same outputs of Test 3.3 were used.

3.6.2 Test Procedure

Two sets of MACCS runs were executed with the following inputs:

Set 1

- POPFRAC = 1
- EFFACY = 0, 0.25, 0.5, 0.75, 1.0

Set 2

- POPFRAC = 0, 0.25, 0.5, 0.75, 1.0
- EFFACY = 1

The results from Set 1 must be identical to the results from Set 2. Results from Set 1 must exhibit linear variation with the variable EFFACY. Results from Set 2 must exhibit linear variation with the variable POPFRAC. The following results were compared between Sets 1 and 2:

- Type C sector average dose
- Type 6 centerline dose
- Type 5 population dose
- Type 1 health effects

- Type 4 average individual risk
- Type 8 population-weighted individual risk

In addition, it was demonstrated that Type C results vary linearly with EFFACY for the Set 1 runs and vary linearly with POPFRAC for the Set 2 runs.

3.6.3 Test Results

Figure 3-35 displays Type C sector average inhalation doses. Type 6 centerline inhalation doses are presented in Figure 3-36. The plots in Figure 3-35 and Figure 3-36 demonstrate that the Set 1 runs (POPFRAC = 1, EFFACY = 0, 0.25, 0.5, 0.75, 1.0) and the Set 2 runs (POPFRAC = 0, 0.25, 0.5, 0.75, 1.0, EFFACY = 1) output identical results. The Set 1 results are indicated with symbols, and the Set 2 results with solid curves. The plot legend represents values of EFFACY for Set 1, or values of POPFRAC for Set 2.

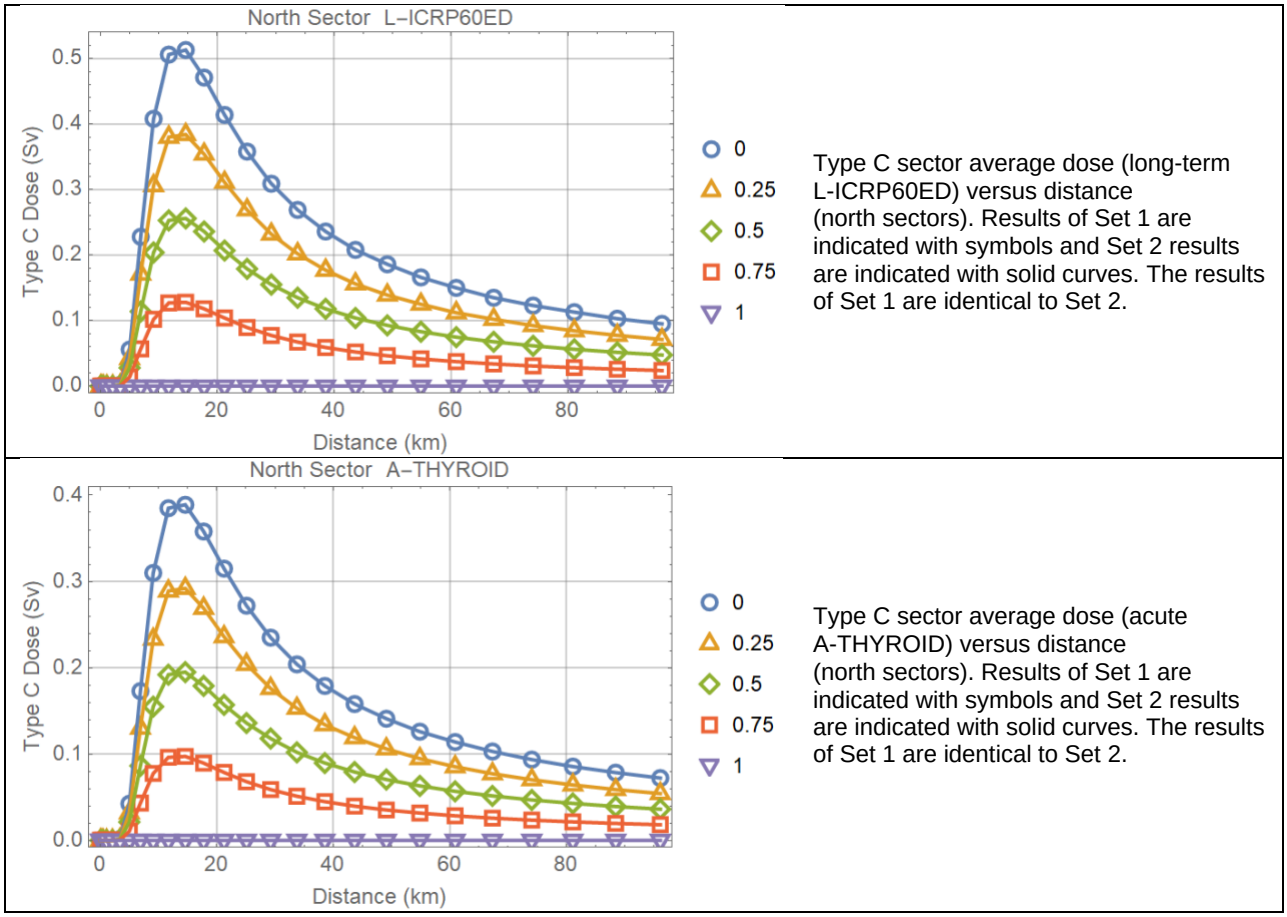

Figure 3-35. Type C inhalation dose versus distance. Each plot displays a different kind of Type C dose. The plots compare Set 1 and Set 2 results.

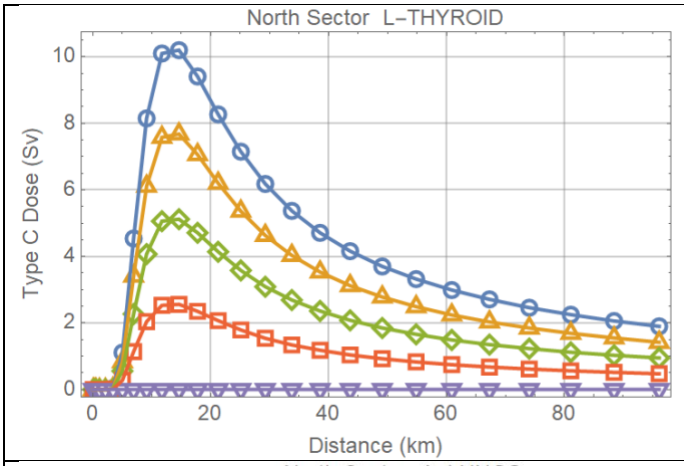

Type C sector average dose (long-term L-THYROID) versus distance (north sectors). Results of Set 1 are indicated with symbols and Set 2 results are indicated with solid curves. The results of Set 1 are identical to Set 2.

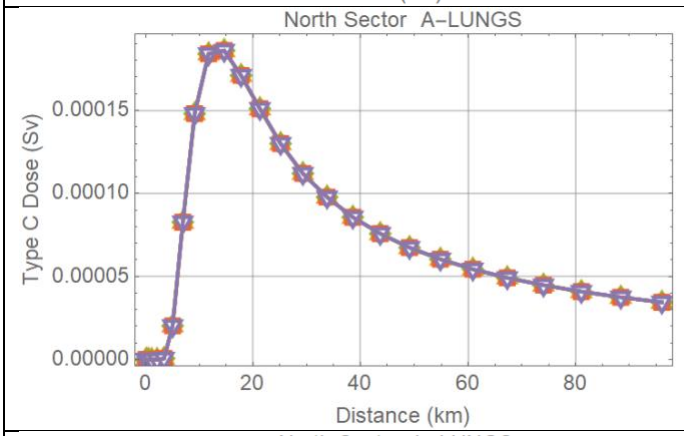

Type C sector average dose (acute A-LUNGS) versus distance (north sectors). In this case, results are independent of the value of POPFRAC and EFFACY because the acute doses to the lung are not reduced by the ingestion of KI pills (only doses to the thyroidal gland are reduced by the ingestion of KI pills).

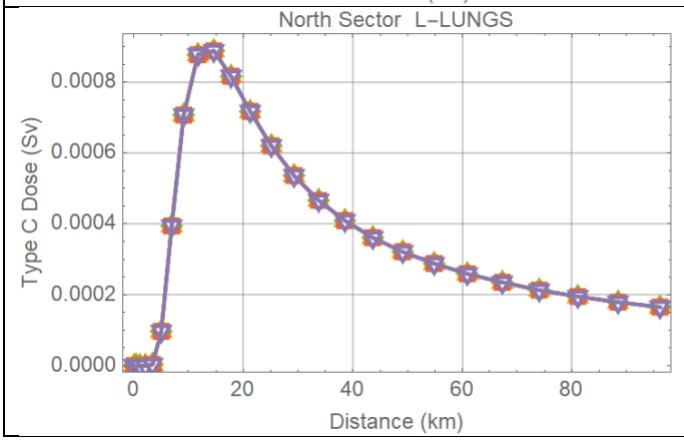

Type C sector average dose (long-term L-LUNGS) versus distance (north sectors). In this case, results are independent of the value of POPFRAC and EFFACY because the lifetime doses to the lung are not reduced by the ingestion of KI pills (only doses to the thyroidal gland are reduced by the ingestion of KI pills).

Figure 3-35 (continued). Type C inhalation dose versus distance. Each plot displays a different kind of Type c dose. The plots compare Set 1 and Set 2 results.

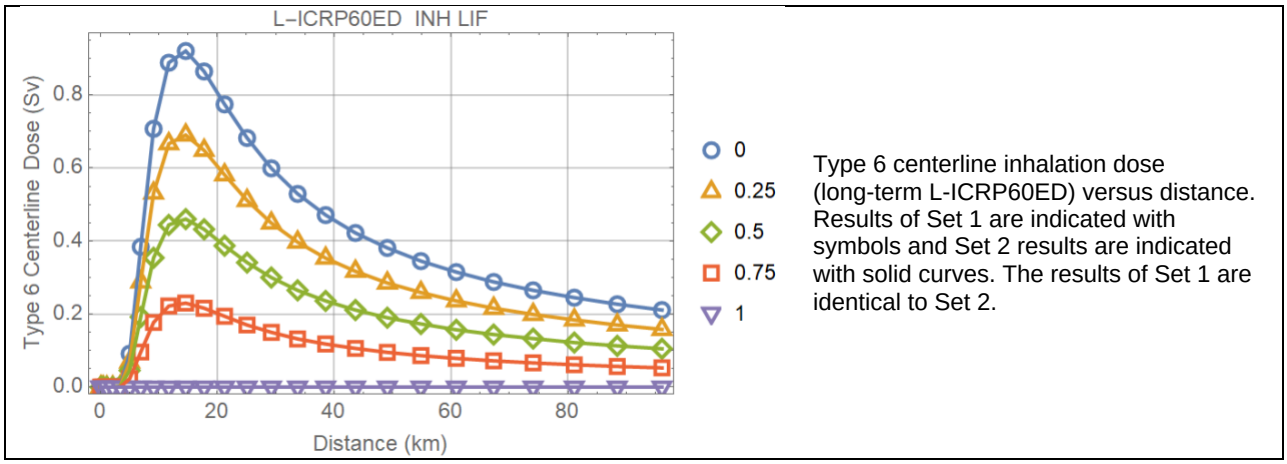

Figure 3-36. Type C inhalation dose versus distance. Each plot displays a different kind of Type c dose. The plots compare Set 1 and Set 2 results.

Figure 3-37 shows the population dose (Type 5 output), population health effects (Type 1 output), and average individual risk (Type 4 output), and population-weighted individual risk (Type 8 output).

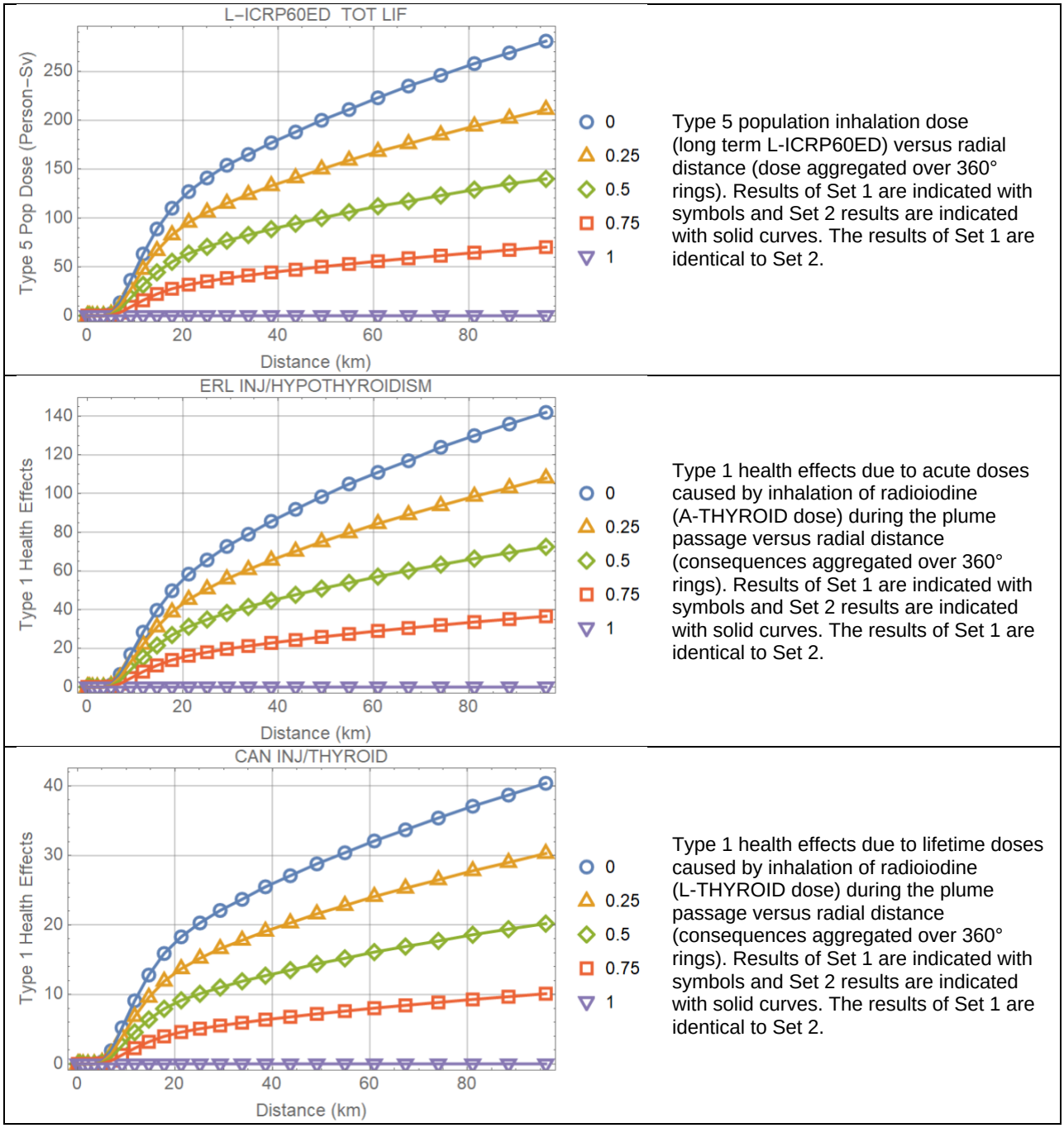

Figure 3-37. Type 5 population dose, Type 1 population health effects, Type 4 average individual risk, and Type 8 population-weighted individual risk versus radial distance. Each plot displays a different kind of output. The plots compare Set 1 and Set 2 results (they are identical).

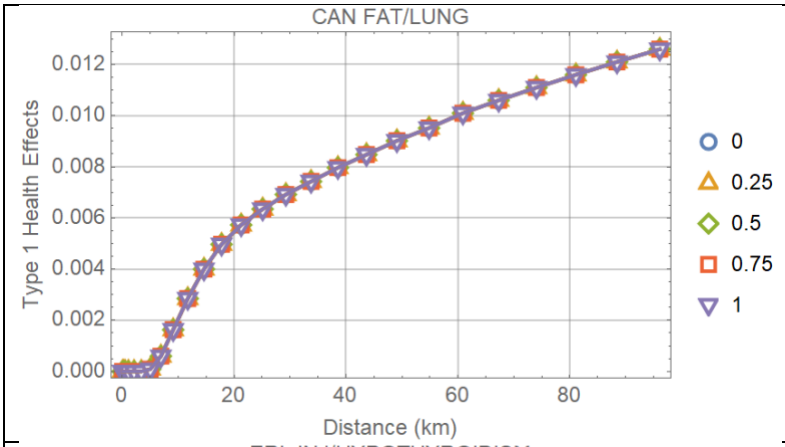

Type 1 health effects (cancer fatalities) due to lifetime doses caused by inhalation of radioiodine (L-THYROID dose) during the plume passage versus radial distance (consequences aggregated over 360° rings). In this case, results are independent of the value of POPFRAC and EFFACY because lifetime doses to the lung are not reduced by the ingestion of KI pills (only doses to the thyroidal gland are reduced by the ingestion of KI pills).

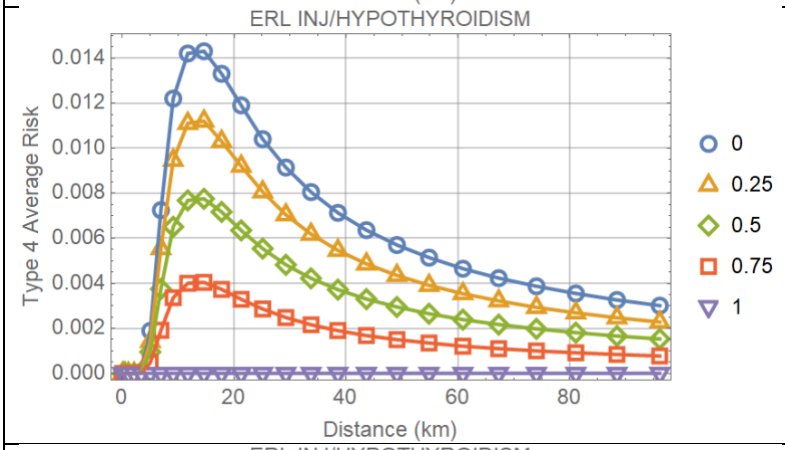

Type 4 average individual risk due to acute doses caused by inhalation of radioiodine (A-THYROID dose) during the plume passage versus radial distance (consequences averaged over 360° rings). Results of Set 1 are indicated with symbols and Set 2 results are indicated with solid curves. The results of Set 1 are identical to Set 2.

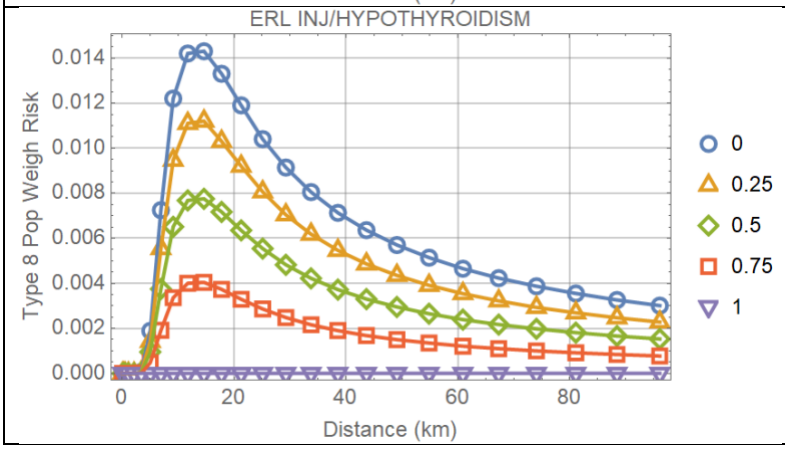

Type 8 population-weighted individual risk due to acute doses caused by inhalation of radioiodine (A-THYROID dose) during the plume passage versus radial distance (consequences aggregated over 360° rings). Results of Set 1 are indicated with symbols and Set 2 results are indicated with solid curves. The results of Set 1 are identical to Set 2.

As expected, Type 4 and Type 8 results are identical due to the use of a uniform population density in the test.

Figure 3-37 (continued). Type 5 population dose, Type 1 population health effects, Type 4 average individual risk, and Type 8 population-weighted individual risk versus radial distance. Each plot displays a different kind of output. The plots compare Set 1 and Set 2 results (they are identical).

Figure 3-38, Figure 3-39, and Figure 3-40 demonstrate the linearity of Type C sector average results on the EFFACY factor, when POPFRAC = 1 (Set 1). Since the results of Set 1 are identical to Set 2, the figure also demonstrates the linear dependence of the Type C results on POPFRAC when EFFACY = 1.

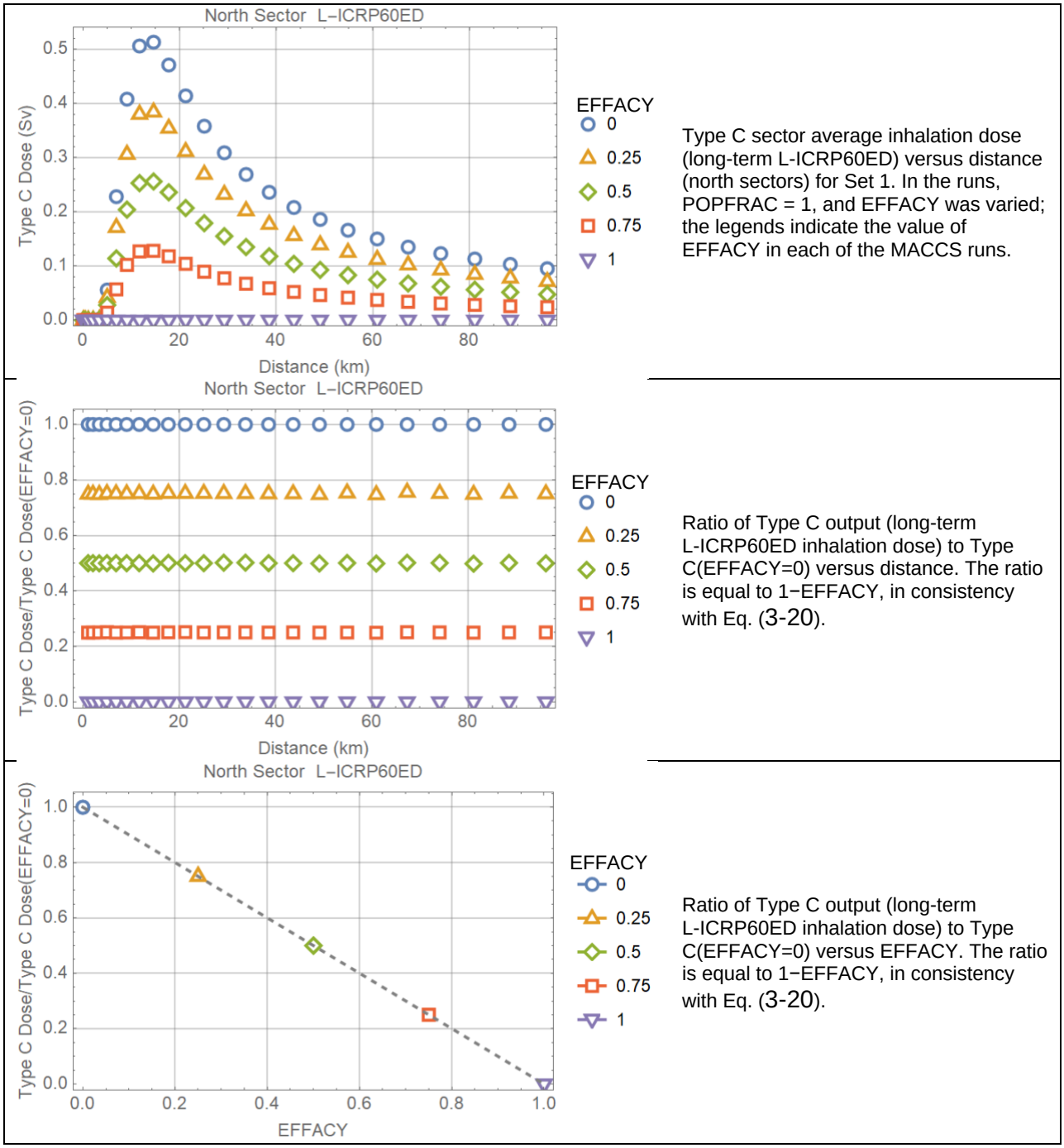

Figure 3-38. Plots demonstrating that the Type C sector average inhalation dose varies linearly with the parameter EFFACY.

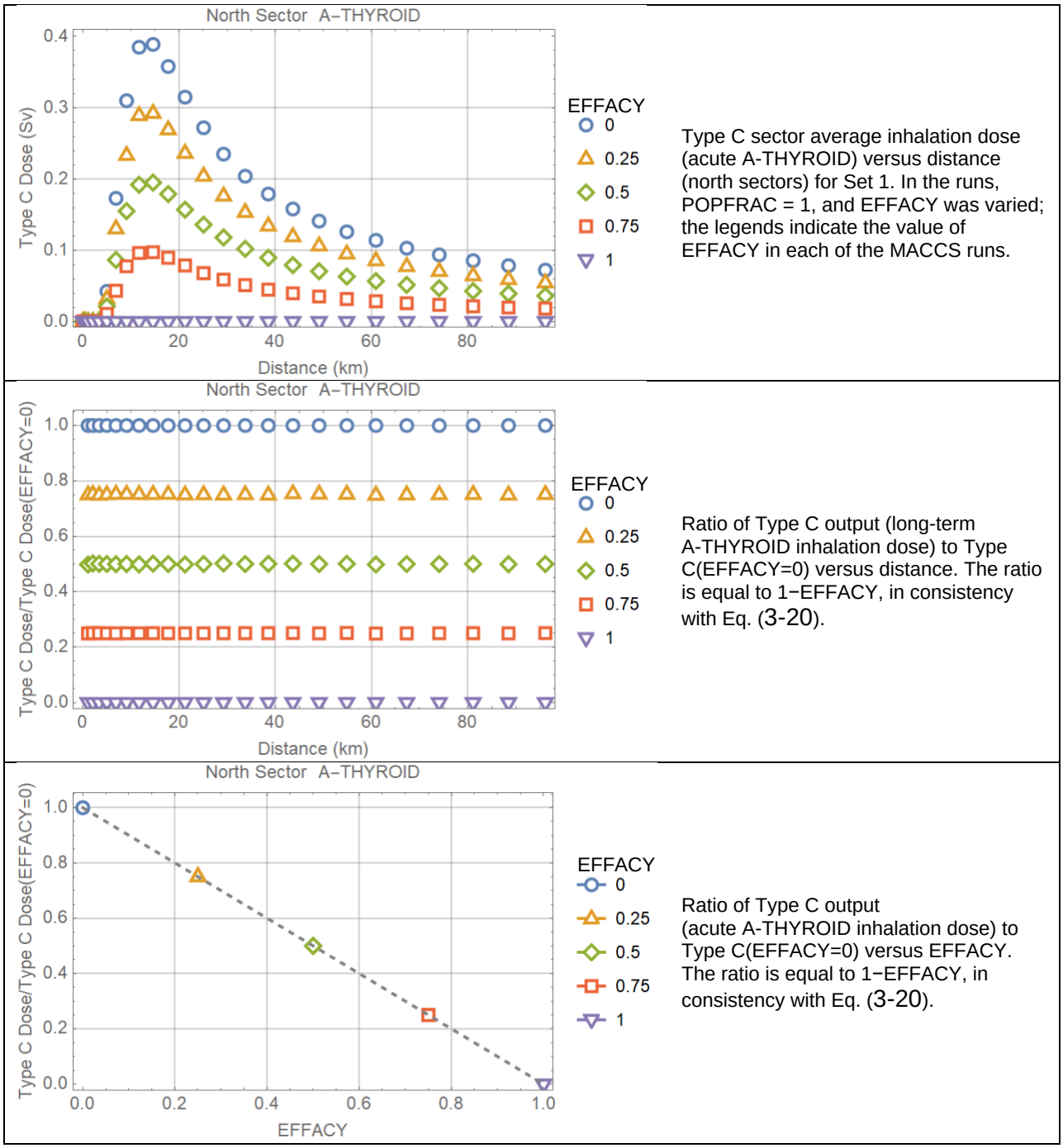

Figure 3-39. Plots demonstrating that the Type C sector average inhalation dose (acute dose to the thyroid) varies linearly with the parameter EFFACY.

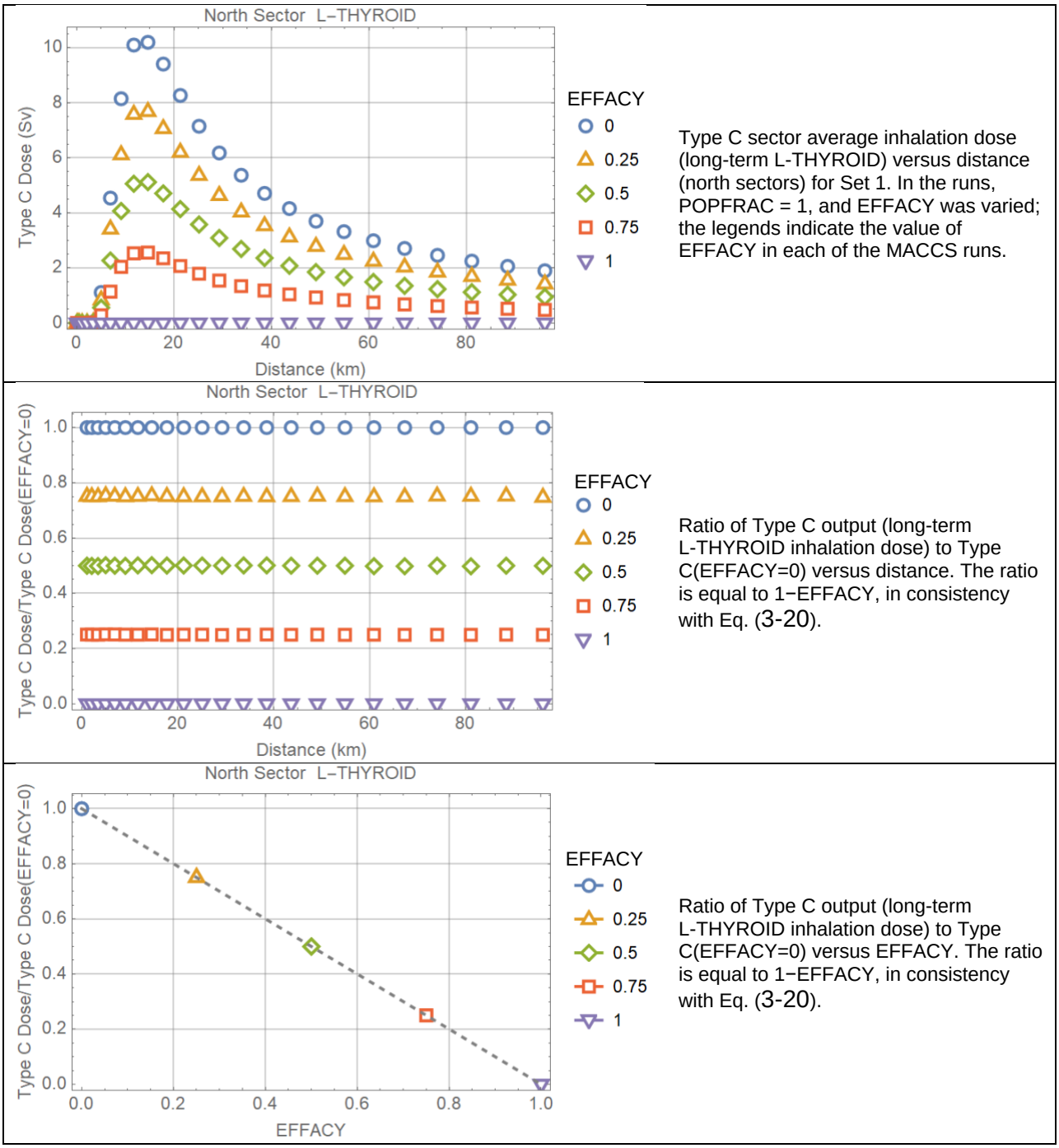

Figure 3-40. Plots demonstrating that the Type C sector average inhalation dose (long-term dose to the thyroid from inhalation of radioactivity during the passage of the plume) varies linearly with the parameter EFFACY.

3.6.4 Test Conclusions

The tests were aimed at examining the implementation of the KI pill ingestion model to mitigate doses to the thyroidal gland in case of inhalation of radioiodine during the plume passage. The tests were successful and verified that the MACCS model is consistent with Eqs. (3-17) to (3-20). The tests indirectly demonstrated that when one cohort is considered with a POPFRAC<1, then averages doses are computed for the different MACCS sectors considering the fraction of the population ingesting and not ingesting KI pills. Average health effects per sector are then computed based on the average doses. If non-linear health effects are modeled (e.g., considering beta shape parameters of risk functions, EFFACB and EIFACB, different than one), the number of health effect cases, Type 1 outputs, are approximations. To derive more accurate results, it is recommended instead to consider two cohorts: one cohort ingesting KI pills and a second cohort not ingesting the KI pills. Again, the two-cohort approach may only be considered when the parameters EFFACB and EIFACB differ from 1. In general, the approximated results are reasonable.

4 CHRONC MODULE

4.1 Test 4.1: Stochastic Health Effects from Groundshine

The objective of the test was examining the computation of the population dose and stochastic health effects from a groundshine dose pathway. The groundshine dose is computed as follows (based on equations 3-19 and 3-20 of the MACCS Theory Manual):

$$DG_k = \left(\sum_i DCG_{ik}\, GC_i \right) SFG\, \frac{1}{\mathrm{DRF}_\ell} \tag{4-1}$$

DG_k	—	groundshine dose to organ k in a sector (Sv)
DCG_{ik}	—	groundshine dose factor to organ k by radionuclide i (Sv-m^2/Bq)
GC_i	—	ground concentration of radionuclide i in a sector after the EARLY period (Bq/m^2)
SFG	—	groundshine shielding factor, specified by LGSHFAC
DRF_ℓ	—	dose reduction factor for decontamination level ℓ, specified by DSRFCT. Decontamination occurs when the dose exceeds a dose threshold DSCRLT over a period TMPACT

The groundshine dose factor DCG_{ik} is computed as

$$DCG_{ik} = DRCG_{ik} \int_{t_1}^{t_2} e^{-\lambda_i t}\, Gw(t)\, dt \tag{4-2}$$

$DRCG_{ik}$	—	groundshine dose rate coefficient to organ k by radionuclide i (Sv-m^2/Bq-s)
t_1	—	initial time for people to reside in a sector (s), t_1=ENDEMP=7 days in the test problem
t_2	—	exposure time end (s), t_2=EXPTIM + ENDEMP=50 years + 7 days in the test problem
λ_i	—	decay rate of radionuclide i (1/s)
$Gw(t)$	—	Gale's groundshine weathering function.

The dimensionless Gale's groundshine weathering function, $Gw(t)$, is a function defined as a sum of exponential decay functions, with time measured with respect to the end of the early phase (or end of the intermediate phase if such phase is enabled). The number of terms in the sum is specified by the parameter NGWTRM. The linear coefficients in the sum are specified by the parameter GWCOEF. Decay rates are specified via effective half-lives through the parameter TGWHLF with units of seconds. In the test problem, weathering was effectively disabled by setting TGWHLF = 10^{12} seconds ≈ 32,000 years, so that $Gw(t) \approx 1$.

4.1.1 Test Input

Identical inputs than Test 3.3 were used with the following changes:

General Properties

- SCOPE
  - Atmospheric Transport and Dispersion: Gaussian
  - Early Consequences

    - Late Consequences
- Food
    - No Food Model
- EARLY, Emergency Cohort One, Shielding and Exposure
    - CSFACT=0 (no cloudshine)
    - PROTIN=0 (no inhalation)
    - GSHFAC = 1 (groundshine pathway only for EARLY period)

Default inputs of the LNT Sample File were used for the CHRONC section, with the following changes:

- CHRONC Shielding and Exposure
    - LPROTIN = 0 (no inhalation pathway)
    - LGSHFAC = 1 (groundshine pathway only for CHRONC period)
- Weathering, Groundshine Weathering
    - NGWTRM = 2 (two exponential terms)
    - GWCOEF(1) = GWCOEF(2) = 0.5
    - TGWHLF(1) = TGWHLF(2) = 10^{12} seconds

Output Controls

Same outputs of Test 3.3 with the following addition

- Type 9 (NUM9) Population Dose Results
    - ORGNAM = L-ICRP60ED
    - IX1DS9 = 1 to 26 (inner radial interval)
    - IX1DS9 = 1 to 26 (outer radial interval)
    - Report Options = NONE

4.1.2 Test Procedure

A single run of the MACCS code was executed with the specified inputs. A python script was written to extract outputs from the file Model1.out. The results are printed in Model1.out in blocks, yielding the following outputs

- ATMOS Block
    - Type 0
- EARLY Block
    - Type 1, 3, 4, 5, 6, 8, A, C
    - Type D results are output in Summary.txt
- Combined Block: EARLY+CHRONC
    - Type 1, 3, 4, 5, 6, 8, A, C, D
- CHRONC Block
    - Type 1, 4, A, C
    - Type 6 results include only groundshine doses. Inhalation doses are not printed. The Type 6 doses are sector average doses for the central sector, and not centerline doses as the Type 6 EARLY module results.
    - Lone Type D results are not available, but combined EARLY+CHRONC Type D outputs are available in the Combined Block
    - Type 9 population dose results

The EARLY Type D ground concentrations (sector average concentrations) were extracted, and the groundshine dose was computed using Eq. (4-1), considering a long-term exposure equal to 50 years (= EXPTIM). The results were compared to the CHRONC Type C sector average doses.

Using the CHRONC C Type C sector average doses, the population dose was computed using the method described in Test 3.2, and compared to the CHRONC Type 9 population dose. Similarly, the stochastic health effects were computed based on the CHRONC C Type C sector average dose, using the method described in Test 3.3, and compared to the Type 1 and Type 4 CHRONC outputs.

4.1.3 Test Results

Comparison of the CHRONC Type C sector average groundshine dose (north sector, centerline sector) to independent computations is presented in Figure 4-1.

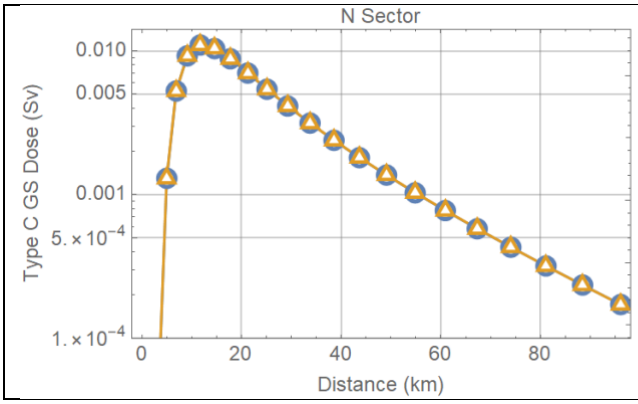

Comparison of the Type C CHRONC output (blue circles) to independent computations based on the Type D (sector average ground concentration) output by the EARLY module (yellow triangles). The comparison includes only the centerline, north sectors.

Figure 4-1. Type C groundshine dose (north sector) versus distance; comparison of MACCS outputs to independent computations.

The CHRONC Type 9 population dose (tracked in the output file Model1.out with the label "LONG-TERM GROUNDSHINE DOSE") was compared to the population dose independently computed based on the Type C individual groundshine dose (L-ICRP60ED) output by the CHRONC module and considering a uniform population density (POPDEN = 10 people/km^2). Independently computed population doses were aggregated over a 360° ring for comparison to the CHRONC Type 9 outputs. The results are presented in Figure 4-2.

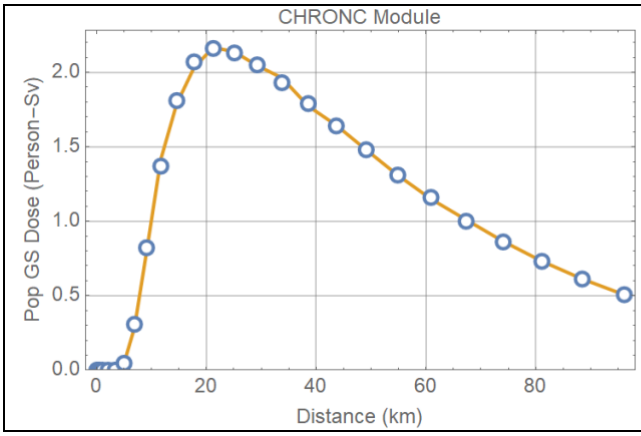

Comparison of the CHRONC Type 9 population dose (blue circles) to independent computations based on the Type C (sector average groundshine dose) output by the CHRONC module (solid curve) and sector outputs aggregated over 360° rings.

Figure 4-2. Type 9 population dose versus radial distance; comparison of MACCS outputs to independent computations.

Stochastic health effects, Type 1 and 4 outputs by the CHRONC module, were compared to independently computed health effects based on the Type C individual groundshine dose output by the CHRONC module (using the methods described in Test 3.3). The results are presented in Figure 4-3.

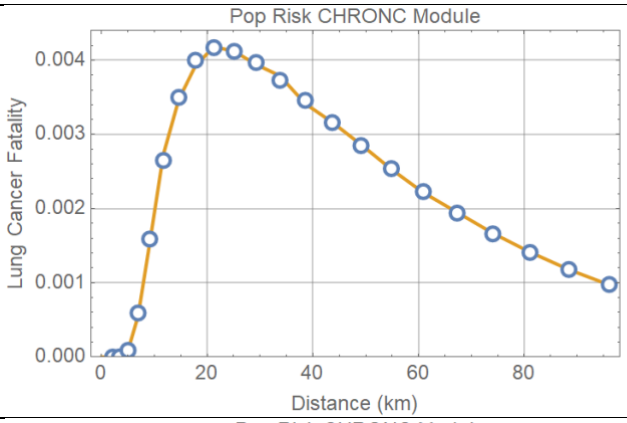

Comparison of the CHRONC Type 1 long-term lung cancer fatality (blue circles) to independent computations based on the Type C (sector average groundshine L-LUNGS dose) output by the CHRONC module (solid curve). The independent computations aggregate risk results over 360° rings.

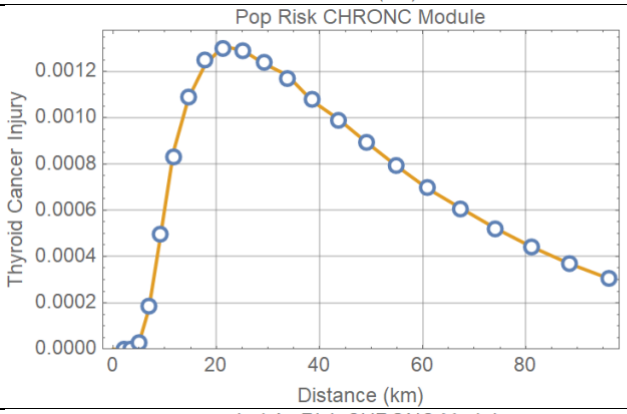

Comparison of the CHRONC Type 1 long-term non-fatal thyroid cancer (blue circles) to independent computations based on the Type C (sector average groundshine L-THYROID dose) output by the CHRONC module (solid curve). The independent computations aggregate risk results over 360° rings.

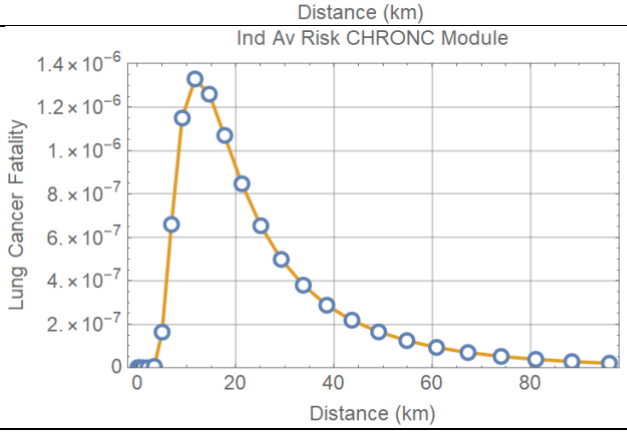

Comparison of the CHRONC Type 4 average individual long-term fatal lung cancer risk (blue circles) to independent computations based on the Type C (sector average groundshine L-LUNGS dose) output by the CHRONC module (solid curve). The independent computations aggregate risk results over 360° rings.

Figure 4-3. Type 1 and Type 4 health effects versus radial distance; comparison of MACCS outputs to independent computations.

4.1.4 Test Conclusions

MACCS successfully passed the designed tests.

4.2 Test 4.2: Stochastic Health Effects from Inhalation of Resuspension

The objective of the test was examining the computation of the population dose and stochastic health effects from an inhalation dose (inhalation of resuspension of radionuclides from the ground) pathway. The resuspension inhalation dose is computed as follows (based on equations 3-22 and 3-23 of the MACCS Theory Manual):

$$DR_k = \left(\sum_i DCR_{ik}\ GC_i \right) BR\ SFI\ \frac{1}{\mathrm{DRF}_\ell} \tag{4-3}$$

DR_k — inhalation dose to organ k in a sector due to resuspension of ground contamination (Sv)

DCR_{ik} — resuspension inhalation dose factor to organ k by radionuclide i for a given time period, defined in Eq. (4-4) below (Sv-s-m^{-1}/Bq-inhaled)

GC_i — ground concentration of radionuclide i in a sector after the EARLY period (Bq/m^2)

BR — breathing rate, specified by LBRRATE (m^3/s)

SFI — inhalation shielding factor, specified by LPROTIN

DRF_ℓ — dose reduction factor for decontamination level ℓ, specified by DSRFCT. Decontamination occurs when the dose exceeds a dose threshold DSCRLT over a period TMPACT

The resuspension inhalation dose factor DCR_{ik} is computed as

$$DCR_{ik} = DCI_{ik} \int_{t_1}^{t_2} e^{-\lambda_i t}\ Rw(t)\ dt \tag{4-4}$$

DCI_{ik} — inhalation dose coefficient to organ k by radionuclide i (Sv/Bq-inhaled)

t_1 — initial time for people to reside in a sector (s), t_1=ENDEMP=7 days in the test problem

t_2 — exposure time end (s), t_2=EXPTIM + ENDEMP=50 years + 7 days in the test problem

λ_i — decay rate of radionuclide i (1/s)

$Rw(t)$ — resuspension weathering function (m^{-1}).

The resuspension weathering function, $Rw(t)$, is a function defined as a sum of exponential decay functions, with time measured with respect to the end of the early phase (or end of the intermediate phase if such phase is enabled). The number of terms in the sum is specified by the parameter NRWTRM. The linear coefficients in the sum are specified by the parameter RWCOEF. Decay rates are specified via effective half-lives through the parameter TRWHLF with units of seconds. In the test problem, weathering was effectively disabled by setting TRWHLF = 10^{12} seconds ≈ 32,000 years, so that $Rw(t) \approx 1$.

4.2.1 Test Input

Identical inputs than Test 4.1 were used with the following changes.

General Properties

- EARLY, Emergency Cohort One, Shielding and Exposure
  - CSFACT = 0 (no cloudshine)
  - PROTIN = 1 (yes inhalation pathway)
  - BRRATE = 10^{-4} m^3/s (breathing rate for the EARLY period)
  - GSHFAC = 0 (no groundshine pathway)
- CHRONC Shielding and Exposure
  - LPROTIN = 1 (yes inhalation pathway)
  - LGSHFAC = 0 (no groundshine pathway)
- Weathering, Resuspension Weathering
  - NRWTRM = 3 (three exponential terms)
  - RWCOEF(1) = 0.5, RWCOEF(2) = RWCOEF(3) = 0.25
  - TRWHLF(1) = TRWHLF(2) = TRWHLF(3) = 10^{12} seconds
- Long Term Dose Criterion
  - DSCRLT (Sv) specified with different values in the different runs
- Decontamination Plan
  - LVLDEC = 2 (2 decontamination levels)
  - TIMDEC = 10^{-6} s (assumed almost instant decontamination, as soon as triggered)
  - DSRFCT(1) = 3, DSRFCT(2) = 15 (decontamination factors)

Output Controls

- The same outputs of Test 4.1 were used.

4.2.2 Test Procedure

This test was similar to Test 4.1, but focused on inhalation dose. The inhalation dose in the tests exceeded the threshold dose to trigger decontamination, DSCRLT. Therefore, in this test, the approach to compute the different decontamination levels was examined. Four runs of the MACCS code were executed with the following values of DSCRLT

- DSCRLT = 1 Sv
- DSCRLT = 5 Sv
- DSCRLT = 10 Sv
- DSCRLT = 100 Sv

In all runs, the long-term projection period for decontamination was TMPACT = 1.58×10^8 s = 5 years. The long-term projection period is used in MACCS to compute an individual dose and compare that dose to the threshold dose DSCRLT. If the individual dose exceeds DSCRLT, the different decontamination levels are applied [either DSRFCT(1) = 3 or DSRFCT(2) = 15] to bring the dose below the threshold. If the highest decontamination level is not enough to bring the individual dose below the threshold, then permanent interdiction is assumed: people are assumed mobilized away from all those sectors that cannot be brought below the target threshold dose. The test was aimed to verify the computational approach to implement decontamination.

4.2.3 Test Results

Figure 4-4 compares the CHRONC Type C individual inhalation dose (circles) for the north sectors to independently computed inhalation doses (yellow, green, and red dashed curves). The independently computed values were based on Type D ground concentrations (north sectors) output by the EARLY module, Eq. (4-3), and considering 50 years of exposure [EXPTIM=1.58×10^9 s]. The yellow curve considers no decontamination, the green curve considers a factor 3 decontamination [decontamination level 1, DSRFCT(1) = 3], and the red curve considers a factor 15 decontamination [decontamination level 1, DSRFCT(1) = 2].

The purple dots represent the inhalation dose after 5 years of exposure. They were computed as

$$D_5 = D_C \frac{\int_0^{5\ \mathrm{yr}} e^{-\lambda_{Cs-137} t}\ dt}{\int_0^{50\ \mathrm{yr}} e^{-\lambda_{Cs-137} t}\ dt} \approx 0.16\ D_C \qquad (4\text{-}5)$$

D_5 — 5-year projected inhalation dose (Sv)
D_C — Type C inhalation dose output by the CHRONC module (sector average dose)
λ_{Cs-137} — decay rate of Cs-137 (7.307×10^{-10} 1/s)

The results of the independent computations are in excellent agreement with the MACCS outputs. The purple dots lie all below the dose threshold, DSCRLT, indicated by a black horizontal dashed line, as expected. The dose threshold concept is correctly applied. The MACCS Type C dose outputs exhibit jumps consistent with the 5-yr projected dose, and it is zero at points where the 5-yr projected dose cannot be made less than DSCRLT after the highest decontamination level (triggering permanent interdiction).

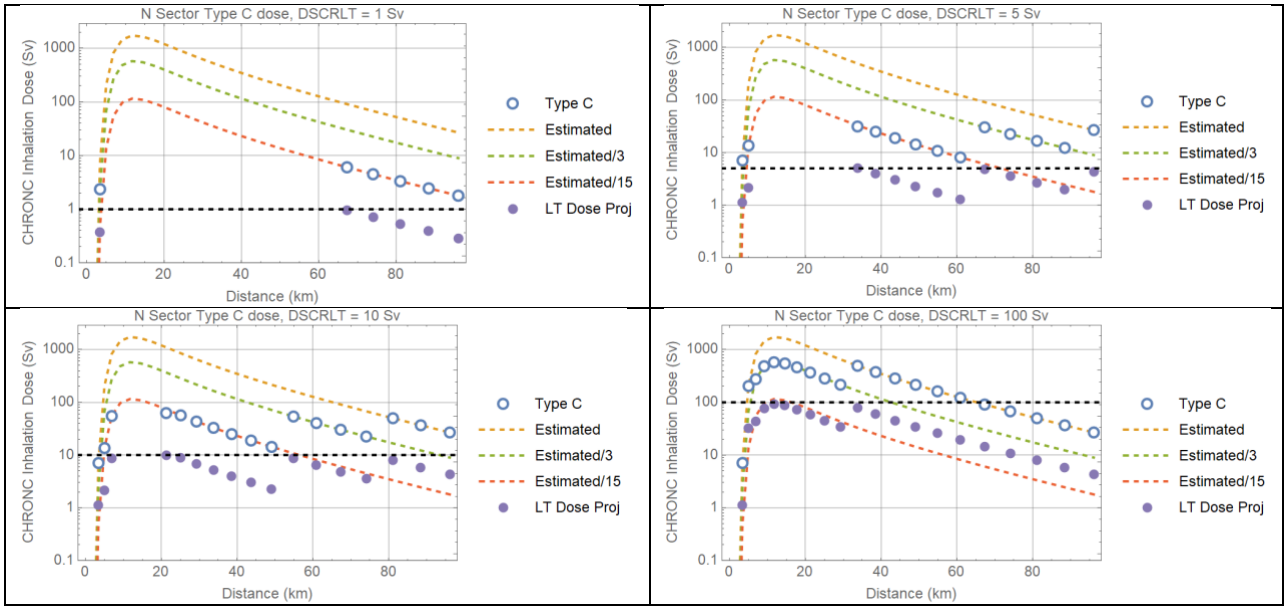

Figure 4-4. Type C inhalation dose versus radial distance; comparison of MACCS outputs (circles) and independent computations (dashed curves). Each plot displays a different case of threshold dose DSCRLT.

The CHRONC Type 9 population dose (tracked in the output file Model1.out with the label "LONG-TERM RESUSPENSION DOSE") was compared to the population dose independently computed based on the Type C individual inhalation dose (L-ICRP60ED) output by the CHRONC module and considering a uniform population density (POPDEN = 10 people/km^2). Independently computed population doses were aggregated over a 360° ring for comparison to the CHRONC Type 9 outputs. The results are presented in Figure 4-5. The symbols correspond to MACCS outputs, and the solid curves correspond to the independently computed population doses.

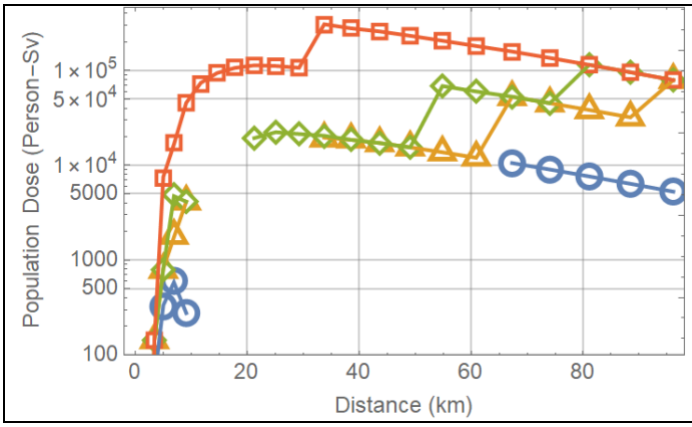

Comparison of the CHRONC Type 9 population dose (symbols) to independent computations based on the Type C (sector average inhalation dose) output by the CHRONC module (solid curves).

Figure 4-5. Type 9 population dose versus radial distance; comparison of MACCS outputs and independent computations.

Figure 4-6 displays stochastic health effects, Type 1 and Type 4 outputs by the CHRONC module, compared to independent computations based on the Type C individual inhalation dose output by the CHRONC module. The computational approach is identical to the approach described in Test 3.3.

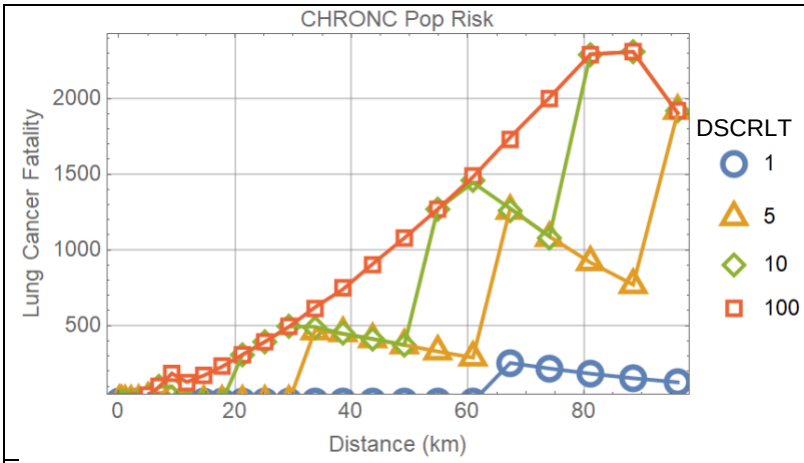

Comparison of the CHRONC Type 1 long-term lung cancer fatality (symbols) to independent computations based on the Type C (sector average inhalation L-LUNGS dose) output by the CHRONC module (solid curves). The independent computations aggregate risk results over 360° rings.

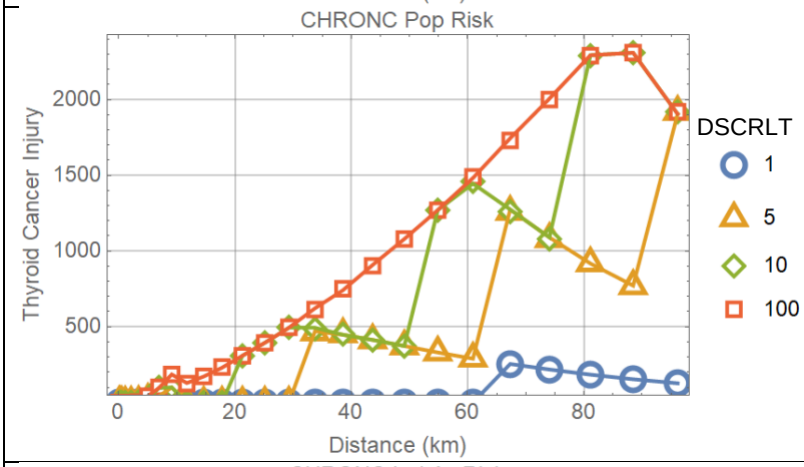

Comparison of the CHRONC Type 1 long-term non-fatal thyroid cancer (symbols) to independent computations based on the Type C (sector average inhalation L-THYROID dose) output by the CHRONC module (solid curves). The independent computations aggregate risk results over 360° rings.

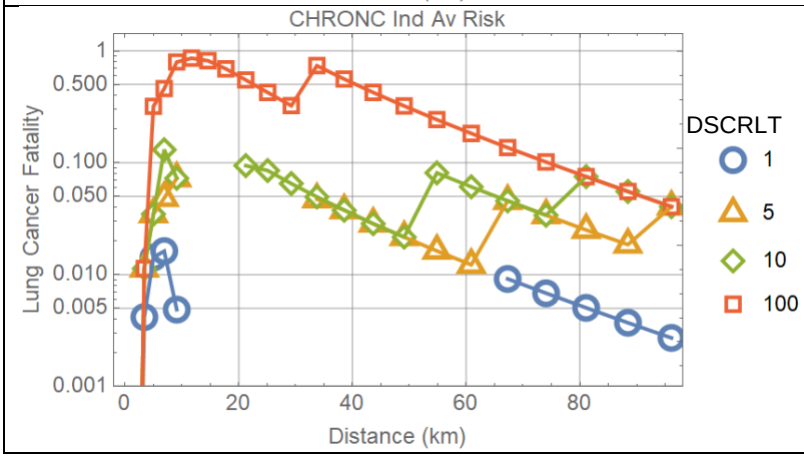

Comparison of the CHRONC Type 4 average individual long-term fatal lung cancer risk (symbols) to independent computations based on the Type C (sector average inhalation L-LUNGS dose) output by the CHRONC module (solid curves). The independent computations aggregate risk results over 360° rings.

Figure 4-6. Type 1 and Type 4 outputs versus radial distance; comparison of MACCS outputs and independent computations.

4.2.4 Test Conclusions

MACCS successfully passed the designed tests.

5 CONCLUSIONS

Numerous tests in this report examined and verified the implementation of numerical algorithms and functions of the MACCS code. The testing was organized in three main sections. Section 2 documents testing of the ATMOS module, Section 3 documents testing of the EARLY module, and Section 4 documents testing of the CHRONC module. Testing focused on equations to compute radionuclide concentrations in air and on the ground, doses from multiple pathways (groundshine, inhalation, cloudshine, and dose to the skin from plume passage), and health effects (injury due to passage of a radioactive plume and acute doses, and long-term cancer), based on examination of simple systems (e.g., constant wind speed and direction, one plume segment, one cohort, one single radionuclide, no mitigation actions, no evacuation, no relocation). Table 5-1 compares the scope of the testing to the table of contents of the MACCS Theory Manual. As demonstrated in the table, the testing covered a broad range of features and functions of the MACCS code, keeping in mind that the systems modeled in the test runs represented simple systems.

The tests were successful in the verification of equations and algorithms of the MACCS code as described in the MACCS Theory Manual (Nosek, et al., 2021). Minor differences of MACCS cloudshine dose outputs with respect to designed benchmarks, likely related to differences in interpolation methods for the computation of the cloudshine factor, which differences do not necessarily indicate deficiencies in the MACCS algorithms but the employment of practical approximations. In general, there was excellent agreement of the MACCS outputs with the designed benchmarks, keeping in mind that benchmarks did not include all details of the MACCS computations, and, thus, differences are expected in a few cases. The results provide confidence that the tested MACCS algorithms were properly implemented and consistent with descriptions in the MACCS Theory Manual.

Testing with MACCS Version 4.0 revealed errors related to the treatment of broad plumes and computation of concentrations in off-center sectors. Those errors were addressed in MACCS Version 4.1, by applying limitations to the lateral spread of plumes (runs are aborted by MACCS if the lateral plume spread is too broad), correctly enforcing practical limits to define off-center sectors with non-zero and zero concentrations, and greatly extending the domain of lookup tables to compute the cloudshine factor. In the tests aimed at examining broad plumes (e.g., Test 3.5), the farthest sectors with non-zero concentrations were the 45° (north-east) and the 135° (north-west) sectors (the wind was assumed to be blowing north, i.e., the plume centerline aligned with the north direction). Trying runs with laterally broader plumes would cause MACCS to abort and print an error message requesting the user to adjust the extent of the lateral plume spread. MACCS Version 4.1 appears to restrict plumes to lie between the 135° and 45° sectors when the wind is blowing north.

MACCS adopts a narrow plume (narrow angle) approximation to convert polar coordinates of the MACCS spatial grid to cartesian coordinates. This conversion is needed, for example, to use steady-state Gaussian plume functions and cloudshine factor functions defined in Cartesian coordinates. The narrow plume approximations become inaccurate in off-center sectors (e.g., north-north-east and north-east sectors if the wind is blowing north). Test 3.5 examined differences in results if accurate polar to Cartesian coordinate conversions were adopted. Given that MACCS Version 4.1 constrains the lateral spread of plumes to few sectors around the central sector, the tests suggest minor differences in both the sector average radionuclide concentrations and the sector average cloudshine doses with respect to simulations using a precise polar to Cartesian coordinate conversion. The differences would be amplified if MACCS allowed the simulation of laterally broader plumes. Although it would be desirable to remove

approximations such as the narrow plume approximation to enhance the applicability of the MACCS models, the Test 3.5 suggests that the gain in precision would be modest if the lateral spread of plumes is kept constrained. Also, the narrow plume approximation tends to overestimate the radionuclide concentration in off-center sectors, which is a conservative approach in MACCS, at least in the few test examples examined in this report.

Table 5-1. Comparison of the table of contents of the MACCS Theory Manual (Nosek, et al., 2021) to tests documented in this report.

MACCS Theory Manual Table of Contents	Test number addressing feature	Comments
2 Atmospheric Transport		
2.1 Introduction	NA	
2.2 Atmospheric Source Term		
2.2.1 Radionuclide Inventory Characteristics	Test 2.1	
2.2.2 Plume Segment Characteristics	Test 2.1	
2.3 Weather		
2.3.1 Weather Data	Indirect testing	During initial and exploratory testing, the input weather file was modified to set a simple weather pattern (constant wind speed, north direction, stability class D). The MACCS run successfully reflected features of the simple weather pattern. Documented tests in this report relied on an alternative approach to set a simple weather pattern, based on the constant or boundary weather inputs (METCOD=4).
2.3.2 Weather Modeling	Limited testing	All tests in this report used the option IPLUME=1 (no wind shift with rotation), with specified wind rose probabilities, WINROS, selected for wind blowing in the north direction only.
2.3.3 Weather Sequence Selection	Not tested	
2.3.4 Mixing Height Model	Not tested	
2.3.5 Boundary Weather	Limited testing	Most of the tests were implemented with constant weather inputs (METCOD=4). Tests 2.3 and 2.4 considered the user supplied weather, METCOD=4.
2.4 Atmospheric Release		
2.4.1 Wake Effects	Indirect testing, Test 2.1	Wake effects are accounted for with selection of initial values of the Gaussian dispersion coefficients. All tests in this report considered SIGYINIT=SIGZINIT=0.1 m, and it was verified that MACCS properly set the dispersion coefficient to those values at x=0.
2.4.2 Plume Rise	Not tested	Tests in this report considered the power model for plume rise, with a sensible heat at the source PLHEAT=0 to disable plume rise. Additional testing is needed for variable plume rise and effect on air and ground concentrations.
2.5 Atmospheric Dispersion		
2.5.1 Gaussian Plume Equations	Tests 2.1, 2.5, Test 3.5	
2.5.2 Dispersion Data	Not tested	
2.5.3 Dispersion Rate Models	Test 2.1, Test 3.5	All tests considered the power law model
2.5.4 Virtual Source Calculation	Test 2.1, Test 3.5	Test accounted for the location of the virtual source to set SIGYINIT=SIGZINIT=0.1 m
2.5.5 Dispersion Scaling Factors	Test 2.1, Test 3.5	The YSCALE and ZSCALE factors were heavily used in the tests in this report to examine the effect of different stability classes on the results

Table 5-1. Comparison of the table of contents of the MACCS Theory Manual (Nosek, et al., 2021) to tests documented in this report.

MACCS Theory Manual Table of Contents	Test number addressing feature	Comments
2.5.6 Plume Meander	Not tested	
2.6 Downwind Transport	Test 2.1	The downwind plume movement was examined in Test 2.1
2.7 Plume Depletion		
2.7.1 Radioactive Decay and Ingrowth	Test 2.1	Test 2.1 examined radioactive decay with the downwind plume movement
2.7.2 Dry Deposition	Test 2.5, Test 3.1	
2.7.3 Wet Deposition	Tests 2.2, 2.3, 2.4	
2.8 Centerline Air and Ground Concentrations	Tests 2.1, 2.2, 2.3, 2.4, 2.5 Test 3.5	
2.9 Atmospheric Transport Model Outputs	Test 2.1	
3 Dosimetry		
3.1 Dose Conversion	Test 2.1, Test 3.1	The tests extracted information from the database of dose conversion factors, provided as input file to MACCS, and verified that those inputs were read by MACCS and used to compute individual acute and lifetime doses.
3.2 Off-Centerline Correction Factors	Test 2.1, Test 3.1	
3.3 Early Doses		
3.3.1 Cloudshine	Test 2.1, Test 3.1	
3.3.2 Groundshine	Test 3.1	
3.3.3 Direct Inhalation	Test 3.1	
3.3.4 Resuspension Inhalation	Not tested	
3.3.5 Skin Deposition	Test 3.1	
3.4 Late Doses		
3.4.1 Groundshine	Test 4.1	
3.4.2 Resuspension Inhalation	Test 4.2	
3.4.3 Food Ingestion	Not tested	Independent extensive testing of the COMIDA module is documented elsewhere (Pensado, et al., 2020)
3.4.4 Drinking Water Ingestion	Not tested	
3.4.5 Decontamination Workers	Not tested	
3.5 Dosimetry Model Outputs	Test 2.1, Test 3.1, Tests 4.1, 4.2	
4 Protective Actions		
4.1 Cohort Data	Limited testing	The tests in this document considered a single cohort, without relocation or evacuation. The cohort shielding parameters (GSHFAC, PROTIN, CSFACT, or SKPFAC) were adjusted so that runs part of Test 3.1 would output groundshine, inhalation, cloudshine, or skin dose. The shielding parameters (LPROTIN, LGSHFAC) were adjusted so that runs part of Test 4.1 would output groundshine doses or inhalation doses from resuspension of contaminants on the ground. It was verified that MACCS properly responded to shielding inputs by the user.
4.2 Early Phase Protective Actions		
4.2.1 Evacuation and Sheltering Model	Not tested	The tests in this document considered a single cohort, without relocation or evacuation.

Table 5-1. Comparison of the table of contents of the MACCS Theory Manual (Nosek, et al., 2021) to tests documented in this report.

MACCS Theory Manual Table of Contents	Test number addressing feature	Comments
4.2.2 Early Relocation Model	Partially tested	In all tests, the threshold dose for early relocation (DOSHOT) was set to a high number (10^{10} Sv) to avoid relocation. Relocation limits the exposure to the plume. In all tests, by avoiding relocation, it was verified that the plume exposure was 100%, as expected.
4.2.3 Potassium Iodide Ingestion Model	Test 3.6	
4.3 Intermediate Phase Protective Actions		
4.3.1 Intermediate Habitation Restrictions	Not tested	
4.4 Long-Term Phase Protective Actions		
4.4.1 Long-Term Habitation Restrictions	Test 4.2	The test accounted for effect of long-term habitation restrictions to explain dose versus distances exhibiting jumps.
4.4.2 Long-Term Farming Restrictions	Not tested	
5 Socioeconomic Impact and Costs		
5.1 Early Phase Costs	Not tested	
5.2 Intermediate Phase Costs	Not tested	
5.3 Long-Term Phase Costs		
5.3.1 Costs in Nonfarm Areas	Not tested	
5.3.2 Costs in Farm Areas	Not tested	
5.4 Socioeconomic Impact and Cost Model Outputs	Not tested	
6 Radiogenic Health Effects		
6.1 Early Health Effects Models	Tests 3.3, 3.6	
6.2 Stochastic Health Effects Models		
6.2.1 Linear No-Threshold Dose Response	Test 3.3, Tests 4.1, 4.2	Tests assumed the linear no-threshold dose response model for the computation of health effects
6.2.2 Linear-Quadratic Dose Response	Not tested	
6.2.3 Annual-Threshold Dose Response	Not tested	
6.2.4 Piecewise-Linear Dose Response	Not tested	
6.3 Health Effect Model Outputs	Tests 3.3, 3.6, Tests 4.1, 4.2	

6 REFERENCES

Bixler, N., et al. 2017. *MELCOR Accident Consequence Code System (MACCS), User's Guide and Reference Manual.* Washington DC : US Nuclear Regulatory Commisssion, 2017. ADAMS Accession No. ML17047A450.

Chang, R., et al. 2012. *State-of-the-Art Reactor Consequence Analyses (SOARCA) Report (NUREG-1935).* Washington DC : US Nuclear Regulatory Commission, 2012.

Clayton, D. J. 2021. *Implementation of Additional Models into the MACCS Code for Nearfield Consequence Analysis.* Albuquerque NM : Sandia National Laboratories, 2021. SAND2021-6924.

Derivations of Continuous Functions for the Lateral and Vertical Atmospheric Dispersion Coefficients. **Eimutis, E. C. and Konicek, M. G. 1972.** 1972, Atmospheric Environment, Vol. 6, pp. 859-863.

Molenkamp, C. R., et al. 2004. *Comparison of Average Transport and Dispersion Among a Gaussian, a Two-Dimensional, and a Three-Dimensional Model.* US Nuclear Regulatory Commission. Livermore CA : Lawrence Livermore National Laboratory, 2004. https://www.nrc.gov/reading-rm/doc-collections/nuregs/contract/cr6853/index.html. ADAMS Accession No. ML043240034.

Nosek, A. J. and Bixler, N. 2021. *MACCS Theory Manual.* Sandia National Laboratories. Albuquerque NM : Sandia National Laboratories, 2021. https://maccs.sandia.gov/docs/MACCS_factsheets/MACCS Theory Manual Final_SAND2021-11535.pdf.

Pensado, O. and Speaker, D. 2020. *Input Parameter Updates to the MACCS COMIDA2 Model.* Center for Nuclear Waste Regulatory Analyses, Southwest Research Institute. Washington DC : US Nuclear Regulatory Commission, 2020. https://www.nrc.gov/docs/ML2035/ML20350B615.pdf. ADAMS Accession No. ML20350B615.

SNL. 2015a. *History of MACCS.* Sandia National Laboratories. Washington DC : US Nuclear Regulatory Commission, 2015a. ADAMS Accession No. ML17047A451.

—. 2015b. *History of WinMACCS.* Sandia National Laboratories. Washington DC : US Nuclear Regulatory Commission, 2015b. ADAMS Accession No. ML17047A452.

—. 2021. MACCS: MELCOR Accident Consequence Code System. *MACCS.* [Online] Sandia National Laboratories, 2021. https://maccs.sandia.gov/default.aspx.

—. 2017b. *MELCOR Accident Consequence Code System (MACCS) Software Quality Assurance Plan, Version 1.5.* Sandia National Laboratories. Albuquerque NM : Sandia National Laboratories, 2017b. ADAMS Accession No. ML17047A458.

—. 2017a. *State-of-the-Art Reactor Consequence Analyses (SOARCA) Project.* Severe Accident Analysis Department, Sandia National Laboratories. Washington DC : US Nuclear Regulatory Commission, 2017a. ADAMS Accession No. ML17340B209.

—. 2019. *State-of-the-Art Reactor Consequence Analyses (SOARCA) Project, Sequoyah Integrated Deterministic and Uncertainty Analyses (NUREG/CR-7245).* Severe Accident Analysis Department, Sandia National Laboratories. Washington DC : US Nuclear Regulatory Commission, 2019. ADAMS Accession No. ML19296B786.

Thoman, D. C., Brotherton, K. M. and Davis, W. 2009. *Benchmarking Upgraded HotSpot Dose Calculations Against MACCS2 Results.* 2009 EFCOG Safety Analysis Working Group, Washington Safety Management Solutions LLC. Washington DC : US Nuclear Regulatory Commission, 2009. https://www.nrc.gov/docs/ML1704/ML17047A449.pdf. ADAMS Accession No. ML17047A449.

Wolfram Reseach. 2021. Wolfram Mathematica. [Online] Wolfram Reseach, 2021. https://www.wolfram.com/mathematica/?source=nav.